


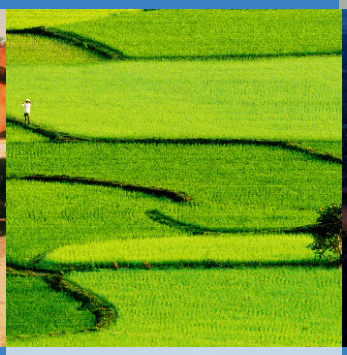


Changes In Global Vegetative Patterns And Their Relationship To Human Activity

A Report of the Aspen Global Change Institute
Elements of Change Series
Susan Joy Hassol
John Katzenberger
Editors

ASPEN GLOBAL CHANGE INSTITUTE

Changes in Global Vegetative Patterns and Their Relationship to Human Activity

A report on the Aspen Global Change Workshop
9 - 22 July, 1995
Aspen, Colorado USA

CO-CHAIRS:
Richard C. J. Somerville
William J. Emery
Compton J. Tucker

WRITER-EDITORS:
Susan Joy Hassol

ELEMENTS OF CHANGE SERIES EDITOR:
John Katzenberger

Furthering the understanding of Earth Systems and global environmental change

FUNDING

The Aspen Global Change Institute gratefully acknowledges support for its 1994 summer science sessions
PROVIDED BY THE
National Aeronautics and Space Administration
Grant Number NAGW-3583,
National Science Foundation
Grant Number OCE-9417138,
Environmental Protection Agency, and interagency support of the Subcommittee on Global Change Research of the U.S. Global Change Research Program

VIDEO AND HARDCOPY

Archival videos of the presentations from this session are available through Aspen Global Change Institute's website, www.agci.org. Hardcopy versions of the report are also available on a cost of reproduction basis. Contact AGCI for more information. Publications of AGCI are available on-line in cooperation with the Global Change Research Information Office (GCRIO) at http://www.gcrio.org/agci-home.html

The views expressed in this report are summaries of participant presentations by the writer, editors, and do not necessarily represent those of the Aspen Global Change Institute, its directors, officers, staff or sponsors.

THE RECOMMENDED CITATION:

Hassol, S.J., and J. Katzenberger, eds. 1996, electronic edition 2008. Changes in Global Vegetative Patterns and Their Relationship to Human Activity. Proc. of an Aspen Global Change Institute Workshop 9-22 July 1995, Elements of Change series, AGCI.

DESIGN AND PRODUCTION:
Original hardcopy edition: Kelly Alford
Electronic edition: Susannah Barr

ASPEN GLOBAL CHANGE INSTITUTE
100 EAST FRANCIS STREET • ASPEN COLORADO 81611
970 925 7376 • agcimail@agci.org • www.agci.org

Table of Contents

Acronyms

APAR: Absorbed Photosynthetically Active Radiation

AVHRR: Advanced Very High Resolution Radiometer

AVIRIS: Airborne Visible/Infrared Imaging Spectrometer

BRDF: Bidirectional Reflectance Distribution Function

BRF: Bidirectional Reflectance Factor

BATS: Biosphere Atmosphere Transfer Scheme

DAAC:Distributed Active Archive Center

EDC: EROS Data Center

EROS: Earth Resource Observation Satellite

FASIR: Fourier-adjusted, solar zenith angle corrected, interpolation and reconstruction

FIFE: First ISLSCP Field Experiment

GCM: General Circulation Model

GIS: Geographic Information System

HTF: Humid Tropical Forest

ISLSCP: International Satellite Land Surface Climatology Project

LAD: Leaf Angle Distribution

LAI: Leaf Area Index

Landsat: Land Remote Sensing Satellite

Lidar: Light Detection and Ranging

MODIS: Moderate-Resolution Imaging Spectrometer

MSS: Multi-Spectral Scanner

NDVI: Normalized Difference Vegetation Index

NIR: Near Infrared

PAR: Photosynthetically Active Radiation

SAIL: Scattering by Arbitrarily Inclined Leaves

SAR: Synthetic Aperture Radar

SiB: Simple Biosphere model

SPOT: System Pour l'Observation de la Terre

TM: Thematic Mapper

Changes in Global Vegetative Patterns - Update and Methodology

Session One Summary

William J. Emery and Compton J. Tucker

Changes to global vegetation cover resulting from human activities have profound implications for ecosystem functioning, biogeochemical cycles, and climatic stability.

Overview

While pre-1972 global vegetation patterns can only be estimated using a variety of his torical sources, post-1972 global vegetation patterns can be directly determined using satellite remote sensing. Our ability to assess and evaluate future changes in these patterns has thus changed dramatically through the application of satellite remote sensing. These data sources (satellite remote sensing and in situ or field studies) have been used to make an up-to-date estimate of the impacts of both natural and anthropogenic changes to vegetation cover in selected regions since the 1970s. For example, recent studies of tropical forest and savanna vegetation in Brazil have documented changes in an area of 7,000,000 square kilometers (km2). While estimates of reported vegetation cover change derived using different methodologies vary, there is agreement that a substantial alter ation of vegetation cover in Brazil has occurred since 1972. The extension of these techniques to other regions of the tropics (i.e., non-Brazilian South America, Southeast Asia, and tropical Africa) was discussed at this Aspen Global Change Institute (AGCI) session, and regional/historical differences between these areas and the Brazilian Amazon were identified.

The various tools for satellite-based assessment were also discussed at this AGCI session. These tools include optical remote sensing, and passive and active (radar) microwave remote sensing, all coupled with "ground truth" validation and numerical model simulations. The model simulations are necessary to evaluate and assess the impact of global vegetation changes on environmental parameters and processes, as ecological, bio-geochemical, and climate models are all needed to completely evaluate the potential impacts of these vegetation changes on the global environment.

Introduction

Changes to global vegetation cover resulting from human activities have profound implications for ecosystem functioning, biogeochemical cycles, and climatic stability. It is generally assumed that human activity has dramatically altered the natural vegetative cover of our planet, especially in the past 300 years (Turner et al. 1990). Upon closer analysis, one discovers not only a considerable ignorance of the present global distribution of terrestrial land cover types, but no systematic, reliable, and comprehensive compendium of human-caused changes to the natural vegetation cover on a global scale (Townshend et al., 1991). In an effort to improve this state of knowledge, the Aspen Global Change Institute devoted its first of three 1995 summer sessions to understanding changes to global vegetation patterns and their relationship to human activity.

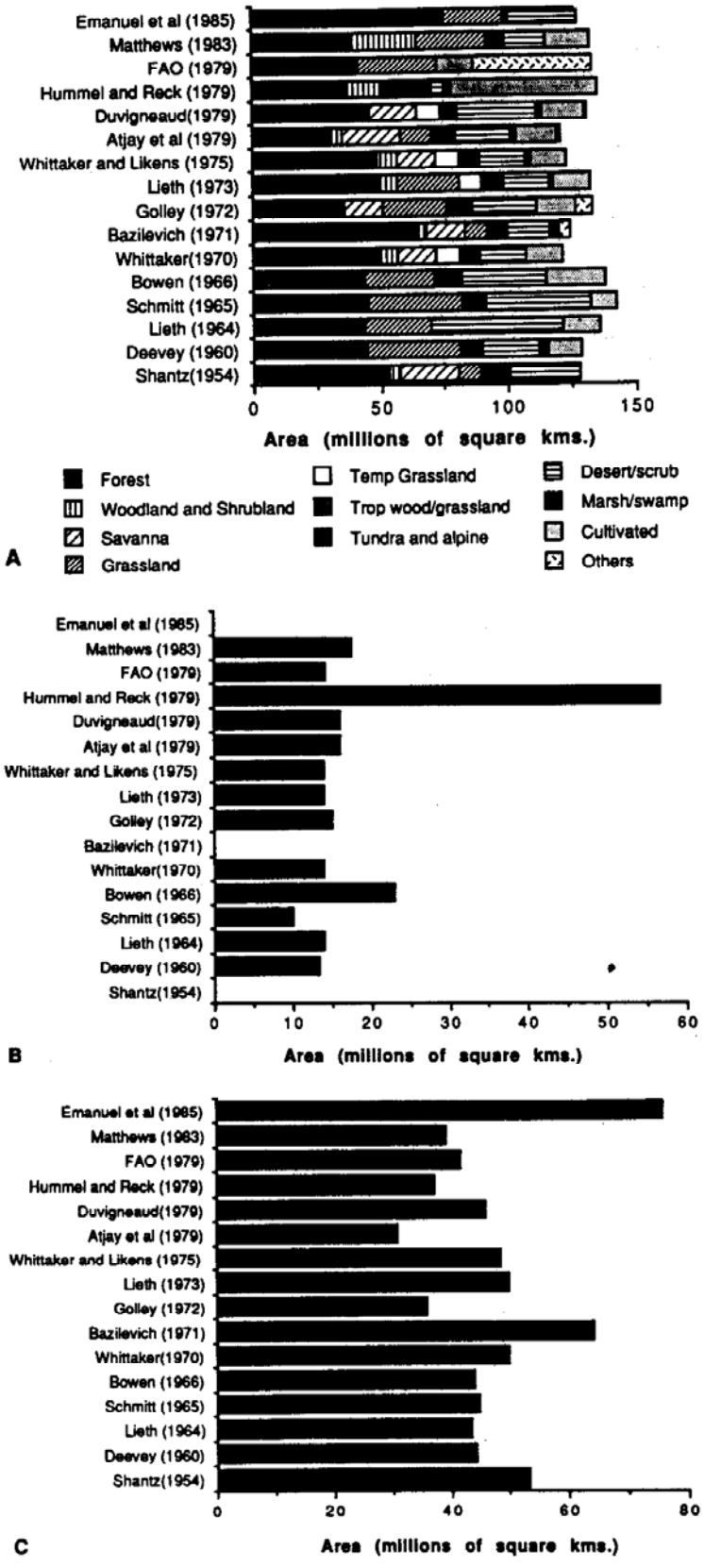

Substantial disagreements in extent of various land cover types globally result from the fact that estimates rely on reconciling numerous separate sources employing widely-varying criteria.

Figure i.1

Variations in estimates of the global extent of cover types for: (a) ten main cover types (the apparent total area varies because of different estimates of the extent of unvegetated categories such as desert and ice caps); (b) cultivated land; (c) forest land

Source: Townshend et al., 1991, Global Land Cover Classification by Remote Sensing: Present Capabilities and Future Possibilities, Remote Sens. Environ., 35:243-255.

A review of existing estimates of global land cover reveals a high degree of disagreement (see figure i.1, Townshend et al., 1991). This is also true for global estimates of agricultural land and forested land, two categories of land cover which can be easily mapped. Substantial disagreements in extent of various land cover types globally result from the fact that estimates rely on reconciling numerous separate sources employing widely-varying criteria. It is thus not surprising that such a high degree of disagreement is present. Furthermore, not only does the total area of the various classes vary substantially among authorities, but the specific spatial distributions of ten vary widely even when the total global estimates of a cover type are similar.

Major efforts have been made to synthesize current global land cover knowledge to generate global digital data bases (Matthews, 1983 and Henderson-Sellers et al., 1986). Although these represent improvements on previous knowledge, they suffer from unavoidable errors inherent in the primary data upon which they are based.

Multi-temporal AVHRR NDVI composites allow classification of the surface based upon photosynthetic capacity and how this varies in time.

Not only are accurate estimates of global land cover of the utmost importance for under standing the coupled Earth-climate system, the extent of land cover type fragmentation is also important. For example, if Earth's climate does become warmer, the ability for terrestrial ecosystems to adapt by "ecosystem migration" could be compromised if natural ecosystems are broken up into non-contiguous pieces. In addition, biological diversity concerns are directly related to habitat destruction and fragmentation.

Regional Examples or Case Studies of Vegetation Changes

Satellite remote sensing has been suggested as a possible means to overcome the tremendous disagreement obvious in figure i.1 (Tucker et al., 1985; Justice et al., 1985; Goward et al., 1985; Townshend and Justice, 1986; Townshend et al., 1987, 1989, 1991; Defries and Townshend, 1995; Loveland et al., 1995). Two different satellite-based approaches have been used to produce estimates of land cover extent:

1. Coarse-resolution (1-10 km) data from the Advanced Very High Resolution Radiometer (AVHRR) sensor on the NOAA-polar orbiting meteorological satellites has been used to map large-scale climatic or vegetation associations, more akin to potential vegetation of regions or continents (Tucker et al., 1985; Justice et al. 1985; Goward et al. 1985; Townshend and Justice, 1986; Townshend et al., 1987, 1989, 1991).

2. Landsat Multi-Spectral Scanner (MSS) and /or Thematic Mapper (TM) data, coupled with a geographic information system (Skole and Tucker, 1993) has been used to map deforestation and surface cover alteration in tropical areas. The use of Landsat data to map land cover is especially important because it can detect many human-caused surface changes which are not detectable using AVHRR data.

Two very different approaches are used to assemble the "seamless" data sets required to study areas millions of km2 in size. With AVHRR data, the daily satellite data are processed into time series composite images which are in turn analyzed to produce land cover type estimates. Thus seamless satellite data are produced and then analyzed. By comparison, for Landsat data hundreds of Landsat scenes are individually analyzed to arrive at the same scene attributes; these determined attributes are subsequently incorporated into a geographic information system, edge-matched, and a seamless data set of those attributes results. The remote sensing determination of tropical deforestation and also the conversion of cerrado or savanna to

agricultural use in Brazil were used to illustrate the AGCI discussions of human modification of the natural environment as detected through the use of satellite data.

AVHRR Data: Continental-Scale Estimates of Land Cover

AVHRR data are useful for large-scale land-cover mapping because of their multi-temporal nature. Daily AVHRR data are formed into normalized difference vegetation index (NDVI) composites which are estimates of vegetation photosynthetic capacity. This follows from the basic relationship of the NDVI to intercepted photosynthetically active radiation (PAR), and this relationship to photosynthesis. Summed over the growing season, PAR and NDVI are highly related to total photosynthesis, and hence to total dry biomass production (figure i.2). Thus, multi-temporal AVHRR NDVI composites allow classification of the surface based upon photosynthetic capacity and how this varies in time.

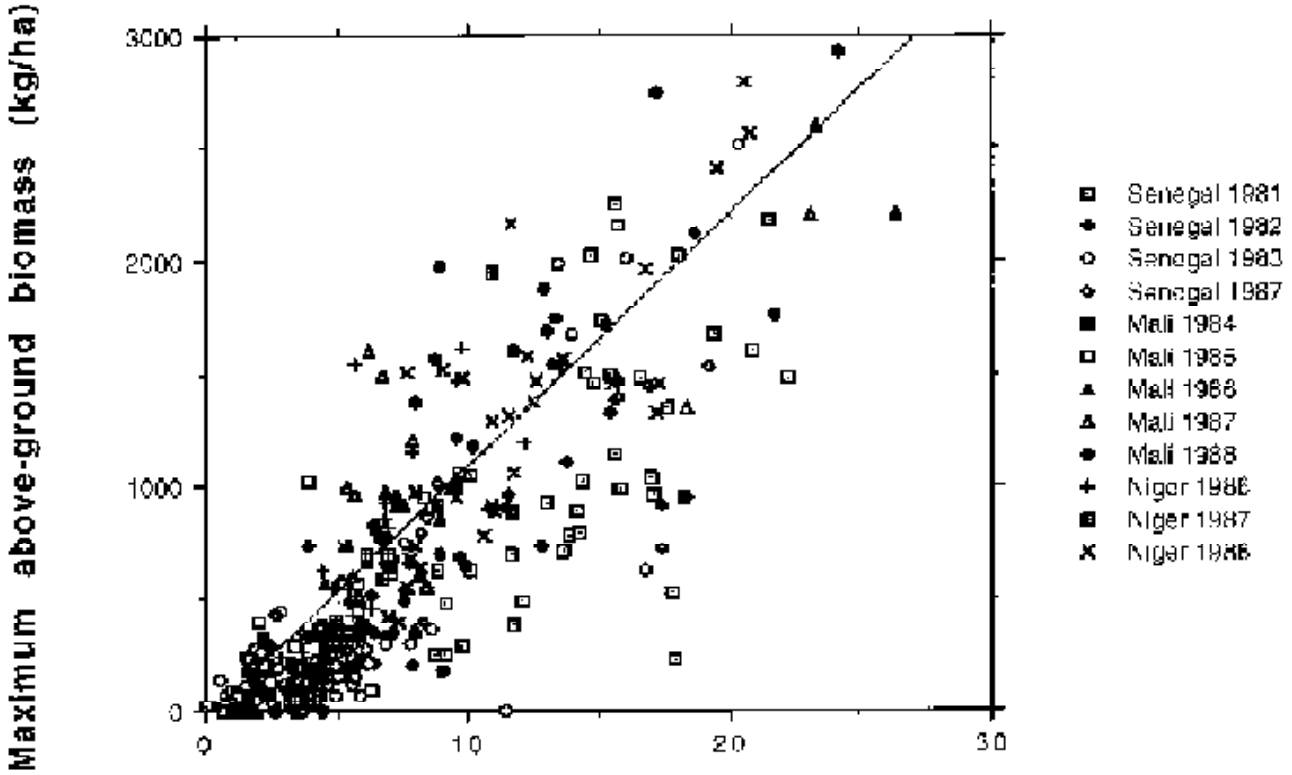

Figure i.2
Temporal sum of NDVI (NDVI days)
Summary figure for NOAA AVHRR 1-km NDVI-Sahelian biomass relationship from 1981-1988. This figure represents the specific comparisons between ground-sampled above-ground total dry herbaceous biomass sampled at the end of the growing season and the integrated or summed NDVI data from the same growing season for these specific locations. From Prince (1991) [biomass (kg/ha)=-86+114*ndvi-days; CIs: @3 ndvi-days,±61 kg/ha;@10 ndvi-days, ±51 kg/ha].

AVHRR data have been formed into time series of the NDVI and used to investigate the possibility of continental land cover determination(s) (Townshend et al., 1985 and 1987; Tucker et al., 1985; Tucker et al., 1991; Tateishi and Kajiwara, 1992; Eastman and Fulk, 1993). The assumption in all of the AVHRR continental land cover studies is that the various large aggregations of land cover have different NDVI responses through time. These different

magnitudes and time variations are the means to classify or discriminate between cover types (desert, semi-arid steppe, savanna, forest, etc.).

Problems arise when more and more land cover aggregations are desired, or when larger and larger areas are studied. Problems also occur when multiple continents are studied together. These problems stem from a lack of clear boundaries between different vegetation aggregations and make exact boundary delineation impossible in many situations.

The Amazon Basin contains ~60% of our planet's remaining tropical forest with Brazil containing ~40% of the global total.

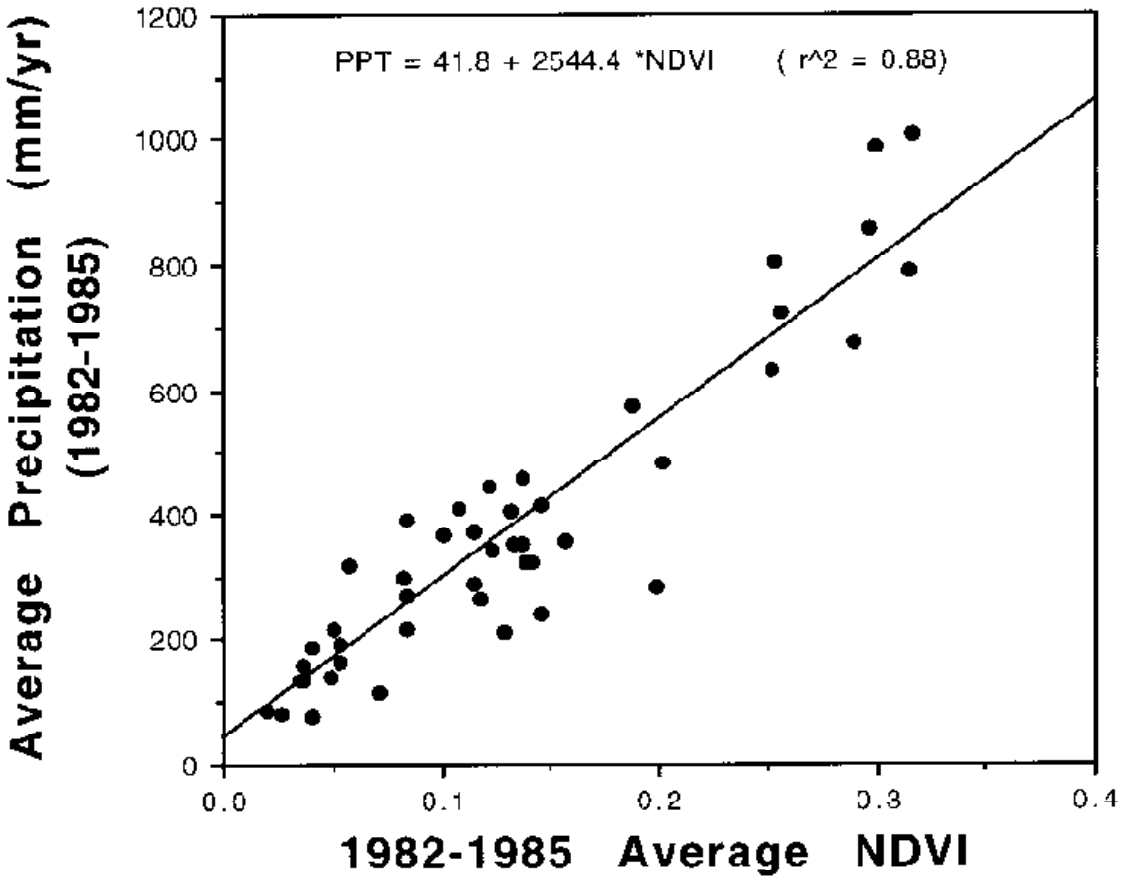

Figure i.3
Comparison between the average precipitation from 1982- 1985 for 24 stations from West Africa and the coincident normalized difference vegetation index averaged from 1982-1985. A similar relationship exists for the 0-600 mm/yr zone between precipitation and the normalized difference vegetation index. From Tucker et al. (1991)

An example of where this has been overcome has been reported by Tucker et al. (1991 and 1994) and involves determining the area of the Sahara Desert from 1980 to the 1990s. In these studies, precipitation data were correlated with coincident NDVI data for 42 Sahelian station locations (figure i.3). This provided the means to use a specific NDVI value as the threshold corresponding to a specific precipitation amount. Tucker et al. , (1991 and 1994) used the 200 mm/year precipitation isoline as the boundary between desert and non-desert, on the south side of the Sahara. This approach was then used from 1980 through the present to document the expansion and contraction of the Sahara to the south. Other land cover determinations must use specified thresholds for assigning areas studied to specific land cover aggregations. Without such thresholds, it is difficult to assign specific boundaries between the various cover types which have meaning.

Figures i.2 and i.3 represent two methods for determining the accuracy of NOAA AVHRR satellite NDVI data in terms of coincident ground observations from specified areas. Other relationships from different locales have been reported by Nicholson and her students (Davenport and Nicholson, 1993; Malo and Nicholson, 1990; and Nicholson et al., 1990).

Landsat Data/GIS Tropical Forest and Savanna Example

At the present time, a substantial alteration of natural vegetation is occurring through out the tropics, in both tropical forests and tropical savannas. Recently researchers have suggested that tropical deforestation plays a major role in the global carbon cycle and has profound implications for biological diversity. Tropical deforestation has also been the subject of intense popular media coverage the past decade. It is thus instructive to review our knowledge of the extent and rate of tropical deforestation, as this is directly pertinent to the theme of this Aspen Global Change Institute session.

Tropical forests (including moist evergreen and seasonal forests) once covered ~24,500,000 km2 of Earth's terrestrial surface (Whittaker and Likens, 1975) and are now estimated to cover only ~10,000,000 km2 (Wilson, 1986). This dramatic decrease has generated widespread concern and calls for tropical forest conservation. These concerns can be traced to the fact that approximately 8,000,000 km2 of tropical land have been converted to agriculture, ~3,000,000 km2 are under shifting cultivation, and ~3,500,000 km2 have been converted to pasture (Salati and Vose, 1983 and 1984). The Amazon Basin contains ~60% of our planet's remaining tropical forest with Brazil containing ~40% of the global total (Mares, 1986).

Tropical forests are home to the greatest diversity of plant and animal life known on Earth, containing over half of our planet's plant and animal species. They are estimated to contain far in excess of 5 million plant and animal species (Prance, 1982). Wilson (1986) notes that ~1.7 million species have been described, including ~750,000 insects, ~47,000 vertebrates, and ~250,000 plants. Some researchers believe the total number of species could be higher than 30 million (Erwin, 1986). Taxonomists have identified only a small percentage of the several million tropical species. One principal adverse effect of tropical deforestation would be mass extinctions comparable to that which last occurred ~60-70 million years ago at the end of the Mesozoic era when the dinosaurs, among many other species, became extinct. These mass extinctions would be expected to result primarily from tropical forest habitat destruction.

Brazil contains the majority of the tropical forests within the Amazon Basin. The so-called "Legal Amazon" covers ~5,000,000 km2, of which 70% is occupied by the non-flooded (terra firme) forest. The rest includes swamp forest, flooded grassland and cerrado (bush land, grassland and savanna). The difficulties of monitoring changes in this large area have resulted in substantial disagreements on the extent of deforestation. For example, the World Bank published figures stating that as of 1988, ~600,000 km2 (~12%) of the Legal Amazon was "cleared" (Mahar, 1989) while Brazilian sources stated that only ~280,000 km2 (~5%) was cleared in 1988 (Tardin and da Cunha, 1990). These two reports, both for 1988, illustrate the late 1980's disagreement over actual figures for deforestation in the Amazon Basin of Brazil (see also Washington Post, 1989) and prompted David Skole at the University of New Hampshire and Compton Tucker at NASA Goddard Space Flight Center to investigate this matter.

Skole and Tucker (1993) have reported 230,000 km2 of deforestation in the Legal Amazon as of 1988, as well as calculating the total areas of isolated forest and deforestation/forest edges. When considering the effect of tropical deforestation upon biological diversity, three

The habitat which remains after parts have been deforested is broken up into fragments which can be isolated to varying degrees. The connectivity with other similar fragments, time since fragmentation, and distance between fragments are all important in determining the biological effects.

components must be considered simultaneously: 1) the deforestation per se (i. e., habitat destruction), 2) areas of isolated forest fragments, and 3) the total area of intact forest in direct contact with areas of deforestation (i.e., the "edge" effect).

Skole and Tucker (1993), drawing upon previous deforestation remote sensing research (Kaufman et al. , 1990; Malingreau and Tucker, 1988; Nelson and Holben, 1986; Nelson et al., 1987a and 1987b; Setzer, 1988; Tardin et al., 1980; Tucker et al., 1984; Woodwell et al., 1983 and 1987), developed a geographic information system approach to analyze tropical deforestation using Landsat TM data as the primary data source (Skole, 1992; Skole and Tucker, 1993). This technique is student-labor intensive but much less expensive than any other means for studying deforestation of large areas while providing a high degree of accuracy. Skole (1992) has reported the accuracies of various analytical approaches (table i.1).

Since 1965, the Brazilian cerrado has been increasingly transformed into cultivated pastures, field crops, dams, urban areas, and degraded areas. It is estimated that ~40% of the natural vegetation of the cerrado has been converted from the natural state.

Method	area estimate (km^2)	% relative to TM digital analysis
SPOT, 20 m, digital, all bands	615	95%
Landsat TM, 30 m, digial, bands 3-5	650	
Landsat TM, ch. 5, 1:250,000, Photo/GIS	600	92%
Landsat TM, ch. 5, 1:500,000, Photo/GIS	710	109%
AVHRR, 1 km, maximum likelihood	875	134%
AVHRR, 1 km, ch. 3 threshold	1175	181%

Table i.1

Comparison of different satellite data and methodologies for estimating tropical deforestation in Rondonia, Brazil (from Skole, 1992). Percent difference is relative to TM digital analysis.

Once the deforestation data are incorporated into the geographic information system, they can be combined with other information such as vegetation distributions, elevation, hydrology, etc., and then used for a variety of purposes. The geographic information system can then be used to determine land cover spatial descriptions such as patch size, edge length, distance between patches, etc. Most importantly, the geographic information system also functions as a data management system. This is an important consideration when dealing with assembling several hundred Landsat images into a "seamless" data set.

Ecological Consequences of Fragmentation

The habitat which remains after parts have been deforested is broken up into fragments which can be isolated to varying degrees (Lovejoy et al., 1984, 1986; Wilcove et al., 1986). The connectivity with other similar fragments, time since fragmentation, and distance between fragments are all important in determining the biological effects of fragmentation (Miller, 1978; Wilcox, 1980; Harris, 1984; Saunders et al., 1991). In order to study this question, the landscape must be specified in terms of fragment size, fragment shape, and location in the landscape (Franklin and Forman, 1987; Ripple et al., 1991). One way to study large-scale habitat fragmentation is to employ a geographic information system using Landsat TM data to provide the required information about surface conditions.

One principal adverse effect of tropical deforestation would be mass extinctions comparable to that which last occurred ~60-70 million years ago at the end of the Mesozoic era when the dinosaurs, among many other species, became extinct.

Savanna Alteration in Brazil Since 1970

While Brazil contains the largest expanse of continuous tropical rain forest on the planet in its Amazon Basin, it also contains a very large area of tropical savanna. The ~5,000,000 km2 of Brazilian Legal Amazon is comprised of 80% tropical forest, 5% open water, and 15% savanna or cerrado. To the south and east of the Legal Amazon is an expansive mosaic of cerrado comprised of evergreen woodland, savanna, and grasslands. This mosaic is often referred to as the Brazilian Cerrado and totals ~2,000,000 km2 of which ~1,400,000 km2 lies outside of the Legal Ama zon (Nepstad et al., 1995).

Cerrado vegetation ranges from open grassland to closed-canopy woodland which differ in proportions of herbaceous and woody vegetation. The herbaceous cover is very active during the rainy season which usually lasts from October to March; ~90% of the cerrado receives between 1,000 to 2,000 mm of precipitation per year. During the dry season precipitation is very low, daytime temperatures high, relative humidity low, and evaporation very high. Consequently, the incidence of fire is very high and the accumulation of dead herbaceous vegetation facilitates fire occurrence (Adamoli et al., 1986).

One principal adverse effect of tropical deforestation would be mass extinctions comparable to that which last occurred ~60-70 million years ago at the end of the Mesozoic era when the dinosaurs, among many other species, became extinct.

The Brazilian Cerrado has experienced and continues to experience large-scale land use conversion, from formerly natural ecosystems to various types of human-managed activities. Because much of the exploitation of these areas has occurred since the early 1970s, this is an ideal area to evaluate the use of Landsat and other satellite data to identify conversion of natural ecosystems to areas of human activity.

It is much more difficult to use Landsat satellite data to quantify land-use changes in areas of cerrado or savanna than in closed-canopy forest. This results from the Brazilian Cerrado being a seasonal savanna with a continuous layer of herbaceous species at peak periods of growth, with scattered trees and bushes that can sometimes form continuous canopies. In addition, corridors of gallery evergreen forest occur along rivers (Klink et al., 1993). The difficulty in using Landsat satellite data to distinguish undisturbed cerrado from cerrado converted to agricultural use is that differences between these are more subtle compared to those in closed-canopy forested areas. It is perhaps most difficult to distinguish undisturbed cerrado from cerrado converted to agricultural use in the dry season when cloud cover is at a minimum. The only way to overcome this dry season limitation is to use Landsat data from more than one date. Complicating this further, there is disagreement regarding the “natural” cerrado vegetation was it open grassland savanna or was it closed canopy woodland that vanished through the increased use of fire since Colombian times?

Until 1965, the cerrado of Brazil was used primarily for cattle grazing. Since 1965, the Brazilian cerrado has been increasingly transformed into cultivated pastures, field crops, dams, urban areas, and degraded areas. It is estimated that ~40% of the natural vegetation of the cerrado has been converted from the natural state (Dias, 1994). Total population in the cerrado area grew from 6.5 million people in 1970 to 12.6 million in 1991. Principal uses of the converted cerrado areas are agricultural and include cultivated pas tures, soybeans, corn, rice, and other crops (Nepstad et al., 1995).

As Nepstad et al. (1995) point out, the lack of information on land-use in the Brazilian Cerrado (and by extension, to all tropical savannas) is remarkable when compared to the attention given to closed canopy tropical forest. The need for information regarding land-use changes in natural non-forested areas can be extended to include not only tropical savannas but temperate grasslands or steppes. Satellite data are the only economically viable means of determining land-use change in savannas and grasslands.

The lack of information on land-use in the Brazilian Cerrado (and by extension, to all tropical savannas) is remarkable when compared to the attention given to closed canopy tropical forest.

References

Adamoli, J. et al., 1986. Caracterizacao da regiao dos cerrados. In: W. J. Goedert. Solos dos Cerrados. Sao Paulo, EMBRAPA and Nobel Press, pp. 33-74.

Adams, J. B., Smith, M. O., and Johnson, P. E., 1986. Spectral mixing modeling: A new analysis of rock and soil types at the Viking Lander 1 site. J. Geophys. Res. 91:8098-8122.

Adams, J. B., Smith, M. O., and Gillespie, A. R., 1989. Simple models for coples natural surfaces: A strategy for the hyperspectral era of remote sensing, in Proceedings of the IEEE Geoscience Remote Sensing Symposium ‘89 , I:16-21.

Cale, P. and Hobbs, R. J., 1991. Condition of road side vegetation in relation to nutrient status. pp. 353-362 in D. A. Saunders and R. J. Hobbs, eds., Nature Conservation and the Role of Corridors. Surrey, Beaty, and Sons, Chipping Norton, Australia.

Davenport, M. L. and Nicholson, S. E., 1993. On the relationship between rainfall and the normalized difference vegetation index for diverse vegetation types in East Africa. Int. J. Remote Sens. (in press).

Dias, B. F., 1994. “Conservacao de natureza no cerrado,” in Cerrado: Caracterizacao, Occupacao, e Perspectivas. Brazilia Univ. Press, Brazilia, pp. 583-640.

Eastman, R. R. and Fulk, M., 1993. Long sequence time series evaluation using standard principal components. Photogram. Eng. Remote Sens. 59:991-996.

Erwin, T. L. 1986. News and Comment. Science , 234:14-15.

Fearnside, P. M., 1986. Spatial concentration of deforestation in the Amazon Basin. Ambio 15:74-81.

Franklin, J. F. and Forman, R. T. T., 1987. Creat ing landscape patterns by forest cutting: Ecological consequences and principles. Landscape Ecology 1:5-18.

Goward, S. N., Tucker, C. J., and Dye, D. G., 1985. North American vegetation patterns observed with the NOAA-7 advanced very high resolution radi ometer. Vegetatio 64:3-14.

Harris, L. D., 1984. The Fragmented Forest: Is land biogeographic theory and the preservation of biotic diversity. University of Chicago Press, Chicago, Illinois.

Harris, L. D., 1988. Edge effects and conservation of biotic diversity. Conservation Biology, 2:330-332.

Henderson-Sellers, A., Wilson, M. F., Thomas, G., and Dickinson, R. E., 1986. Current Global Land Surface Data Sets for Use in Climate-Related Studies. NCAR Technical Note 3 272-STR, National Center for Atmospheric Research, Boulder, Colorado.

Janzen, D. H., 1983. No park is an island: increase in interference from outside as park size decreases. Oikos 41:402-410.

Justice, C. O., Townshend, J. R. G., Holben, B. N., and Tucker, C. J., 1985. Analysis of the phenology of global vegetation using meteorological satellite data. Int. J. Remote Sens. 6:1271-1318.

Kaufman, Y. J., C. J. Tucker, and I. Y. Fung, 1990. Remote sensing of biomass burning in the tropics. J. Geophysical Res. 95(D7) :9927-9939.

Klink, C. A., Moreira, A. G., and Solbrig, O. T., 1993. "Ecological impacts of agricultural development in the Brazilian cerrados," in The World's Savannas: Economic Driving Forces, Ecological Constraints and Policy Options for Sustainable Land Use . Young, M. D. and Solbrig, O. T. eds., pp 259-283, Man in the Biosphere Series 12, Parthenon Publishing, London.

Lovejoy, T. E. et al., 1984. "Ecosystem decay of Amazon forest fragments," pp. 295-325 in Ex inctions, M. H. Niteki, ed., University of Chicago Press, Chicago, Illinois.

Lovejoy, T. E. et al., 1988. "Edge and other effects of isolation on Amazon forest fragments," pp. 257-285 in Conservation Biology, M. E. Soule, ed. The Science of Scarcity and Diversity. Sinauer Associates, Sunderland, Massachusetts.

Mahar, D. J., 1989. Government Policies and De forestation in Brazil's Amazon Region. World Bank, Washington, D. C., 56 pp.

Malingreau, J. P. and C. J. Tucker, 1988. Large-scale deforestation in the southern Amazon Basin of Brazil. Ambio 17:49-55.

Malo, A. R, and Nicholson, S. N., 1990. A study of rainfall and vegetation dynamics in the African Sahel using normalized difference vegetation index. J. Arid Environ. 19:1-24.

Mares, M. A., 1986. Conservation in South America: Problems, consequences, and solutions. Science 233:734-739.

Matthews, E. 1983. Global vegetation and land use: new high resolution data bases for climate studies. J. Appl. Meteorol. 22:474-487.

Miller, R. L.,1978. Applying island biogeographic theory to an East African reserve. Environmental Conservation 5:191-195.

Nelson, B. W., 1992. "Natural Forest Disturbance and Change in the Brazilian Amazon." Presented at the World Forest Watch Meeting, Sao Jose dos Campos, SP, Brazil, 6 pp.

Nelson, R. F. and B. N. Holben. 1986. Identifying deforestation in Brazil using multiresolution satellite data. Int. J. of Remote Sensing 7(3):429-448.

Nelson, R. F., D. Case, N. Horning, V. Anderson, and S. Pillai. 1987a. Continental Land Cover Assessment Using Landsat MSS Data. Remote Sensing of Environment 21:61-81.

Nelson, R. F., N. Horning, and T. A. Stone. 1987b. Determining the rate of forest conversion in Mato Grosso, Brazil, using Landsat MSS and AVHRR data. Int. J. Remote Sensing 8(12):1767-1784.

Nepstad, D. C. et al., 1995. Land-use in Amazonia and the cerrado. Ciencia e Cultura (in press).

Nicholson, S. E., Davenport, M. L., and Malo, A. R., 1990. A comparison of the vegetation response to rainfall in the Sahel and East Africa, using normalized difference vegetation index from NOAA AVHRR. Climate Change 17:209-242.

Panetta, D. and Hopkins, A. J. M., 1991, "Weeds in corridors: invasion and management," pp. 341 -351, in Nature Conservation the Role of Corridors , D. A. Saunders and R. J. Hobbs, eds. Surrey, Beaty, and Sons, Chipping Norton, Australia.

Prance, G. T., 1982. Extinction is Forever , Columbia Univ. Press, New York.

Ripple, W. J., Bradshaw, G. A., and Spies, T. A., 1991. Measuring forest landscape patterns in the Cascade Range of Oregon, USA. Biological Conservation 57:73-88.

Sabol, D. E. Jr., Adams, J. B., and Smith, M. O., 1992, Quantitative subpixel spectral detection of targets in multi-spectral images. Journal of Geophysical Research 97:2659-2672.

Salati, E. and P. B. Vose, 1983. Depletion of tropical rainforests. Ambio 12:67-71.

Salati, E. and P. B. Vose, 1984. Amazon Basin: A system in equilibrium. Science 225:129-138.

Saunders, D. A., Hobbs, R. J., and Margules, C. R., 1991. Biological consequences of ecosystem fragmentation: A review. Conservation Biology 5:18-32.

Setzer, A. W., 1988. Relatorio de atividades do projecto IBDF-INPE "SEQE"Ano 1987, Relatoria INPE-4534-RPE/565 (Instituto Nacional de Pesquisas Espaciais, Sao Jose dos Campos).

Skole, D. L., 1992. Comparison of SPOT, thematic mapper, and AVHRR for quantifying deforestation in Rondonia. Ph. D. Dissertation, Univ. of New Hampshire, Durham.

Skole, D. L. and Tucker, C. J., 1993, Tropical deforestation and habitat fragmentation in the Brazilian Amazon: satellite data from 1978 to 1988. Science 260:1905-1910.

Tardin, A. T. et al., 1979. Levantamento de areas de desmatamento na Amazonia Legal atraves de imagens do satellite Landsat. Relatoria INPE 411 -NTE/142 (Instituto Nacional de Pesquisas Espaciais, San Jose dos Campos).

Tardin, A. T. et al. , 1980. Relatoria INPE 1649 -RPE/103 (Instituto de Pesquisas Espaciais, Sao Jose dos Campos).

Tardin, A. T. and R. P. da Cunha, 1990. Evaluation of deforestation in the Legal Amazon using Landsat TM images. INPE-5015-RPE/609 (Instituto de Pesquisas Espaciais, Sao Jose dos Campos).

Tardin, A. T. et al., 1992. Evaluation of deforestation in the Legal Amazon using Landsat TM images. INPE-5015-RPE/609 (Instituto de Pesquisas Espaciais, Sao Jose dos Campos).

Tateishi, R. and Kajiwara, K., 1992. Global land cover monitoring by AVHRR NDVI data. Earth Environ . 7:4-14.

Terborgh, J., 1976, Island biogeography and conservation: strategy and limitations. Science 193:1029-1030.

Townshend, J. R. G., Goff, T. E., and Tucker, C. J., 1985. Multitemporal dimensionality of images of normalized difference vegetation index at continental scales. IEEE Trans. Geosci. Remote Sens. GE-23:888-895.

Townshend, J. R. G. and Justice, C. O., 1986. Analysis of the dynamics of African vegetation using the normalized difference vegetation index. Int. J. Remote Sens. 7:1189-1207.

Townshend, J. R. G., Justice, C. O., and Kalb, V. T., 1987. Characterization and classification of South American land cover types using satellite data. Int. J. Remote Sens. 8:1189-1207.

Townshend, J. R. G., Justice, C. O., Li, W., Gurney, C., and McManus, J., 1991. Global land cover classification by remote sensing: present capabilities and future possibilities. Remote Sens. Environ. 35:243-255.

Tucker, C. J., B. N. Holben, and T. E. Goff, 1984. Intensive forest clearing in Rondonia, Brazil as detected by satellite remote sensing. Remote Sensing of Environment 15:255-261.

Tucker, C. J., Townshend, J. R. G., and Goff, T. A., 1985. African land cover classification using satellite data. Science 227:369-375.

Tucker, C. J., Dregne, H. E., and Newcomb, W. W., 1991. Expansion and contraction of the Sahara Desert from 1980 to 1990. Science 253:299-301.

Turner, B. L., Clark, W. C., Kates, R. W., Richards, J. F., Mathews, J. T., and Meyer, W. B. (editors), 1990. The Earth as Transformed by Human Action. Cambridge Univ. Press, Cambridge UK, 713 p.

Washington Post , 1989. “Brazil angrily unveils plan for the Amazon.” April 7, 1989, pp. 1 and 18.

Whittaker, R. H. and G. E. Likens, 1975. “Primary production: The biosphere and man,” in Primary Production of the Biosphere, eds. Lieth, H. and Whittaker, R. H.; Springer Verlag, New York.

Wilcove, D. S., McLellan, C. H., and Dobson, A. P., 1986. “Habitat fragmentation in the temperate zone.” pp. 273-256 in Conservation Biology. The Science of Scarcity and Diversity, M. E. Soule, ed. Sinauer Associates, Sunderland, Massachusetts.

Wilcox, B. A., 1980. “Insular ecology and conservation.” pp. 95-117 in Conservation Biology an Evolutionary-Ecological Perspective, M. E. Soule and B. A. Wilcox, eds., Sinauer, Sunderland, Mas sachusetts.

Wilson, E. O., 1986. News and Comment, Science 234:14-15.

Woodwell, G. M. et al. , 1983. Global deforestation: contribution to atmospheric carbon dioxide. Science 222:1081-1086.

Woodwell, G. M., R. A. Houghton, T. A. Stone, R. F. Nelson, and W. Kovalick. 1987. Deforestation in the Tropics: New Measurements in the Amazon Basin Using Landsat and NOAA Advanced Very High Resolution Radiometer Imagery. J. of Geophysical Research 92(D2):2157-2163.

Estimation of Vegetation Characteristics Over Large Areas Using Inverse Modeling

Bobby H. Braswell

Climate System Modeling Program / National Center for Atmospheric Research
Boulder, Colorado

Braswell and colleagues have demonstrated a method for extracting biophysical characteristics over large regions using coarse resolution remote sensing data and inverse radiative transfer modeling. The objective of this approach is to obtain variables which can assist process modeling of terrestrial biogeochemistry and land surface energy balance. These variables are important for understanding how the terrestrial biosphere is coupled to the physical climate system. An example of this coupling is the effect of climate change/variability on net terrestrial carbon dioxide exchange. While the interactions between human activity and terrestrial vegetation can be studied with higher resolution data, the issues under investigation here are inherently low or course resolution problems.

The hot-spot parameterization is necessary in order to account for the effect of self-shading by the vegetation.

In order to extract variables like fPAR (the fraction of absorbed photosynthetically active radiation) and albedo from remote sensing, a model is needed. One approach is to use empirical relationships between vegetation indices and a variable (e. g., Leaf Area Index [LAI], fAPAR). The first requirement of this method is a good index that is invariant with respect to atmospheric contamination, soil variability, and other contaminating factors. Then, one must construct relationships based on field data. Another approach is to use a physical model, as is discussed here. In contrast, the physical model uses parameters describing the architectural and optical characteristics of vegetation components and produces reflectance that is a function of wave length and sun-sensor geometry, known as the bidirectional reflectance factor (BRF). In order to calculate the parameters, an optimization routine is used to determine the parameter set that minimizes the difference between the measured and modeled BRF.

This research utilized a modified version of the Scattering by Arbitrarily Inclined Leaves (SAIL) model (Verhoef, 1984). Modifications include a hot-spot parameterization by (Kuusk, 1991) and the inclusion of a second set of canopy elements (Qin, 1993) that allows for the distinction between leaf and non-leaf scattering and absorption of light. The hot-spot parameterization is necessary in order to account for the effect of self-shading by the vegetation, and the second (non-photosynthetically active) component allows for more accurate simulation of real canopies that contain significant amounts of stems or senescent vegetation. The two-component SAIL model (SAIL2) parameters include optical and structural characteristics for leaves and stems, background reflectance, and the relative abundance of the components (leaves, stems, and bare soil). There are 18 parameters in all.

Braswell and colleagues have performed an informal validation of the model by comparison with field data (a Maize canopy) from Qin (1993). Their model has roughly the same complexity as Qin's so that an almost identical parameterization was possible. SAIL2 was successful in simulating the canopy near infrared and visible reflectances under a number of

illumination conditions. With one component only it was impossible to fit the data. Inclusion of a stem fraction in the canopy introduces more anisotropy (not the same in all directions) to the predicted BRF, especially by decreasing forward scatter transmittance. The model also reveals significant differences in computed Normalized Difference Vegetation Index (NDVI) from forward scatter to backscatter directions. This strong variation suggests that there are considerable problems interpreting NDVI observed from different angles.

Braswell presented an integrated algorithm for the use of Pathfinder 8x8 km AVHRR data to estimate vegetation parameters Figure 1.1). In order to obtain enough information to perform a parameter retrieval, he constructed a BRF by treating all pixels within some neighborhood (in this case a circle of radius 50 km) as if they were the same target. Because of the way the data is composited, adjacent pixels in a scene often are from observations on different days and thus may have very different view zenith and relative azimuth angles. This additional information enables the successful inversion of the model. Supporting the main flow of the algorithm (boxed portion of Figure 1.1) are a series of analyses involving a vegetation index. An NDVI climatology was constructed from three years of data (1986-88) and a principal component rotation was performed to obtain a continuous land surface characterization (LSC) based on the time trajectory of the index. The LSC is used in two ways, the first of which is to ensure spatial continuity of a neighborhood. All pixels which have a significantly different annual pattern of NDVI are treated as outliers and neglected. The second use of the LSC is to stratify a region of interest, for example, by applying parameters and constraints differently for different functional ecosystem types. Finally, Figure 1.1 shows that field measurements may be applied directly to the inversion process by defining fixed parameter values and constraints.

An NDVI climatology was constructed from three years of data (1986-88) and a principal component rotation was performed to obtain a continuous land surface characterization based on the time trajectory of the index.

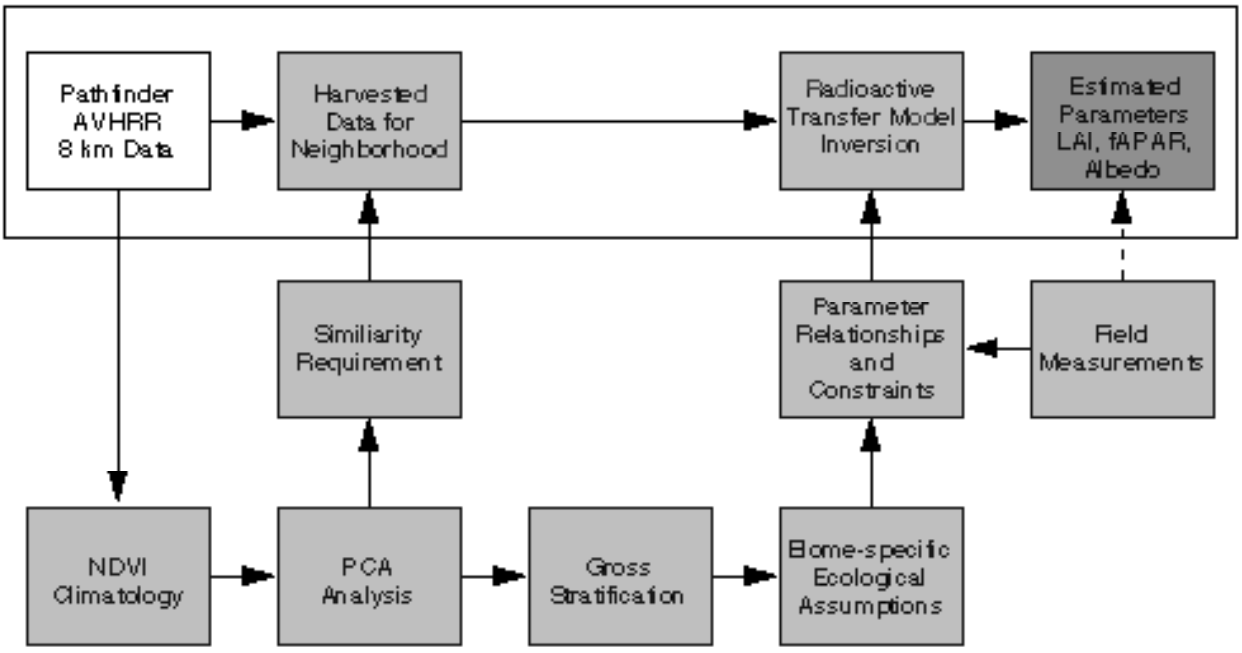

Figure 1.1
Algorithm for Inversion of a Radiative Transfer Model on Pathfinder AVHRR Data

There are a number of advantages associated with using model inversion:

1. The approach is based on physical modeling and thus the relationships between parameters and reflectances are self-adjusting; no catalog of empirical relationships is needed.

2. It allows for the explicit use of soil and leaf optical properties.

3. It allows for the incorporation of a priori knowledge of land-surface type.

4. It complements (and utilizes) broad-brush vegetation index approaches. Any factor that leads to uncertainty in biophysical estimates derived from Radiative Transfer Model inversion also results in uncertainty in results derived from vegetation index methods. In theory, however, inversion is a tool that can allow for reduction in the uncertainty through the use of ecological knowledge and field measurements.

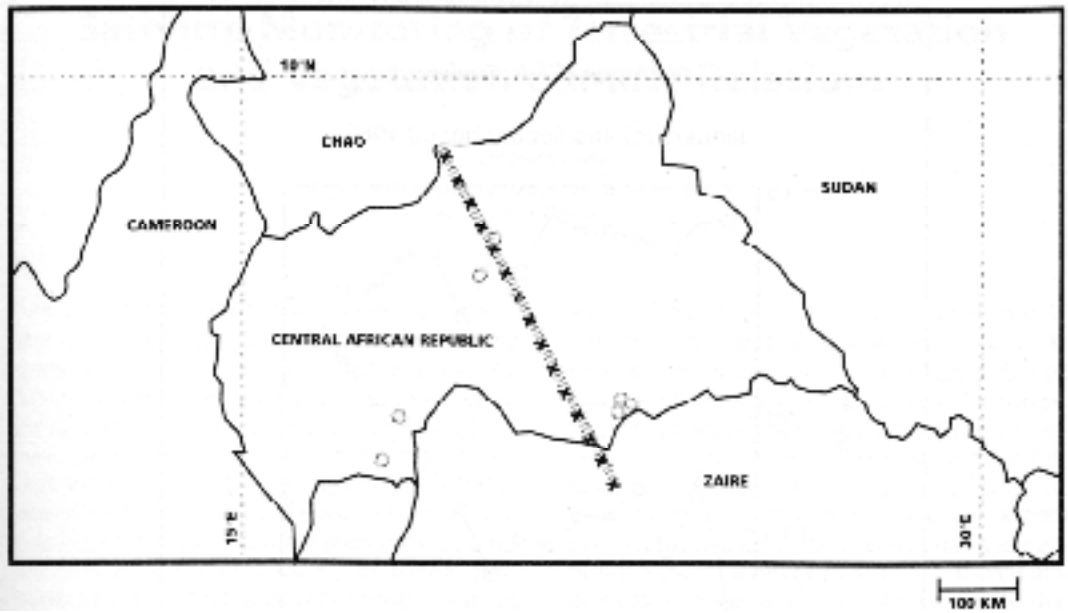

Figure 1.2
15 Point AVHRR Transect Across the Central African Republic and 7 Study Sites from the 1995 EOS-IDS Field Campaign

In the dry season there is a sharp gradient beginning with patch number nine (approximately midway), from the sparse woodlands to the evergreen forest. In the wet season, the fAPAR is more or less constant along the transect, with a slight decline.

An initial investigation was focused on a transect across the Central African Republic (Figure 1.2). This transect represents a steep ecological gradient from dry, seasonal grass land in the north near Chad to moist, evergreen forest in the south near Zaire. In between, there are savannas, woodland systems, and drought-deciduous forest. Each circle represents a field site where soil/litter background spectral measurements were taken as well as some LAI measurements. Each cross represents a "site" (neighborhood) where data was gathered from the AVHRR for the inversion analysis. Each of the 15 sites initially contained 121 8x8 km pixels. Through the imposed requirement of spatial continuity as discussed above using the LSC, as many as half of the pixels may have been rejected. Two time periods were focused on: January (dry season) and September (wet season) of 1988. The inversion was performed to estimate the canopy parameters of each patch and for both time periods. Then, a series of forward integrations were applied using those parameters to generate fAPAR and albedo estimates.

Figure 1.3 shows some preliminary results. The top panel is folar fAPAR for the transect (the x-axis is the distance from the northernmost point). It is evident that in the dry season there is a sharp gradient beginning with patch number nine (approximately midway), from the sparse woodlands to the evergreen forest. In the wet season, the fAPAR is more or less constant along the transect, with a slight decline. Both these results are reasonable qualitatively as well as quantitatively, based on knowledge of these systems, but it is not known whether the small scale features are real or artifacts. Specifically, the slight decline in wet-season fAPAR going south could be due to the fact that the same fixed parameters and the same mode of inversion were used along the whole transect. The albedo results in the bottom panel are more difficult to interpret, but show season-to-season differences that are reasonable.

The preliminary results presented here indicate that inversion techniques have the potential to provide accurate estimates of surface properties that are physically and ecologically based. Continued development of this approach will include investigation of how to apply fixed parameters and parameter constraints on a biome-by-biome basis. More careful validation of the SAIL2 model for both forward and inverse modes is also planned. Eventually, this technique will be mature enough to produce time varying, two-dimensional fields of these quantities for use in terrestrial biogeochemical and climate modeling studies.

The preliminary results presented here indicate that inversiontechniques have the potential to provide accurate estimates of surface properties that are physically and ecologically based.

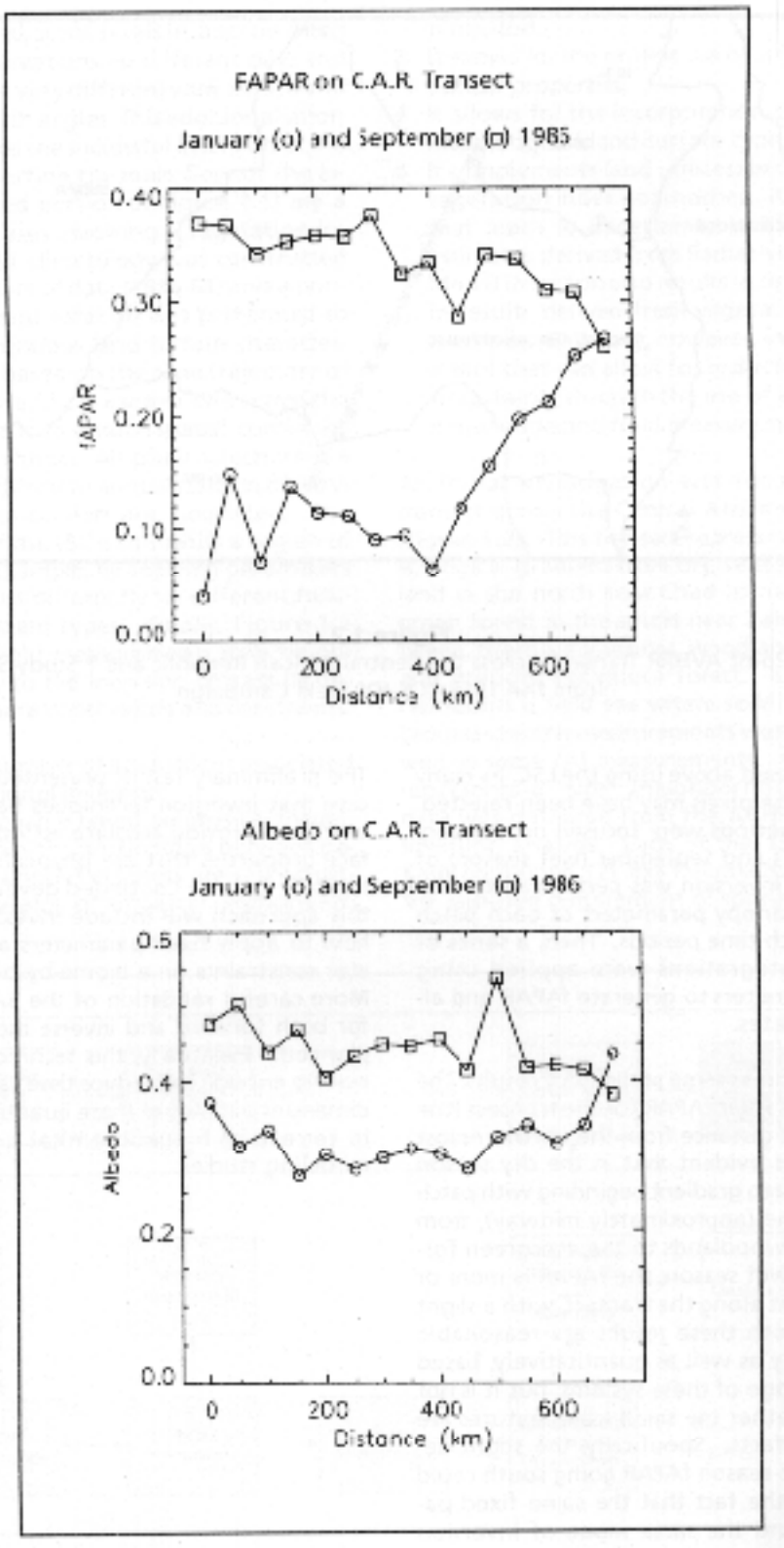

Figure 1.3
January (circles) and September (squares) 1986

Satellite Monitoring of Terrestrial Vegetation and Vegetation-Climate Relations

Dennis Dye

Institute of Industrial Science
University of Tokyo, Japan

Human-caused land cover changes generally result in a net reduction in biomass and photosynthetic activity relative to undisturbed conditions.

Terrestrial vegetation plays a central role in the functioning and sustained existence of the Earth's biosphere. Primary production -- the photosynthetic process by which green plants produce biomass -- regulates the flow of energy and the cycling of carbon, water and nutrients in terrestrial ecosystems. Reliable assessment of the global carbon budget and prediction of future climate scenarios requires an improved understanding of global patterns and dynamics of primary production, as well as the environmental, climatic and human factors that influence those patterns. Dennis Dye and colleagues are employing satellite remote sensing to evaluate terrestrial primary production and related processes at the global scale. The research is bringing new insight and understanding about the interrelationships between vegetation processes, climate and human-caused changes in land cover.

With the advent of agriculture and the growth of human populations and industrial activities, humans have shifted from an essentially benign presence on the Earth to be come major agents of global environmental change. Remotely sensed satellite observations have proven invaluable for detecting, mapping and evaluating human-caused land cover changes at local-to-global scales. Relatively high spatial resolution data from earth observation satellites such as Landsat are effective for assessing land cover patterns and dynamics at local-to-regional scales. At continental-to-global scales, course spatial but high temporal resolution data, such as those acquired with the Advanced Very High Resolution Radiometer (AVHRR) on the NOAA polar orbiting satellites have been successfully employed to examine continental scale land cover change and vegetation dynamics.

A simple but effective method for assessing land cover change by remote sensing involves determination of the undisturbed, potential vegetation cover based on empirically derived relationships with climate variables. Comparison of the potential vegetation patterns with contemporary patterns observed by satellite provides an indication of the magnitude and spatial distribution of land cover change. Such an approach applied to the North American continent using AVHRR data revealed dramatic, broad-scale changes in vegetation cover relative to the pre-European settlement era. Human-caused land cover changes generally result in a net reduction in biomass and photosynthetic activity relative to undisturbed conditions. Land cover change, however, may occasionally increase the biomass and photosynthetic activity relative to undisturbed conditions. For example, in arid, sparsely vegetated regions such as the Imperial Valley of California, highly productive crop vegetation may be introduced and supported by irrigation, producing an overall increase in biomass and photosynthetic activity.

A physically-based, mechanistic modeling approach is proving particularly effective for evaluating net primary production (NPP) at the regional-to-global scale. NPP may be estimated by accounting for the efficiency with which the photosynthetically active radiation (PAR, 400-700 nm) that is absorbed (APAR) by a vegetation canopy is converted to plant matter (Figure 2.1). The approach accounts for factors that alter energy use efficiency, such as physiological and physiognomic attributes of the vegetation canopy, and effects of temperature and moisture stress.

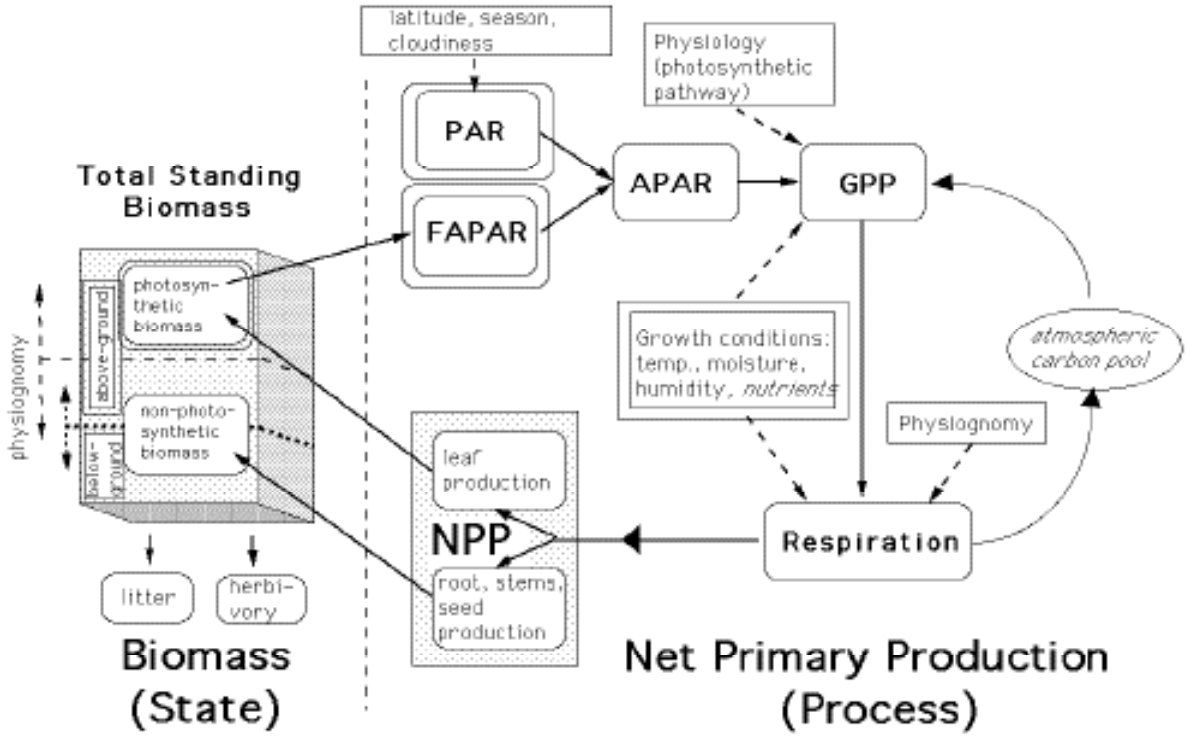

Figure 2.1
Conceptual diagram of the energy conversion model of terrestrial primary production.

A major advantage of the energy conversion model is that key variables can be estimated and monitored on a global basis using contemporary satellite remote sensing tech niques. APAR is estimated as the product of surface-incident PAR, and the fraction of incident PAR that is absorbed by the vegetation canopy (fAPAR). A recently developed methodology employs ultraviolet (370 nm) reflectivity data from the Total Ozone Mapping Spectrometer (TOMS) to estimate and map incident PAR over the globe. fAPAR may be estimated and mapped on a global basis using normalized difference vegetation index (NDVI) measurements from the Advanced Very High Resolution Radiometer (AVHRR).

The increasing time period of satellite data records provides unique opportunities to examine interannual and decadal patterns of variation in biospheric energy flow and primary production (Figure 2.2). A recent, initial investigation of time series data of incident and absorbed PAR revealed distinct patterns of interannual and decadal variation at both regional and global scales. A distinct reduction in global and zonal average terrestrial incident PAR was detected following the eruption of the El Chichón volcano in 1982. Other interannual variations were detected, some of which appear related to anomalous conditions associated with El Niño/Southern Oscillation (ENSO) events during the observation period.

A distinct reduction in global and zonal average terrestrial incident PAR was detected following the eruption of the El Chichón volcano in 1982.

Between 1979 and 1989, global and zonal average terrestrial APAR exhibits a distinct rising trend. It is noteworthy that this trend corresponds in time with an anomalous rise and fall in the rate of increase in atmospheric concentration of CO2 reported by C. D. Keeling and colleagues (Figure 2.3). These trends are indicative of interactions and feedback between variations in solar radiation at the surface, temperature, moisture conditions, and net ecosystem productivity (NEP, which accounts for both net carbon storage by primary production and carbon release by soil respiration). The nature of these interactions, the causes and reliability of the observed trends and their significance for global climate are being addressed in the current research.

Detection of these previously unrecognized patterns and trends in energy flow to primary production underscores the tremendous value of on-going satellite-based monitoring of the biosphere. The growing archive of time-series satellite observations of global vegetation and related variables should soon be significantly enhanced by improved data sets from the Earth Observing System (EOS). These improved data, together with a growing time period of observations, promise further advancements in understanding of the role of vegetation processes in the global Earth system and of the impact of human activities on those processes.

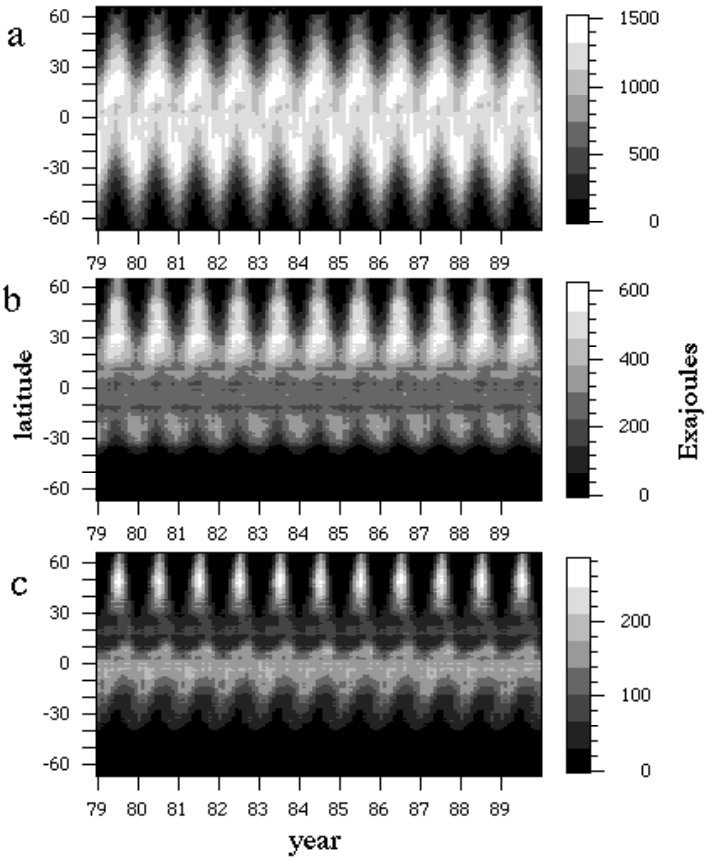

Figure 2.2

Variation in the 1° zonal totals of combined land /ocean incident PAR (top), terrestrial incident PAR (middle), and terrestrial vegetation-absorbed PAR (bottom) for the period from January 1979 to December 1989.

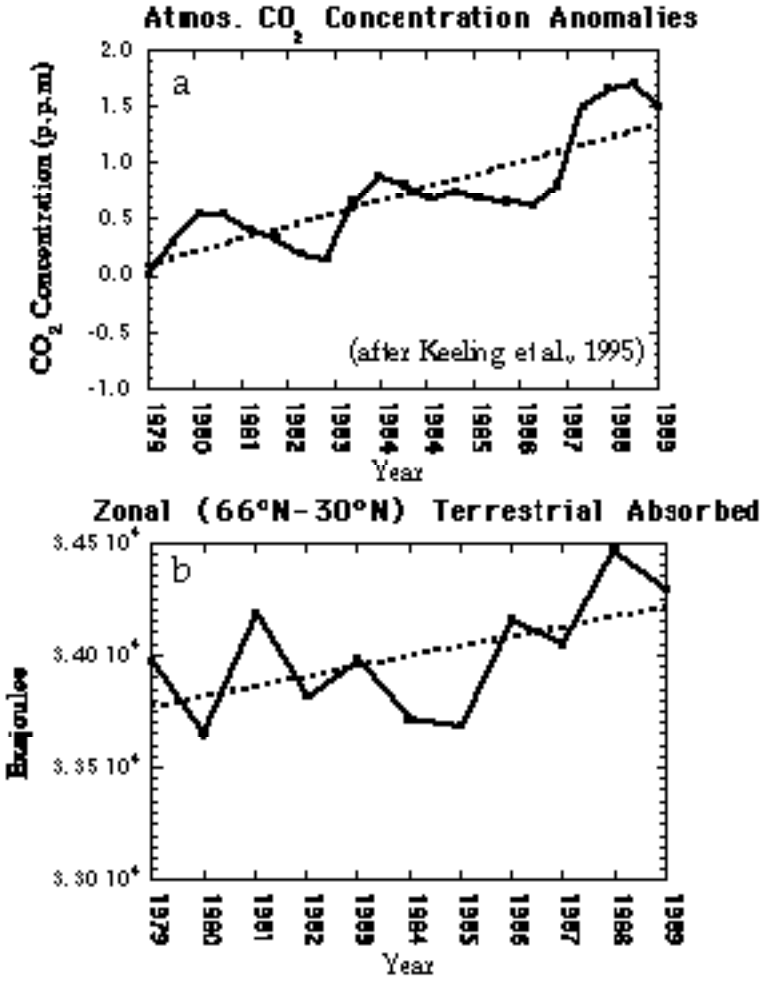

Figure 2.3

a) Anomalies in the atmospheric CO2 growth rate reported by Keeling et al. (Nature, 22 June 1995, 375 :666); b) Annual time series of terrestrial vegetation-absorbed PAR (APAR) for 66°N to 30°N latitudes from Nimbus-7 TOMS and NOAA AVHRR measurements. Dashed lines indicate least-squares linear fit.

Between 1979 and 1989, global and zonal average terrestrial APAR exhibits a distinct rising trend. It is noteworthy that this trend corresponds in time with an anomalous rise and fall in the rate of increase in atmospheric concentration of CO2 reported by C. D. Keeling and colleagues.

Satellite Remote Sensing Technologies for Monitoring Vegetation

William J. Emery

Center for Remote Sensing and Image Processing
University of Colorado Boulder, Colorado

AVHRR data lends itself to the study of many land surface processes, including monitoring snow pack for river runoff, detecting/ monitoring forest fires and assessing the extent of vegetation damage, and monitoring the status of large areas of terrestrial vegetation.

Remote sensing of the Earth began with the advent of aerial photography and in a relatively short time, advanced to the mounting of cameras in rockets. In 1957, the Russian satellite Sputnik demonstrated the viability of operating systems in low Earth orbit (LEO). This began a series of meteorological satellites designed to monitor cloud conditions on Earth. Known as the Television Infrared Observing Satellite (TIROS), the first U. S. space craft in the early 1960s was spin stabilized with its camera pointing towards Earth only for the latitudes of North America. A change in the spin axis led to the series of "wheel" satellites with cameras pointing outwards giving daily global coverage.

In the early 1970s, ballistic missile guidance technology was incorporated into LEO satellites making it possible to operate a 3-axis stabilized spacecraft. This was accomplished through a considerable increase in weight (from ~300 to over 700 lbs. (136 to over 317 kg). Today, LEO environmental satellites typically weigh over 3,000 lbs. (1,360 kg) and carry a multitude of instruments including imagers, radiometric profilers, space environment monitors, and data collection systems. A summary of the presently operating Earth observing spacecraft and instruments is shown in Table 3.1.

1. NOAA/TIROS-N **AVHRR**	2 satellites with daily coverage 5 channels from visible to thermal IR
2. Landsat **MSS** **TM**	5 visible channels, 80 m resolution 7 band (6 visible, 1 thermal IR), 30 m resolution
3. SPOT	multiple visible channels, 20 m resolution, 10 m resolution panchromatic

Table 3.1
Operational Environmental Satellites/Instruments
Low-Earth Orbit

EOSDIS

One of the biggest stumbling blocks in the routine analysis of satellite data is the need for considerable processing to correct for image distortions and sensor calibration. At present, individual groups perform most of these functions. In addition, there is considerable difficulty in gaining access to digital satellite data. NASA is planning a new data system called the Earth Observing System Data and Information System (EOSDIS) that will ingest, process and distribute all NASA (and some non-NASA) satellite data. There will be a number of Distributed Active Archive Centers (DAACs) in the U. S. responsible for the processing, archiving and distribution of these data.

AVHRR Applications

The regular daily coverage of the Advanced Very High Resolution Radiometer (AVHRR) lends itself to the study of many land surface processes. These include: monitoring snow pack for river runoff, detecting/monitoring forest fires and assessing the extent of vegetation damage, and monitoring the status of large areas of terrestrial vegetation. As an example, Figure 3.1 shows AVHRR images converted into the Normalized Difference Vegetation Index (NDVI) before and after a severe freeze in Florida on Christmas Day 1989. The reduced vegetation indicated by the brown colors in the second image indicates the damage to the orange groves brought about by this freeze. Similar analyses can be used to infer the conditions of the corn crop in Iowa or the wheat crop in Kansas. Agribusinesses are beginning to use this technology to increase their knowledge of crop productivity.

Agribusinesses are beginning to use this technology to increase their knowledge of crop productivity.

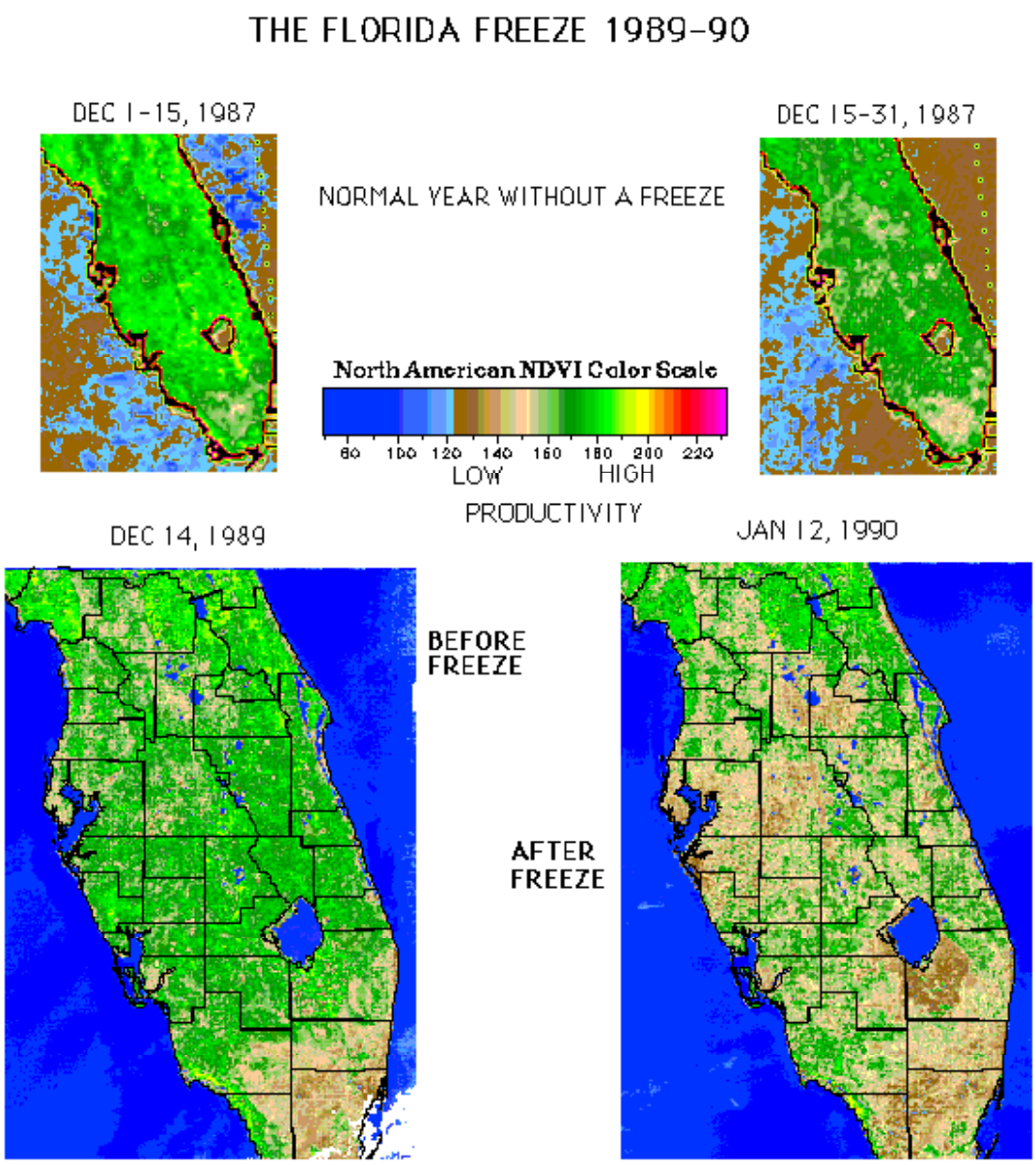

Figure 3.1
Change in Vegetation Due to a Freeze

High Resolution Surface Reconstruction from AVHRR Data

It is possible to use the fact that repeat coverage by the AVHRR instrument never covers the same exact spot. This oversampling at a scale smaller than the 1 km resolution of the AVHRR images can be used with a Bayesian reconstruction technique to produce 180 m (and possibly 120 m) images from 18 AVHRR images of the same area. Applied to Death Valley, California (Figure 3.2) this technique resolved spatial features that could only be seen clearly in the higher resolution (80 m) of Multi Spectral Scanner (MSS) data for the same region. A statistical test of this procedure using two-dimensional Fourier transforms (Figure 3.3) demonstrates that the finer-scale features of the MSS image are mostly resolved by the 180 m AVHRR surface reconstruction.

This surface reconstruction technique has the potential for generating higher spatial resolution satellite imagery from repeat images from lower resolution images without the need for more complex or dedicated imaging systems.

This surface reconstruction technique has the potential for generating higher spatial resolution satellite imagery from repeat images from lower resolution images without the need for more complex or dedicated imaging systems.

In addition using a reflectance model provides a technique for routine subpixel image navigation.

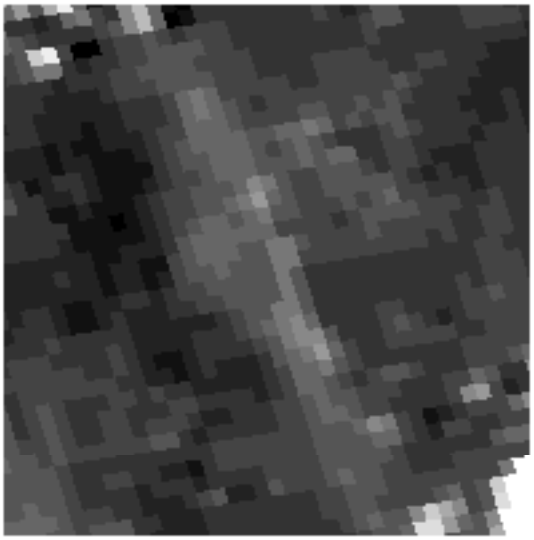

Figure 3.2a
Raw AVHRR image

Figure 3.2b
180 m resolution reconstruction from 18 1 km AVHRR images

Figure 3.2c
80 m resolution MSS image of the same area

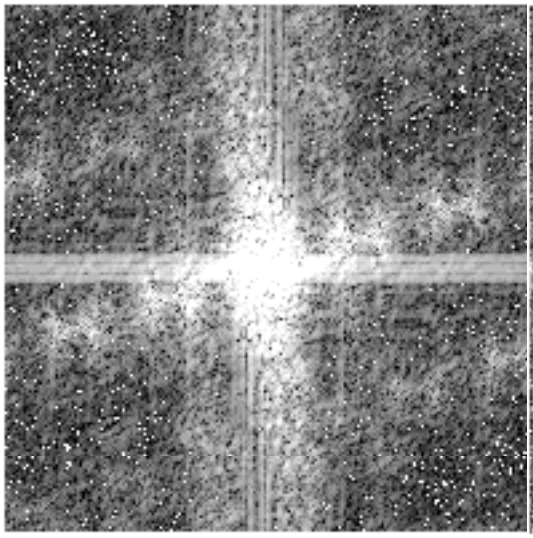

Figure 3.3a
2D FFT of Figure 3.2a

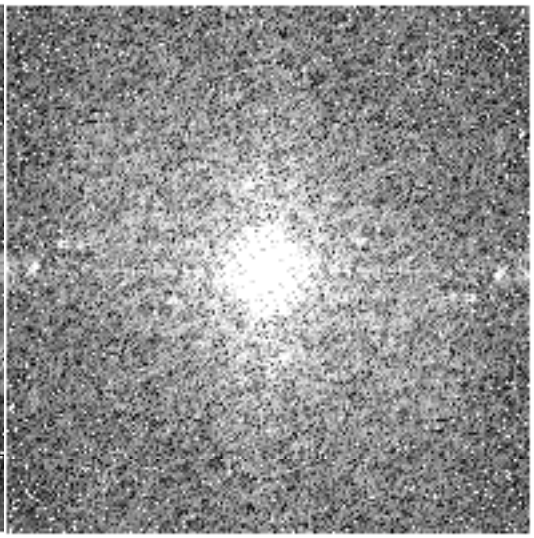

Figure 3.3b
2D FFT of Figure 3.2b

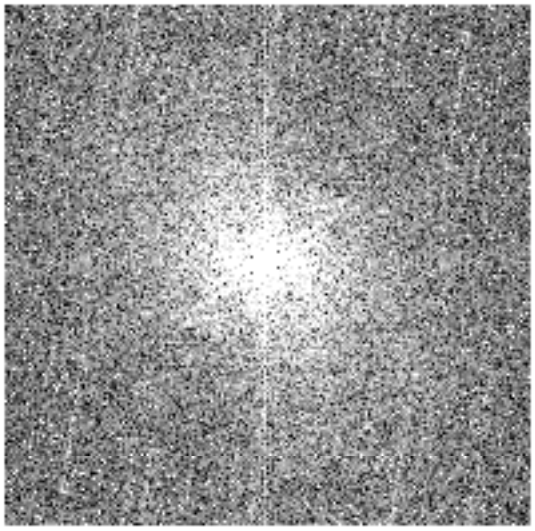

Figure 3.3c
2D FFT of Figure 3.2c

A statistical test of this procedure using two-dimensional Fourier transforms (Figure 3.3) demonstrates that the finer-scale features of the MSS image are mostly resolved by the 180m AVHRR surface reconstruction.

Soil Radiative Transfer Influences in Satellite Monitoring of Vegetation

Alfredo Huete

University of Arizona
Tucson, Arizona

With greater disturbances and land use changes, patterns of asynchronous soil and vegetation development emerge and it becomes vital to remove radiometric soil influences in operational vegetation monitoring programs.

The role and importance of canopy background signals in the global assessment and monitoring of vegetation from satellites are critically examined by Huete. The coupling of soils and vegetation occurs in both a "biome" sense as well as in a radiometric sense. Variations in soil background occur at all spatial scales, including continental variations of dark, organic-rich grassland soils, reddish iron-rich forest soils, and highly variable, geologically exposed arid region soils. Temporally, canopy background signals vary with wetting, presence of snow, and the dynamic behavior of leaf fall and decomposition. Since soils and vegetation co-vary in nature, it is not a simple matter to separate and isolate soil influences on canopy spectral response. However, with greater disturbances and land use changes, patterns of asynchronous soil and vegetation development emerge and it becomes vital to remove radiometric soil influences in operational vegetation monitoring programs.

Operational monitoring of the Earth's vegetative cover currently involves the utilization of vegetation indices (VIs) as a precise radiometric measure of spatial and temporal patterns of vegetation photosynthetic activity. Only with such precise consistency can one utilize VIs for change detection. The normalized difference vegetation index (NDVI), which is the difference of the near-infrared and red bands divided by their sum, has been the most widely used index in global vegetation studies. Its success and accuracy, however, depends on how well it is able to depict actual vegetation differences amidst widely varying soil, atmosphere, and sun-target-sensor variations. Another use of the NDVI is to derive canopy biophysical parameters such as fraction of absorbed photosynthetically active radiation (fPAR), leaf area index (LAI), and % green cover. Many studies have concluded that the translation from NDVI to biophysical parameter is biome dependent and requires knowledge of biome type.

Soil Influences on Vegetation Indices

Two distinct forms of soil influences on vegetation indices (VIs) can be examined. The first concerns the spectral properties of bare soils and background surfaces. Since these signals represent non-photosynthetic elements of a canopy, they form a "baseline" against which the "green" vegetation signal is measured. There are two spectral effects on the NDVI, one due to "brightness" variations and the second associated with "color" variations. Brightness variations plot along a "soil line" in NIR-red space, whereas color differences create secondary sources of variation plotting away from the soil line. The NDVI is susceptible to both forms of variation and cause the NDVI to vary from 0 to 0.2 units on a scale of 0 to 1.

The second form of soil influence concerns soil-plant mixtures and radiant transfer processes within the canopy. Two cases of radiative mixing of soils and plants can be compared. In the first case, the leaf elements of a canopy are assumed opaque resulting in a spectrally-independent, linear mixture model. In the second case, the leaves possess transmissive properties (particularly in the near-infrared) and one can utilize Beer's law to model radiant transfer through the canopy. Figure 4.1 shows the high extent of soil back ground-induced variability in the NDVI for both cases. At zero percent cover, one can see the NDVI vary from 0 (snow) to 0.2 (organic, black soil). At intermediate levels of green cover, however, the soil noise problem increases and becomes maximum at 30-40% green cover, before decreasing to zero at 100% green cover. The same results are seen with more complex canopy models (SAIL, Myneni), with both observational ground and satellite data sets.

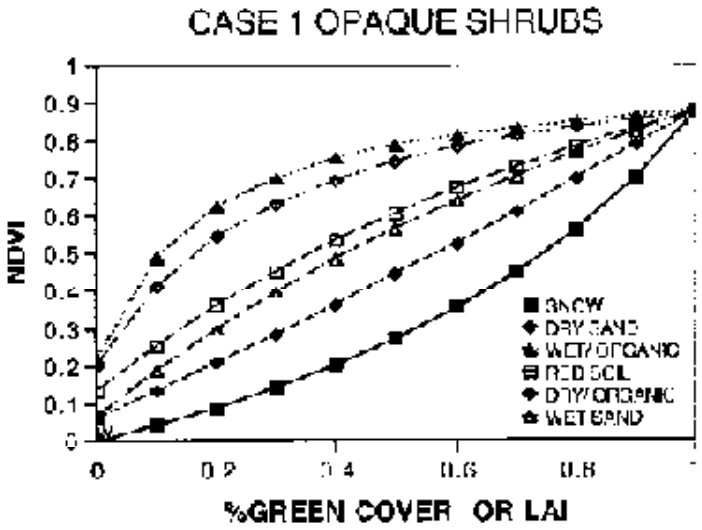

Figure 4.1a

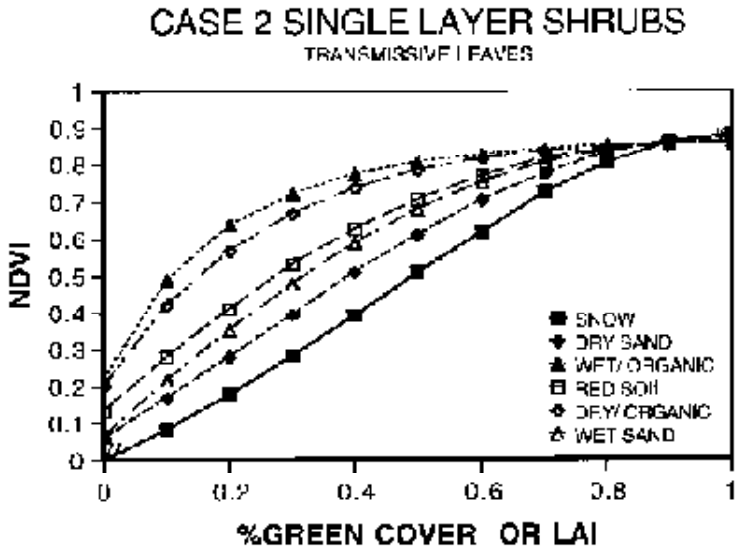

Figure 4.1b

Canopy background-induced variations in the NDVI for both 4.1a opaque and 4.1b transmissive leaf cases.

The removal of one source of noise will require consideration of the additional influences. ... New methods have been developed to render the VI inherently less sensitive to atmospheric variations.

The soil adjusted vegetation index (SAVI) utilizes a constant "L" to remove the soil back ground noise (Figure 4.2). The "L" factor is related to the differential extinction properties between the red and NIR (Huete, 1988). As long as the canopy is actively photosynthesizing, red extinction through a canopy will exceed that of the NIR and a soil correction is necessary. One of the benefits of soil correction is to make the VI more linear with biophysical plant parameters. This benefits vegetation studies by minimizing saturation problems at high levels of vegetation, and allows for more accurate aggregation or scaling of multi-resolution data sets.

Atmosphere and Angular Considerations

Numerous ground, air, and simulation studies over a wide variety of canopies have demonstrated large "potential" influences of soil background, atmosphere, canopy architecture, solar zenith, and view zenith angles on the NDVI response. These influences, however, are intricately coupled as, e. g., the proportions of soil and plant viewed or "remotely sensed" varies with sun-target-sensor geometry. The NDVI has benefited greatly in having many of these influences cancel out. For example, in the presence of an atmosphere, soil influences on the NDVI start to become smaller and are nearly removed in turbid at mospheric conditions. The NDVI function is also more linear with LAI in the presence of an atmosphere. The presence of an atmosphere also offsets canopy anisotropic behavior resulting in less variable NDVI differences with satellite viewing angles. Thus, atmospheric correction of satellite data sets will aggravate soil background and sun-view angular problems in the NDVI. The removal of one source of noise will require consideration of the additional influences.

One of the benefits of soil correction is to make the VI more linear with biophysical plant parameters This benefits vegetation studies by minimizing saturation problems at high levels of vegetation, and allows for more accurate aggregation or scaling of multi-resolution data sets.

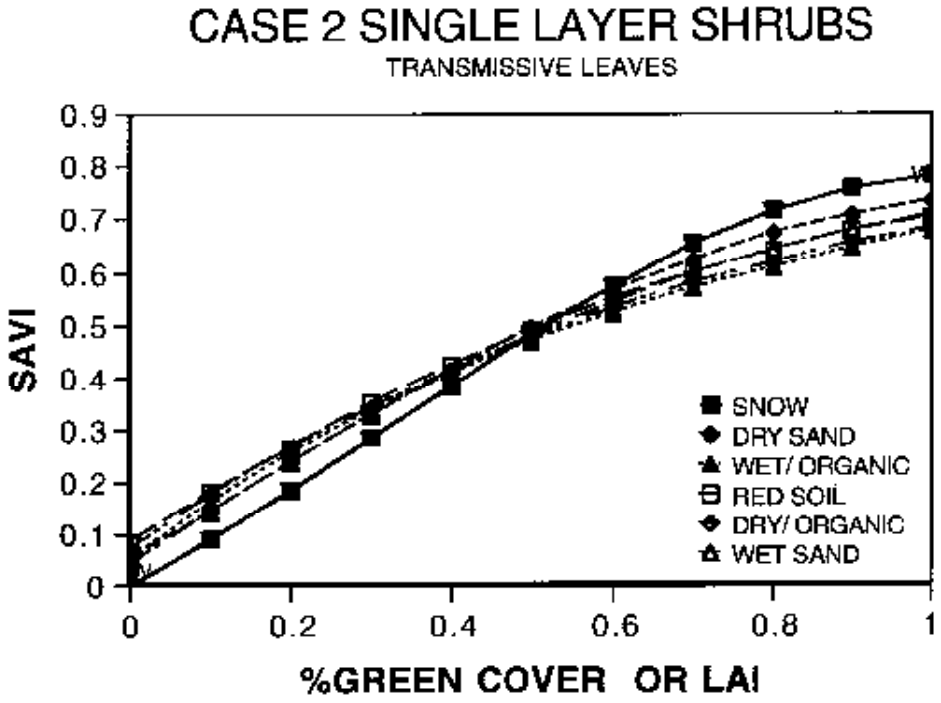

Figure 4.2
Canopy background variations in the SAVI.

New methods have been developed to render the VI inherently less sensitive to atmospheric variations. These involve incorporation of the blue band, which utilizes atmospheric scattering of blue light to adjust scattering in the "red" band. Kaufman and Tanré (1992) developed the atmospherically resistant vegetation index (ARVI) by including the blue band in an NDVI-like

equation. Liu and Huete (1995) incorporated both soil adjustment and atmospheric resistance concepts into a single index, the modified NDVI (MNDVI) (Figure 4.3). In Figure 4.3 we see the progressive decline in soil and atmospheric-induced noise with improved VIs which incorporate soil and atmospheric adjustment factors. The MNDVI has been shown to remove smoke plumes and cirrus clouds from Landsat TM imagery, an indication of its ability to minimize atmospheric aerosols on a pixel by pixel basis.

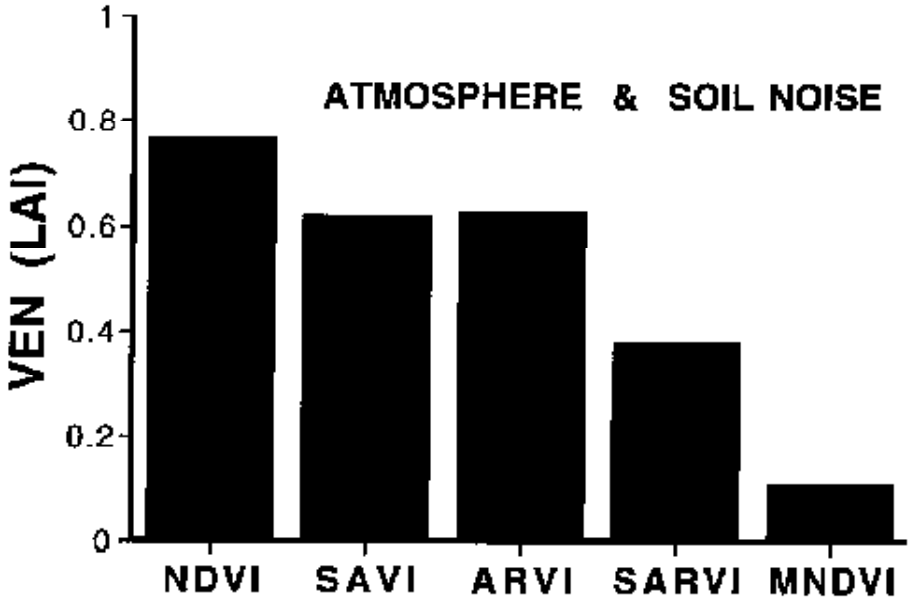

Figure 4.3
Atmospheric- and canopy background-induced "vegetation equivalent noise" (VEN) values for the NDVI and improved indices.

The improved indices, which represent state of the art research, will refine vegetation change detection by physically incorporating soil, atmosphere, and bidirectional effects.

Conclusion

Improved indices will compliment the NDVI in global vegetation monitoring studies in the Earth Observation System (EOS) era to begin in 1998 with the launching of the MODIS sensor (Running et al., 1994). The NDVI will serve as a "continuity" index in order to exploit a 15+ year AVHRR-NDVI global data set. The improved indices, which represent state of the art research, will refine vegetation change detection by physically incorporating soil, atmosphere, and bidirectional effects. Furthermore, there is some evidence that the new indices, such as SAVI and MNDVI are more related to LAI, whereas the NDVI is more correlated to fPAR. This will enable improved methods in extraction of canopy biophysical parameters for global change and land use studies.

References

Running, S. W., Justice, C., Salomonson, V., Hall, D., Barker, J., Kaufman, Y., Strahler, A., Huete, A., Muller, J. P., Vanderbiblt, V., Wan, Z. M., Teillet, P., and Carneggie, D., 1994, Terrestrial remote sensing science and algorithms planned for EOS/MODIS, Int. J. Remote Sensing, 15:3587-3620.

Huete, A. R., 1988, A soil adjusted vegetation index (SAVI), Remote Sens. Environ. 25:295-309.

Kaufman, Y. J. and Tanre, D., 1992, Atmospherically resistant vegetation index (ARVI) for EOS-MODIS, IEEE Trans. Geosci. Remote Sensing, 30:261-270.

Liu, H. Q., and Huete, A. R., 1995, A feedback based modification of the NDVI to minimize canopy background and atmospheric noise, IEEE Trans. Geosci. Remote Sensing , 33:457-465.

Canopy Bidirectional Reflectance Modeling/ Inversion

Jean Iaquinta

Lab of Physical Meteorology
University Blaise Pascal Aubiere, Cedex, France

The primary objective for terrestrial remote sensing is to provide qualitative and quantitative information about the state and behavior of continental surfaces. This depends on the resolution of an inverse problem to retrieve several parameters that characterize surface radiances measured by satellite sensors. Such an inversion is made up of two basic elements, namely a model of the radiance field and a numerical algorithm that determines models parameters by an optimal fitting between observed and predicted radiance fields.

The objectives of the project discussed here were to understand the radiation transport within plant canopies and within the atmosphere (aerosol layers, water and ice clouds), to develop a physical modeling of relevant processes, and to extract information of interest about land surface characteristics through an inversion procedure.

A number of canopy bidirectional reflectance models have been developed in recent decades, generally falling into three categories. (1) Computer simulation models (including Monte-Carlo and radiosity) require an explicit description of the medium and of all interaction processes taking place between light and the targets, principally according to the laws of geometrical optics. The resolution of the problem is made on a photon-by-photon basis. These models are very realistic, generally very time consuming, and use too many parameters to allow for their inversion. (2) On the other extreme, empirical or semi-empirical models only describe the shape of the Bidirectional Reflectance Factor (BDRF) by using more or less simple mathematical functions. The parameters used generally have no intrinsic physical meaning. (3) Conversely, physical models, such as those described below, can be inverted, use measurable quantities as variables, and are based on the analytical or numerical resolution of a transport equation with appropriate boundary conditions. Hybrid models have also been developed with some of the advantages and disadvantages of the three types.

In the classical radiation transport equation in a plane-parallel medium the extinction coefficient is modified to take into account the hot-spot effect. Very simple boundary conditions are selected: at the ground there is a Lambertian surface, and a clear-sky at mosphere overlays the canopy. The leaf scattering phase function is computed using the bi-Lambertian model of Ross and Nilson. In this model a fraction rL of the intercepted energy is re-radiated as a cosine distribution around the leaf normal, another part tLis transmitted on the other side in the same manner, and the residual fraction is absorbed.

When observing the radiation exiting a vegetation canopy near the retro-solar direction (where no shadows occur) we can observe a specific signature called the hot-spot effect,

An important element of the model discussed here is a parameterization which compensates for the hot-spot effect.

corresponding to an increase of reflectance. This feature is related to the finite size of the leaves and to the holes between these leaves. An important element of the model discussed here is a parameterization which compensates for this hot-spot effect.

With these specifications and parameterizations, it is possible to solve the radiation transport problem and derive a physical BDRF model. Some analytical solutions can be obtained for uncollided and first-collided radiations including the hot-spot effect. The computation of multiple scattering contribution is made by means of the Discrete Ordinates Method. Finally, a model emerges using a limited number of parameters for describing the architecture of the canopy, the Leaf Area Index, a hot-spot parameter, parameters for the leaf angle distribution, specified leaf optical properties, and soil albedo. An example of what the model can produce is seen in Figure 5.1, a polar plot of the BDRF of an erectophile canopy as a function of the viewing angle.

Advantages of this model include the fact that it is about 30 times faster than the exact resolution version, with discrepancies of less than 1% in the visible range. This simplified model presents a good compromise between accuracy and computational time.

Typical values were used for the canopy parameters, and the hot-spot parameter was 2rL=0.20

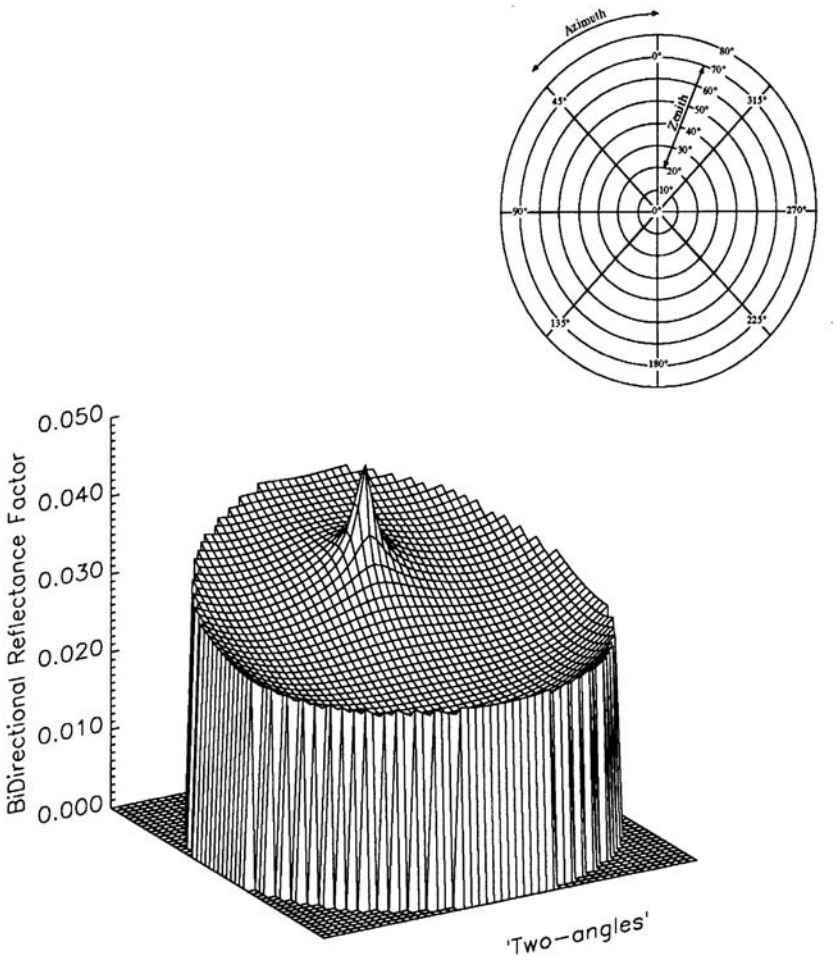

Figure 5.1
The plot for an erectophile canopy observed in the visible region.
Example of a Polar Plot

COMPARISONS WITH A MONTE-CARLO RAY-TRACING

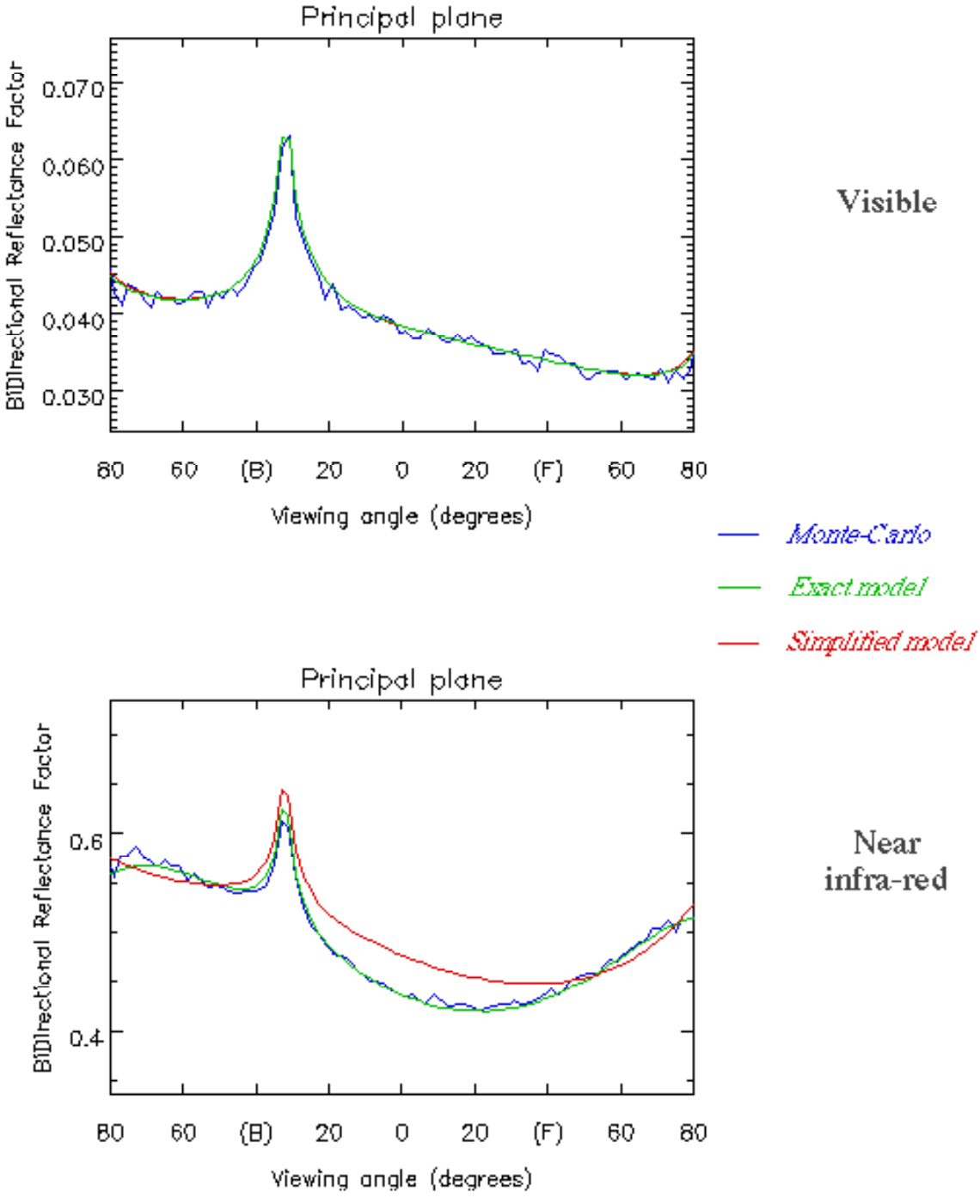

Figure 5.2a and Figure 5.2b
Comparisons with Monte Carlo ray-tracing

As can be seen in the figures, the agreement between the three models is excellent in the visible, especially in the hot-spot region.

For some applications (for instance as the bottom condition in atmospheric problems or for inversion purposes) it is necessary to have fast, but still realistic models. Therefore a simplified version of the model was developed to accelerate BDRF calculations. In this model the multiple scattering contribution was approximated considering an isotropic scattering phase function and non-dependence on the viewing angle. Advantages of this model include the fact that it is about 30 times faster than the exact resolution version, with discrepancies of less than 1% in the visible range. The principle drawback is that the simplified model shows about 5% average difference with respect to the exact resolution in the near infra-red (because multiple scattering was considered as independent of the viewing angle the difference is important at nadir and for large viewing zenith angles). Accordingly, this simplified model presents a good compromise between accuracy and computational time.

There is a need to couple the vegetation canopy with the atmosphere, making corrections that account for the effects of aerosol layers, water clouds and ice clouds above the surface.

These two models were compared with a Monte-Carlo ray-tracing code developed by Yves Govaerts at the JRC in Ispra, Italy. In this model the hot-spot is not parameterized but appears naturally because of the finite size of the leaves and their spatial arrangement while it was simply included in the previous models by means of a geometrical modification of the extinction coefficient. Figure 5.2a compares the results of the three models for a planophile canopy over a dark soil in the visible region; Figure 5.2b compares model results for an erectophile canopy and a bright soil in the near infra-red.

As can be seen in the figures, the agreement between the three models is excellent in the visible, especially in the hot-spot region. In the near infra-red the exact model is still in very good agreement with the Monte-Carlo, and as expected, the simplified model diverges slightly. These comparisons validate the parameterization used for the hot-spot effect.

The Inversion Problem

In the inverse problem the data are BDRFs and the unknowns are the model canopy characteristics. For solving this problem we minimize a non-linear merit function using an iterative numerical algorithm to find the set of model parameters that best fit the data. The minimization process starts with an initial guess for each of the parameters, which are also subject to fixed upper and lower bounds (chosen according to physical constraints). Results of a sensitivity study reveal that in this inversion, retrievals of the Leaf Area Index (LAI) are easier in the visible over bright soils and in the near infra-red over dark soils (i. e. in the regions where there is the maximum contrast between soil and canopy). The computational time increases non-linearly with the number of inverted parameters and there are difficulties in simultaneously inverting more than seven parameters. There is also a need for sampling in the hot-spot direction to improve the retrieval of all parameters. Leaf reflectance and transmittance were shown to be little influenced by errors made on the retrieval of other parameters and are always accurately retrieved. Finally, the soil albedo is found to be very difficult to estimate.

This model was then applied to the FIFE 1989 data set, for measurements made by Don Deering with the PARABOLA instrument for three wavelengths. The data set includes measured BiDirectional Reflectance Factors for several solar zenith angles ranging from 33.5° to 74.1°. Canopy characteristics were also measured (site 916, 4439-PAR) or determined through an averaging scheme taking account of the species abundances. Inversions were made separately in each channel and for each solar zenith angle. In a first step, perfect clear-sky conditions were assumed. Simultaneously inverting all of the parameters yielded the following results: the estimation of leaf optical properties is very accurate; the LAI was better estimated than expected from the previous sensitivity study; and the retrieved average leaf inclination angle

indicates erectophile leaves. Good agreement was found between retrieved and measured canopy characteristics, with the near infra-red channel delivering the best results for canopy architecture.

The diffuse part of incident radiation was found to be about 5%, 10% and 15% respectively in channels 1, 2 and 3. Then another series of inversions was conducted consider ing direct plus diffuse sky light. The results were not very different from the previous ones, except for the Leaf Angle Distribution which was found slightly more erectophile with an Average Leaf Inclination Angle about 64° in all channels while the measured ALA was 65°. These results show that it is possible to accurately retrieve all canopy characteristics from actual reflectance measurements by means of an inversion procedure.

IWACS Models

There is a need to couple the vegetation canopy with the atmosphere, making corrections that account for the effects of aerosol layers, water clouds and ice clouds above the surface. Coupled models are also required because the assumption that downward radiation at the top-of-the-canopy is the sum of direct plus isotropic diffuse components is inadequate. In addition, it is wrong for atmospheric problems to approximate vegetated surfaces as Lambertian reflectors. With all of this in mind, an Ice-Water-Aerosols -Canopy-Soil (IWACS) model was developed.

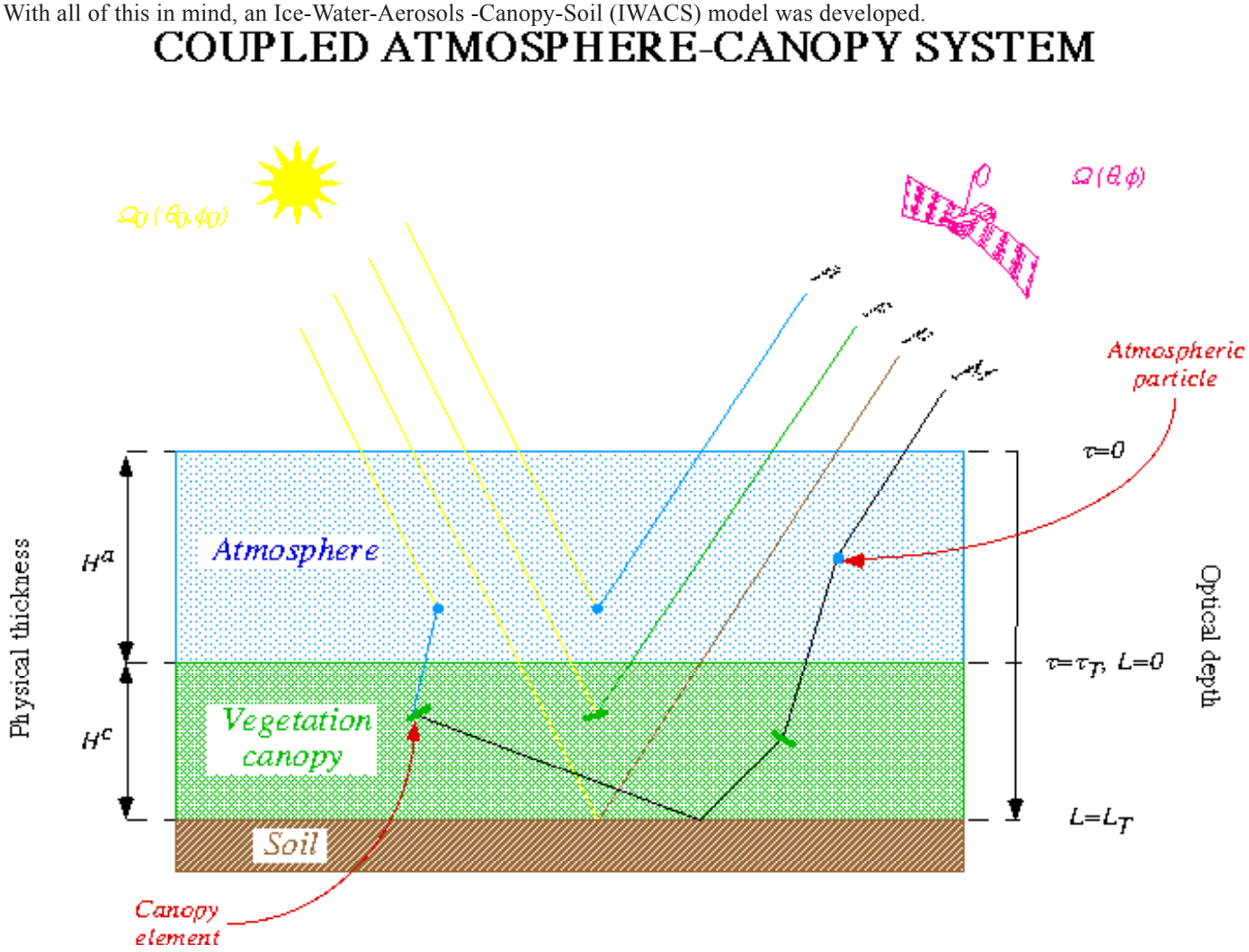

Figure 5.3
The coupled atmosphere/canopy model concept. Ia represents first scattering by the atmospheric particles, Ic the first scattering by the canopy elements, and Iu uncollided radiation and IM multiply scattered radiations.

Figure 5.3 shows the concept behind a coupled atmosphere-canopy model. The first step is specifying the properties of the atmosphere. Atmospheric layers are considered as turbid media with a random orientation of the scattering elements in 3-dimensional space, so their scattering phase function is rotationally invariant. For aerosols, it is calculated using Henyey-Greenstein function, for spherical water droplets the Mie theory was used, and for ice crystals, computations were made with a Monte-Carlo ray-tracing code. The ice crystals modeled were bullet-rosettes with four branches because cirrus clouds are known to be composed of this type of particle. The scattering matrix for ice crystals and water droplets was determined and the transport problem could then be solved.

The upward radiation at the top of the atmosphere in the visible range is plotted when a typical vegetation canopy is surmounted by an aerosol layer, a cirrus cloud, or a water cloud, for several small optical depths (see Figure 5.4).

These results emphasize the importance of atmospheric corrections for both satellite- and ground-based measurements.

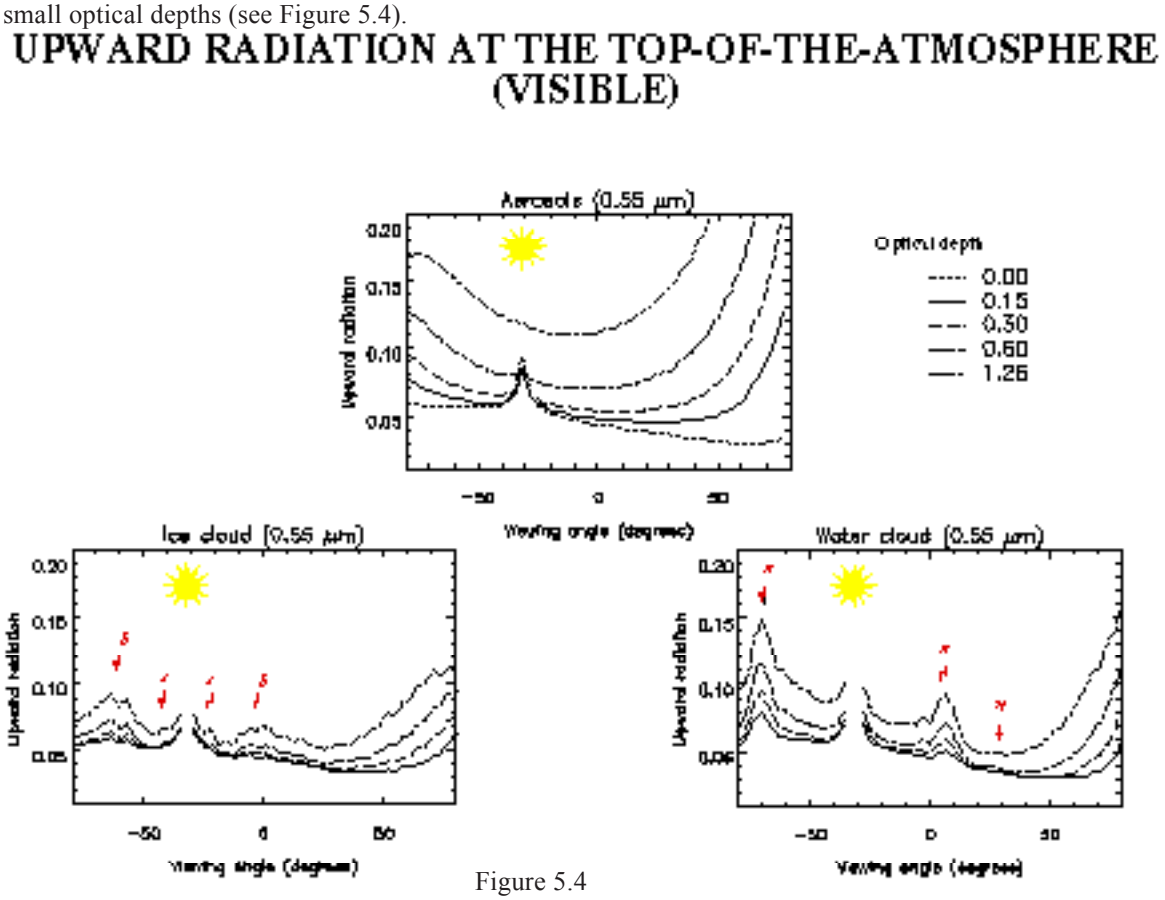

Figure 5.4
Upward radiation at the Top of the Atmosphere

When the optical depth increases, the hot-spot peak disappears and the reflectance increases at large viewing angles. For water clouds and ice clouds, this peak was cut because it extended beyond the graphs. In both cases the shape of the curves are very different from the previous case and we can recognize on both sides of the hot-spot peak typical features characteristic of ice clouds and water droplets (rainbows). In the near infra-red region, the behavior is very similar, but the net atmospheric effect is to decrease reflectance instead of increasing it.

When there are thin water or ice clouds above the vegetation canopy they are easy to detect, but thin aerosols layers are difficult to detect and may have a significant impact on the retrieval of canopy characteristics by means of inversion techniques or by using vegetation indices. These results emphasize the importance of atmospheric corrections for both satellite- and ground-based measurements.

Satellite Data Sets for Global Land-Atmosphere Modeling

Sietse O. Los

NASA/Goddard Space Flight Center
Laboratory for Terrestrial Physics
Greenbelt, Maryland

Los and colleagues at the NASA/Goddard Space Flight Center have assembled a global data set by month of the normalized difference vegetation index (NDVI) from 1982-1990, using daily global meteorological satellite observations from the Advanced Very High Resolution Radiometer (AVHRR). These data exist in two forms: a data set by month for each continent at ~7.6 km resolution; and a global data set at 1° latitude by 1° longitude. The 1° by 1° data set is being used to provide boundary conditions for general circulation models (GCMs) and is also being used in various primary production models of global vegetation (e. g. CASA of Potter et al., NASA Ames). The ~7.6 km resolution data sets are being used for various research projects, such as identifying linked El Niño Southern Oscillation (ENSO)-NDVI anomalies, determination of desert boundaries, and modeling primary production at regional, continental, and global scales. Data have not been processed beyond 1990 due to the Mt. Pinatubo volcanic eruption in mid-1991 which necessitated atmospheric correction over most of the planet. A complete reprocessing of the entire 1981-1995 AVHRR data set is presently underway by Los and colleagues at NASA /Goddard Space Flight Center.

One of the goals of this work is to provide terrestrial time-varying satellite data sets of the NDVI from which the fraction of the intercepted photosynthetically active radiation (fPAR) could be determined. Using a combination of a global land cover classification based on Ruth DeFries' (University of Maryland) data and the AVHRR-derived NDVI time series, the following biophysical variables are generated for each land surface 1° x 1° grid cell: fPAR, leaf area index, albedo, surface roughness, and photosynthesis. Two years of these data (1987 and 1988) have been made available to the public (ISLSCP CD-ROM).

The satellite 1° x 1° data set was intended to be used as a simple interactive biosphere representation which would be coupled to general circulation models and global primary production models. By varying the prescribed surface vegetation classification(s), the effects of human modification of the natural environment can be evaluated as they affect global climate through GCM simulations. For example, Shukla, Nobre, and Sellers have simulated precipitation and temperature changes in the climate of South America by making GCM runs for the Amazon Forest intact and for varying degrees of large-scale Amazon deforestation. Shukla, Nobre, and Sellers have shown that significant drying of South America will result from large-scale deforestation in the Amazon.

By varying the prescribed surface vegetation classification(s), the effects of human modification of the environment can be evaluated as they affect global climate through GCM simulations. Shukla, Nobre, and Sellers have shown that significant drying of South America will result from large-scale deforestation in the Amazon.

Before an accurate representation of the global land surface NDVI could be produced, a significant amount of satellite data processing was necessary. Not only were daily satellite data processed from the NOAA 7, 9, and 11 satellites from 1982-1990, but satellite inter-calibration

was necessary, as was cloud filtering, solar zenith angle correction, compensation for the 1982 El Chichón volcanic eruption, and replacement of missing satellite data (see Figure 6.1).

The satellite data were processed to produce NDVI from the first two channels of the AVHRR instruments as (2-1)/(2+1). This index is bounded between -1 and +1 and is directly related to the fraction of absorbed photosynthetically active radiation. Daily satellite data were mapped into an equal area projection and combined into monthly maximum value NDVI composites, thus minimizing scan angle, cloud, and atmospheric effects. Next the ~7.6 km NDVI data were averaged into 1° x 1° grid cells.

After the satellite data were inter-calibrated from 1982-1990 by month, the data were "sanitized" into a more robust data set, referred to as the FASIR NDVI.

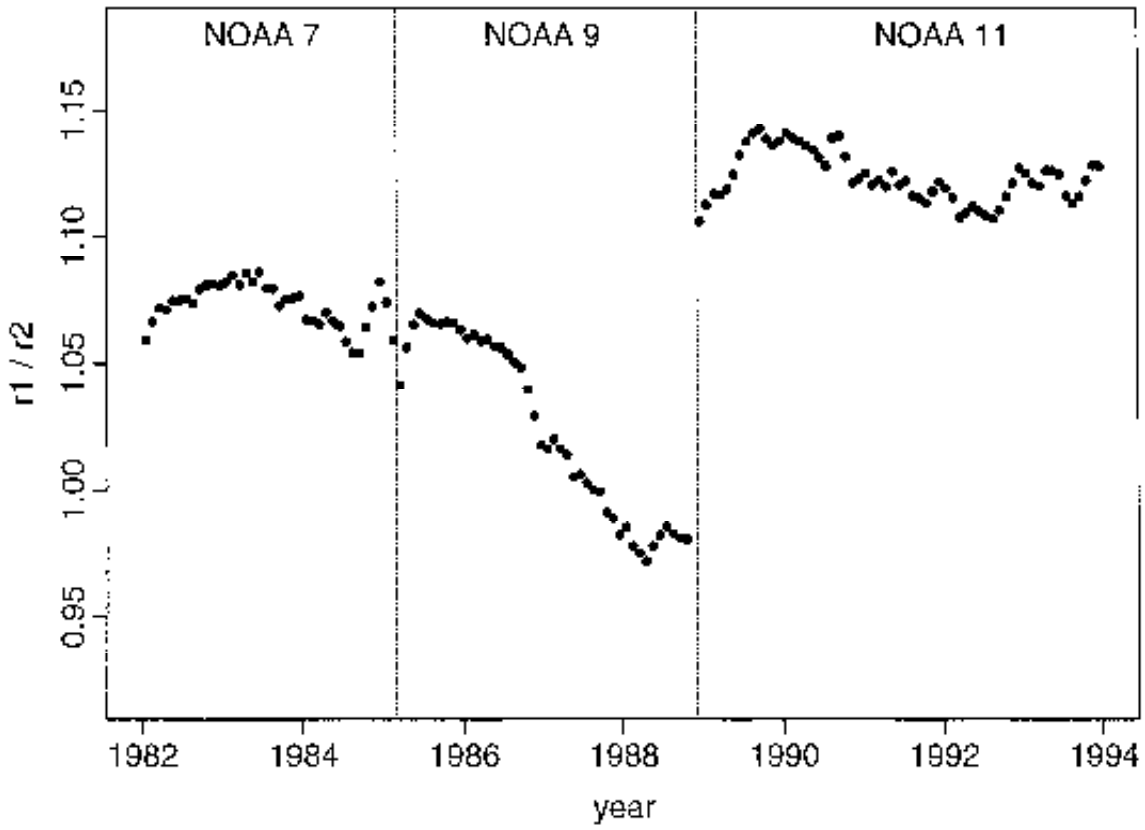

Figure 6.1
Calibration Time Series from 1981-1990

Empirical methods were developed to calibrate the AVHRR instruments' channel 1 and channel 2 to a fixed target through time. This is necessary to ensure that the satellite data sets are consistent and are not introducing calibration error into the simulations carried out using these data.

After the satellite data were inter-calibrated from 1982-1990 by month, the data were "sanitized" into a more robust data set, referred to as the "FASIR NDVI" which stands for Fourier Adjusted, Solar zenith angle corrected, Interpolation, and Reconstruction of missing data (see Figure 6.2). This was accomplished on a pixel by pixel basis at the 1° by 1° grid cell scale.

Fourier adjustment was used to remove extreme outliers from the time series. Solar zenith angle correction was necessary to compensate for illumination effects and increased atmospheric

path lengths at high latitudes. Interpolation of missing data was necessary to represent the boreal forest and other cold areas in winter. Reconstruction of tropical data was necessary because of the very high cloud frequencies in humid tropical forests.

Los and colleagues have produced a global satellite data set from which actual surface conditions can be derived and used in GCMs and ecological simulation models, making possible study of both large-scale human modifications to natural vegetation and of naturally-occurring interannual variability.

The cleaned FASIR-NDVI data were used to calculate land surface parameters at 1° by 1°. A linear relationship between NDVI and fPAR was empirically derived from the assumption that grid cells with NDVI values close to the maximum correspond to conditions of close to maximum (fPAR = 0.95) and that close to minimum NDVI values correspond to close to minimum fPAR (fPAR = 0.001). Leaf area index was calculated from fPAR using an exponential relationship between fPAR and LAI for broadleaf vegetation types and a linear relationship for needleleaf venation and shrubs (see Figure 6.3). The LAI was used to calculate roughness length, the amount of green leaves as a fraction of total leaf area, and, by assigning optical properties dependent on vegetation type, the albedo. Because the land surface parameters were derived from one series of instruments, they show realistic spatial, annual and interannual variations of the physical properties of vegetation.

Los and colleagues have produced a global satellite data set from which actual surface conditions can be derived and used in GCMs and ecological simulation models, making possible study of both large-scale human modifications to natural vegetation of the planet and of naturally-occurring interannual variability.

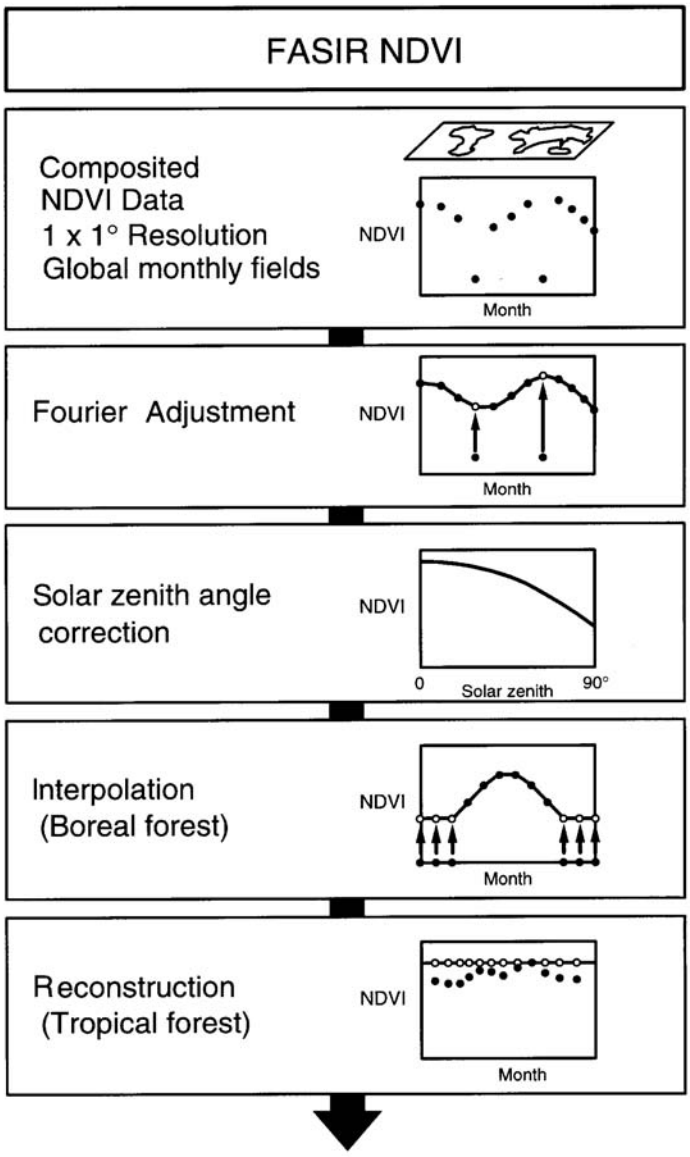

Figure 6.2
Summary of the FASIR Process

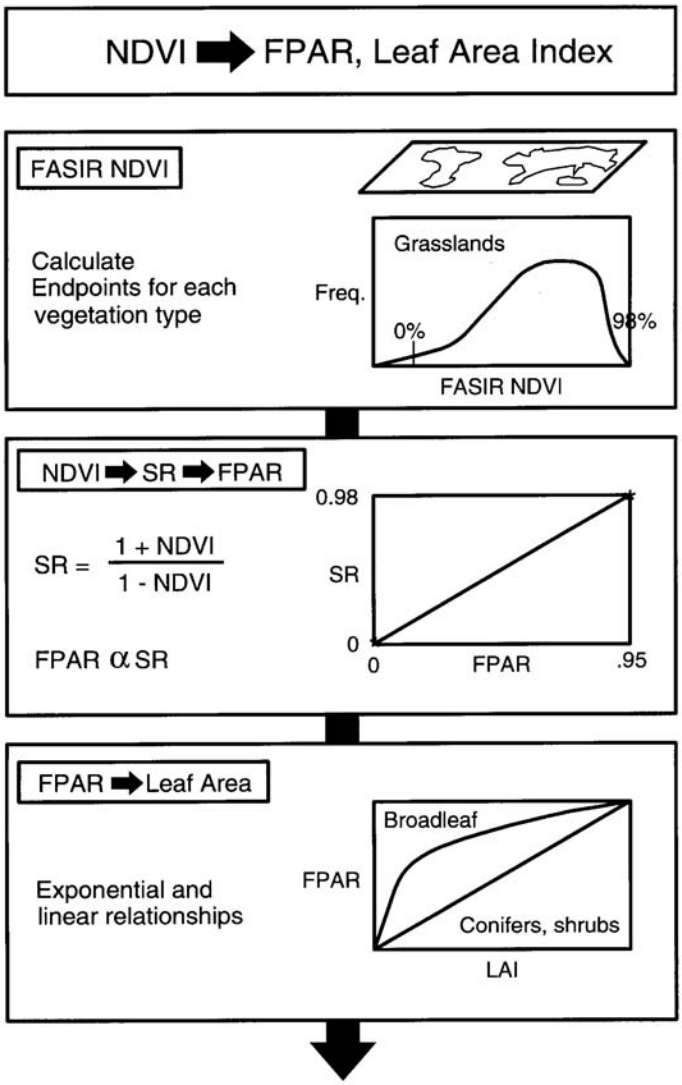

Figure 6.3
FASIR-NDVI to fPAR and LAI

Global Land-Surface Data Sets from Traditional Data Sources

Elaine Matthews

NASA/Goddard Institute for Space Studies
New York, New York

Matthews' digital data sets of global vegetation and land use rely on traditional sources of data, such as maps and statistics, which contain a large amount of underexploited information. The information content of these data bases can be leveraged by combining series of data sets developed from traditional sources with each other or with remote sensing data. In particular, the traditionally-based data sets can provide detailed information about surface features whose gross characteristics are determined by remote sensing, as well as provide longer time histories than the ~20-year histories possible from satellite-based instruments.

Information on the current and past status of the global land surface is needed for many types of investigations but varies with the research area. For global carbon cycle studies, it is important to know more than just the current status of land cover; information is needed regarding historical conversions and dispositions of disturbed lands, including length and intensity of use. Because the character and level of detail of required land surface information is a function of the questions asked, it is crucial to define data needs including thematic detail, and spatial and temporal resolution. For example, for questions regarding surface albedo, a high level of land surface detail is not needed because albedos do not vary a great deal among vegetation types. Alternatively, studies of the methane cycle, whose emissions from individual sources often originate from point sources, require great detail about selected areas, and essentially no information exists about most of the Earth. While it is possible to design flexible data sets that can be tailored to a wide variety of research areas, no data set will fulfill all needs.

Traditionally-based data sets can provide detailed information about surface features whose gross characteristics are determined by remote sensing, as well as provide longer time histories than the ~20-year histories possible from satellite-based instruments.

Vegetation and Land Use Data Bases

Matthews' interest in global vegetation data arose in the late 1970s, primarily in order to improve prescriptions of land surface boundary conditions in the GISS GCM (Goddard Institute for Space Studies' General Circulation Model). At that time, land cover in GCMs was divided into a few types such as forest, grassland, desert, and ice. There was no global digital data set of land cover, no globally consistent series of vegetation maps, and no internationally accepted classification system in use. The closest thing to such an international system was that of UNESCO but the only UN FAO vegetation map in existence (Mediterranean Zone) did not use the UNESCO system; later FAO maps covering South America and Africa also did not use the system. At the time, detailed, digital information was a major improvement over what was available.

For the global vegetation data base published in 1983, Matthews compiled information from about 100 sources (primarily maps) at one degree latitude/longitude resolution. Legends from these maps were translated into, and recorded with, the 5-tier hierarchical UNESCO

classification system. Information from the maps was then recorded using the UNESCO codes. Classification criteria include lifeform, density, seasonality, climate, plant architecture, altitude, and environmental setting. The philosophy underlying this approach was to provide for flexibility both in recording the variable amount of detail available from sources, and subsequently in tailoring the data sets to a variety of research areas.

In the UNESCO classification scheme used in Matthews' vegetation data base, five lifeform categories comprise the first level of the hierarchy; these are closed forest, woodland, shrubland, dwarf scrub and related communities, and herbaceous vegetation. Each of these is further broken down into subcategories primarily on the basis of seasonality. For example, closed forest may be evergreen, deciduous or xeromorphic. Evergreen forests are broken down into ten classes, such as tropical rainforest; tropical rainforest is further refined into eight categories, and so on. Globally, Matthews' vegetation data base identifies 178 vegetation types. For GCM applications, including e. g., surface reflectance features, these types are condensed to about 10; for carbon studies, about 30 types are used. Other applications dictate alternative divisions.

Estimates of pre-agricultural and present biomass suggest that about 12% of the original global biomass was replaced by agriculture.

A land use data set was compiled at the same time, and at the same spatial resolution, as the vegetation data. Because there was no existing land use classification scheme appropriate for a global study, a triple-tier hierarchical system was developed by Matthews for the project. In a manner similar to the UNESCO system for vegetation classification, major categories of farming systems are further broken down to reflect a greater level of detail. Classification of major farming systems into, e. g., intensive subsistence farming or large-scale commercial farming, is based on their permanence and extent of disturbance. At the most detailed level, the data set identifies 119 land use types many of which include crop combinations. For example, the system distinguishes three categories of subsistence farming: rudimentary, extensive, and intensive (i. e., rice). Other categories are extensive and intensive grazing, plantations, mediterranean, large- and small-scale commercial, dairying, lumbering, and no use.

Because land use maps generally do not provide precise boundaries, Matthews developed a relationship between farming systems and cultivated area to integrate the vegetation and land use data sets in order to define land cover. The major farming systems were qualitatively scaled with respect to their impacts on the natural vegetation. Each system was assumed to replace a fraction of the natural vegetation. The assumptions are broad and the scale is simple. This procedure resulted in simple categories of cultivated fractions for 1° cells which range from 20% to 100% of cell areas; subsistence agriculture is associated with low cultivation intensities, while large-scale commercial agriculture is associated with 100% cultivated area. Problems remain particularly with characterizing the impact of less intensive land use systems.

The vegetation and land use data sets provide snapshots of pre-agricultural and present land cover conditions but do not reflect historical trends in change. These data sets have been used to estimate anthropogenically imposed biomass reductions from replacement of natural vegetation with agriculture. Estimates of pre-agricultural and present biomass suggest that about 12% of the original global biomass was replaced by agriculture. Penetration of large- and small-scale commercial agriculture into temperate forests between 30°N and 55°N accounts for about 60% of the global reduction in biomass. Due to poor land use data for the tropics, tropical reductions are probably under-estimated.

Global data bases such as those described here can be considered in three levels. Primary data bases are directly compiled, extrapolated or interpolated. They define topically detailed, large-scale characteristics of the Earth; many are nominal data (e. g., vegetation, soils, countries).

Secondary data bases provide global distributions of source categories identified with properties important for exchanges of particular constituents. They are derived from primary data bases and supplemental information (animal densities = country + land use + population statistics); they contain nominal, interval, or ordinal data; and may have a seasonal component. Tertiary data bases provide global distributions of gas exchanges for individual sources and are derived from combinations of primary and secondary data bases and emission factors.

For example, methane emission from wetlands is derived from combining vegetation, soils and inundation data to produce the wetland distribution; emission factors and in undation periods are applied to the wetland ecosystems to estimate the global methane emission from this source. Uncertainty increases from the primary through the tertiary level, and the tertiary level is most subject to revision as new emissions measurements are available. Information at each stage can be leveraged by coupling the data sets.

Characterizing Disturbance

A key issue is distinguishing areally extensive disturbances (i. e., agriculture) from point-intensive disturbances (i. e., mineral extraction) and characterizing ecosystem disturbances that result from them. In addition to knowing the area of land converted, for which remote sensing is especially valuable, it is crucial to know what ecosystems are disturbed by various activities as well as the disposition of disturbed lands. More predictable mechanisms of anthropogenic disturbance include cultivated land and pastures; less predictable mechanisms include subsistence agriculture, human relocations, forest fires, extractive activities, and dams. Techniques to characterize disturbances include remote sensing (success varies with ecosystem), determining types of land uses present and changing, and developing indices for extensive and intensive disturbances.

Two indices are probably required to characterize land use status and changes: one reflecting areally extensive features (e.g., ranches), and the other to reflect intensive, point uses (e.g. , extractive activities).

Current vegetation-land use associations confirm differential penetration of land uses into ecosystems. Such relationships vary among regions and can be useful for historical reconstructions of global land use. For example, in South America, 40% of grazing is concentrated in xeromorphic woods/shrublands which occupy 25% of the land area; 25% of grazing is in wooded grasslands which occupy 15% of the area; and 7% of grazing is in tropical/ subtropical rainforests which occupy 35% of the area.

Information on extent and type of disturbance can also be deduced from historical map series showing progressions of anthropogenic features. One such attempt to characterize the distribution of human impacts is a landscape disturbance data set, developed by Matthews and compatible with the vegetation and land use data sets. The disturbance index, based on the prevalence of anthropogenic features, is based on Operational Navigation Charts (ONCs) dating mostly from the 1980s. These maps, designed for use by pilots, are at scale of 1:1 M and include a great deal of information on anthropogenic features ranging from urban areas and dense road networks to oases and isolated airstrips. Global coverage comprises about 250 map sheets. An advantage of the ONCs is that the first sheets were published in the 1960s and areas in transition are frequently updated.

The landscape intensity index, determined for each 1° cell, is a qualitative ranking from zero (no human structures at all) to five (maximum disturbance). Of the total global, ice-free land area, about 25% is ranked completely undisturbed (index = 0), and nearly 50% is ranked minimally disturbed (index = 1). A test case was carried out in which a historical series of the landscape intensity index was developed for a portion of the Brazilian Amazon. Based

on this study, it appears that two indices are probably required to characterize land use status and changes: one reflecting areally extensive features (e. g., ranches), and the other to reflect intensive, point uses (e. g., extractive activities).

Global Litter Pools

There are uncertainties in the background conditions against which land use changes are occurring and must be measured. An example of one of these background conditions is global litter production and litter pools which have implications for modeling carbon-related impacts of human disturbances. Historically, global estimates of litter production have ranged from 25-70 Pg C/yr (1 Pg = 1015 g), and estimates of the fine litter pool have ranged from ~50-200 Pg C/yr. (The atmosphere contains ~700 Pg C; ~600 Pg C are held in live vegetation; and ~1500 Pg C are in soils. Under steady state conditions, another 50-60 Pg C are exchanged annually between the atmosphere and biosphere through photosynthesis and respiration.)

Litter measurements from >1000 sites were collected. Global distributions of litter production were developed using the published measurements stratified by ecosystem and simple regression models of litter production and its proxy, net primary production. The series of ten distributions of litter production from the models and measurements reveal a range from 25-70 Pg C for litter production; measurement- and model-based estimates for the litter pool range from 40 to 200 Pg C. Similar global totals of litter production are commonly underlain by large discrepancies in geographic litter distributions. The measurement compilation lead to a survey of how well ecosystems are represented. Measurements of litter production represent ecosystems that cover ~60% of the Earth's ice-free surface; litter pool measurements represent ecosystems that cover only ~50% of the land surface. Climate-based litter production or pool models tend to overestimate values in arid regions which occupy ~30% of the land surface. The availability of systematic validation data for ecosystem/biochemistry models, such as the litter data presented here, will reduce uncertainties in fluxes and pools, and hopefully reduce uncertainties in identifying the "missing carbon sink" which is equal to a small imbalance in large fluxes and stores.

Reference

Matthews, E., Global vegetation and land use: New high-resolution data bases for climate studies. J. Climate and Applied Meteorology, 22:474-487.

Synthetic Aperture Radar Sensing of Vegetation Coupling SAR Observations to Carbon Flux Models

Kyle McDonald

Terrestrial Science Research Element
Jet Propulsion Laboratory
Pasadena, California

Synthetic aperture radar (SAR) can be used to study carbon flux in boreal forests by coupling SAR observations to ecosystem carbon flux models, thus allowing improved quantification of canopy transpiration and C02flux. The seasonal C02flux in boreal forests is characterized by a large increase at the start of the growing season in the Spring and a collapse into senescence in the Fall. The research thrust for using SAR is to:

1. quantify the landscape in terms of functional groups of species and their relative magnitude of flux,

2. define growing season length (thus bounding the period during which flux occurs), and

3. quantify short-term variations observed during the growing season.

The goal of this research is to use the backscatter signature to assist with landscape classification, determination of growing season length, and changes in vegetation water status as related to canopy C02flux in boreal forests. Benefits of using radar include the fact that it penetrates clouds, can be used at night, and is directly related to surface structure and dielectric properties.

Benefits of using radar include the fact that it penetrates clouds, can be used at night, and is directly related to surface structure and dielectric properties.

Radar imagery can provide inputs to process models and biosphere/atmosphere models by supplying ecological parameters such as classification of vegetation functional groups. Each functional group is characterized by a unique behavior in C02flux; this is the reason for partitioning the landscape into different classes. Radar is also useful in determining the timing of deciduous leaf onset and leaf drop, as well as the timing of soil and vegetation thaw and freeze.

The radar backscatter signature of a forest is determined by a combination of the geometric and dielectric properties of the vegetation and soil. Vegetation dielectric properties are related to fluid chemistry (sugars, electrolytes) and vegetation water status (water content, precipitation, dew, temperature, freeze/thaw state, xylem water potential, xylem flow). Soil dielectric properties are related to soil composition (textural components, organic materials) and soil water status (water content, freeze/thaw state, snow). The vegetation structural class is related to geometric properties of the canopy. Canopy phenology, variations of which define growing season, is determined by a combination of geometric and dielectric properties. Vegetation hydrologic status is related to the dielectric properties alone.

A C02flux estimate model is used to determine how the carbon flux varies for various species or functional groups within a landscape. It provides an estimate of C02flux in a region. Figure 8.1 shows the major controls on seasonal C02flux in boreal forests. Generally, growing season length is bound by vegetation freeze/thaw state in coniferous species and by leaf on/off in deciduous species. For coniferous species, radar data are used to bound the start of the growing season, when the vegetation thaws, and the end of the growing season, when the vegetation freezes. These estimates can be used to complement CO 2 flux models and improve their estimates of the total C02flux for a boreal landscape.

At the Bonanza Creek experimental forest near Fairbanks, Alaska, landscape classification by radar successfully identified areas of Balsam Poplar, White Spruce and Black Spruce. Large backscatter decreases (6 to 8 dB at L-band) were observed when the landscape underwent a transition from a thawed to a frozen state. Marked changes were also observed when conditions changed from flooded to unflooded. In this area of discontinuous permafrost, the timing of the freeze and thaw as detected by the radar help bound the growing season, and thus the C02flux.

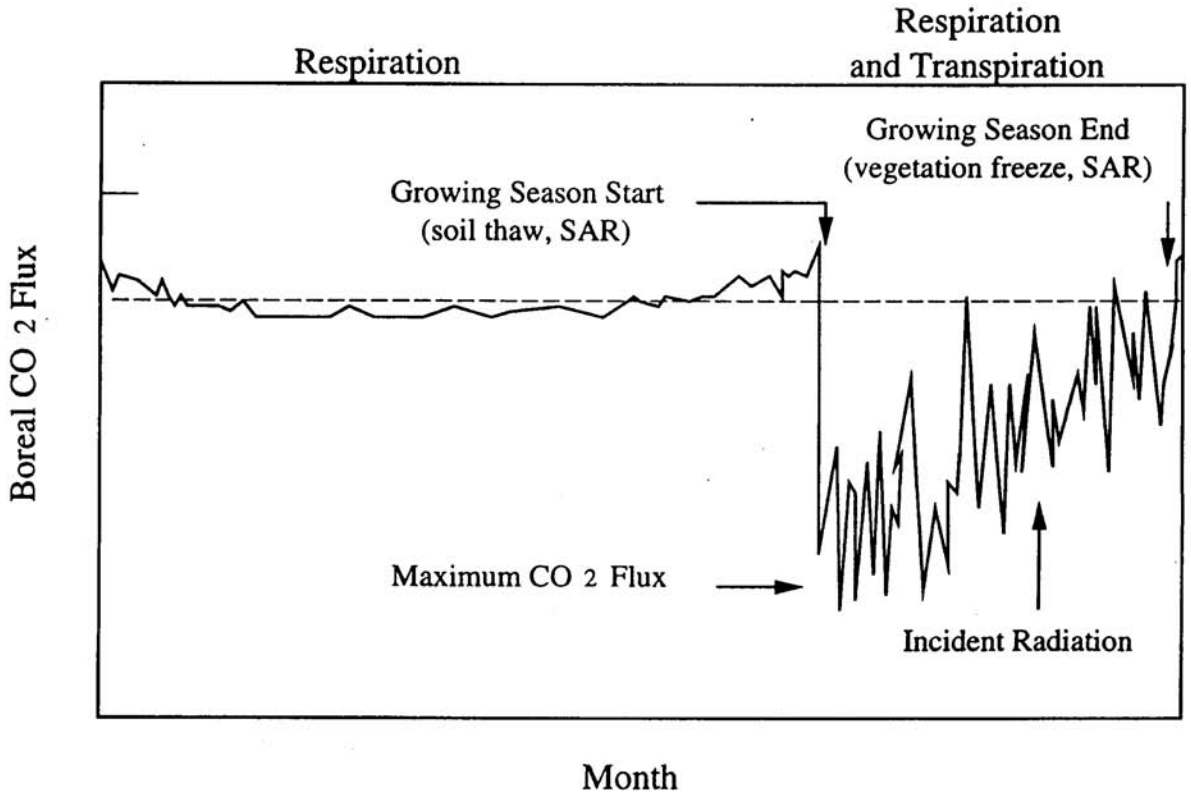

Figure 8.1
Major controls on seasonal CO2 flux in boreal forests. Growing season in coniferous tree species is bound by vegetation and soil freeze-thaw state in the Spring and Fall. Maximum CO2 flux varies with functional group while short-term variations in flux are driven by such parameters as incident radiation.

Quantification of C02flux with flux models revealed radical differences over just 3 days in Spring. Ground truth measurements verified this rapid shift. Temperature measurements made with thermisters in the soil and trees revealed that the thaw occurred in the soil, tree stems,

and needles and twigs at distinctly different times. With the soil thaw begins the period of respiration the start of carbon exchange.

In a regional extension of this approach, ERS multi-temporal transects collected by the ERS -1 spaceborne SAR from August through November across Alaska were used to determine when the landscape froze. This was accomplished by use of a change detection algorithm based upon the difference in backscatter between unfrozen and frozen conditions.

As part of a canopy water status monitoring study carried out in California, dielectric probes were placed in trees to monitor dielectric properties of different parts of the trunk to characterize temporal variance of the dielectric constant. Order of magnitude changes in trunk dielectric constant were found over 24 hour periods. At mid-day, during the period of maximum evapotranspirative demand, the trunk dielectric constant was very low, resembling that of frozen trees. At night, levels recovered, and approached the dielectric constant of pure water. These large diurnal changes in dielectric constant were also reflected as observable changes in radar backscatter.

In situ observations from the Boreal Ecosystem-Atmosphere Study (BOREAS) sites in Manitoba and Saskatchewan were recorded during long-term seasonal and short-term focused field studies to monitor dielectric properties and other variables. As an example, Figure 8.2 shows seasonal xylem water flux, vapor pressure deficit, air temperature, soil temperature profile, bole temperature, and bole dielectric constant, over an entire growing season for an old black spruce site in northern Manitoba.

There is normally a low point in the dielectric constant during the midday high evapotranspiration period, followed by recovery during the pre-dawn hours. However, it has also been observed that during nighttime periods when no mass transport of water occurs, there may still be a marked decrease in dielectric constant. This may be related to some chemical diffusion or mass diffusion laterally in the trunk related to electrolyte exchange and is reflected in the dielectric constant. However, the variation in dielectric constant from tree to tree may be significant, and this highlights the need to study a number of trees in a given stand. These variations could be related to the insertion depth of the probes in each tree or to differences in sizes between trees.

There is normally a low point in the dielectric constant during the midday high evapotranspiration period, followed by recovery during the pre-dawn hours.

In situ observations from the BOREAS sites were recorded during long-term seasonal and short-term focused field studies to monitor dielectric properties and other variables.

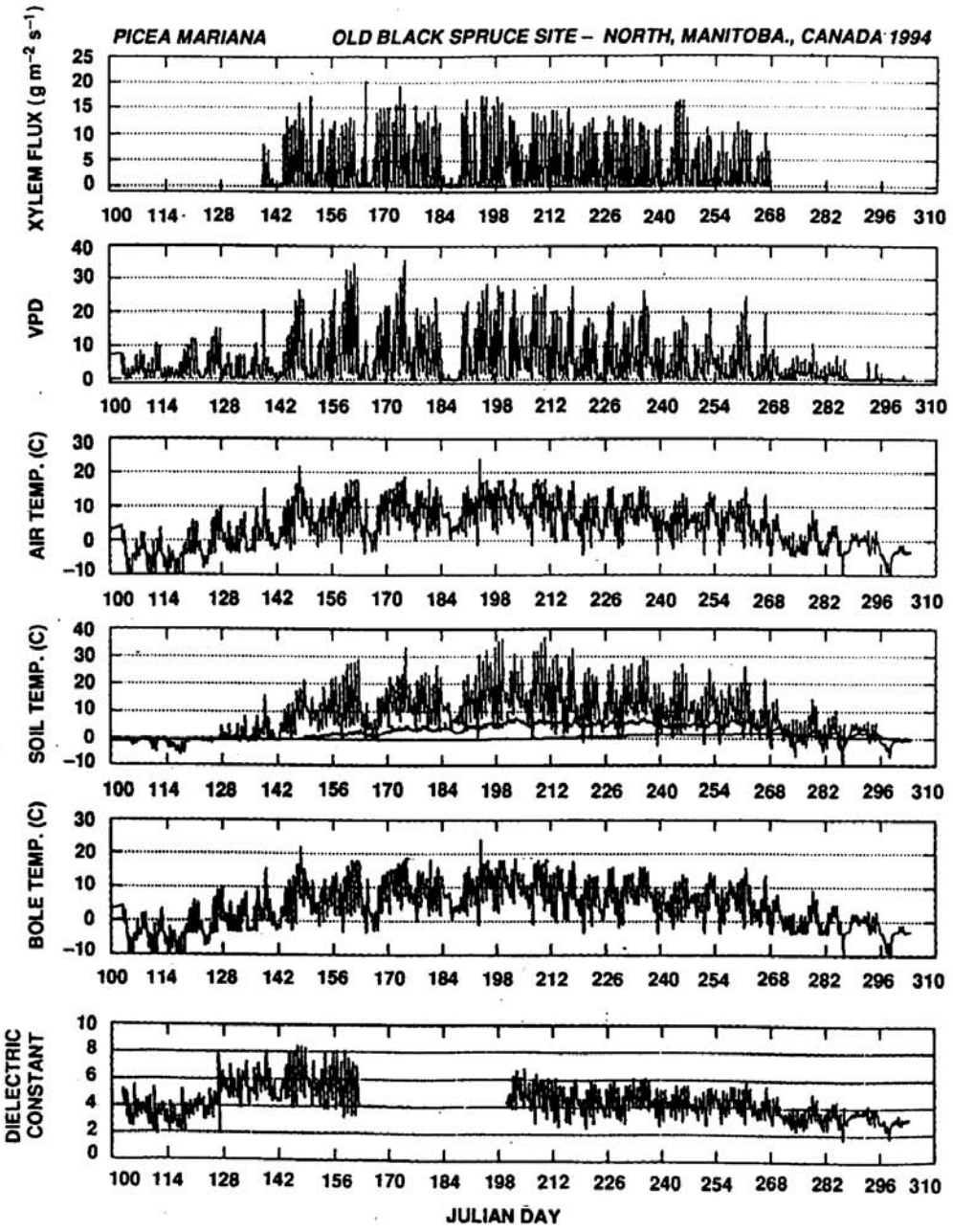

Figure 8.2

This data shows, in order from the top, (a) xylem water flux, (b) vapor pressure deficit, (c) air temperature, (d) soil temperature profile, (e) bole temperature, and (f) bole dielectric constant (real part, C-band) as observed in the NSA old black spruce stand from April 10 (DOY 100) through November 6 (DOY 310), 1994.

Effects of El Niño on Global Vegetative Patterns and Radiative Transfer Models

Ranga Myneni

Biospheric Sciences Branch, Laboratory for Terrestrial Physics
NASA/Goddard Space Flight Center
Greenbelt, Maryland

The FASIR NDVI data set described by Sietse Los was used by Myneni to estimate global gross primary production and to investigate the relationship with El Niño Southern Oscillation (ENSO) induced land precipitation anomalies, using the FASIR NDVI data as a surrogate for precipitation in arid and semi-arid regions of Australia, Africa, and South America. In addition, in an attempt to derive land cover classes consistent with radiative transfer theory, a simplified land cover classification scheme was developed which contained six global classes.

Gross primary production was estimated using the FASIR NDVI to represent Leaf Area Index and coupled with Photosynthetically Active Radiation data set. Assuming net primary production to be proportional to gross primary production (GPP), the results show that heterotrophic respiration and GPP respond similarly to climate, but with different magnitudes.

Significant variations in global GPP were observed for the 1982-1990 time period evaluated, including variations seemingly closely associated with the major 1982-1990 ENSO cycle sea surface temperature (SST) anomalies in the tropical Pacific. This then lead Myneni and co-workers to investigate the possible ENSO-NDVI relationship in order to determine the magnitude of natural variations resulting from SST anomalies on vegetation. There were four major ENSO cycle SST anomalies during the 1982-1990 time period; these two cooling events and two warming events are shown in Figure 9.1.

Spatially-continuous ENSO-precipitation anomalies were investigated for Africa, Australia, and South America using SST data and the GIMMS NDVI continental 7.6 km data for the 1982-1990 time period. The operating assumption is that NDVI data are highly correlated to precipitation data up to ~1000 mm/yr; thus this analysis is restricted to the arid and semi-arid zones of the 3 continents studied. Africa, Australia, and South America were selected for study as they are adjacent to the 5° N to 5° S from 90° W to 150° W SST area of the tropical Pacific (also referred to as the “Niño3” area).

NDVI anomalies were calculated by month from 1982 to 1990 at each 7.6 km pixel for the 3 continents and then correlated with the Niño3 SST anomalies for four 12-month periods during the SST anomalies; each of the 12-month periods corresponded to the Southern Hemisphere summer. The SST-NDVI anomalies were then summarized for the 4 ENSO cycle SST anomalies and represented where they occurred on the 3 continents, as shown in Figure 9.2, as darker areas.

Significant variations in global GPP were observed for the 1982-1990 time period evaluated, including variations seemingly closely associated with the major 1982-1990 ENSO cycle sea surface temperature anomalies in the tropical Pacific.

These results are indicative of the magnitude of impacts natural forcings can have on the global climate system through SST-related precipitation anomalies.

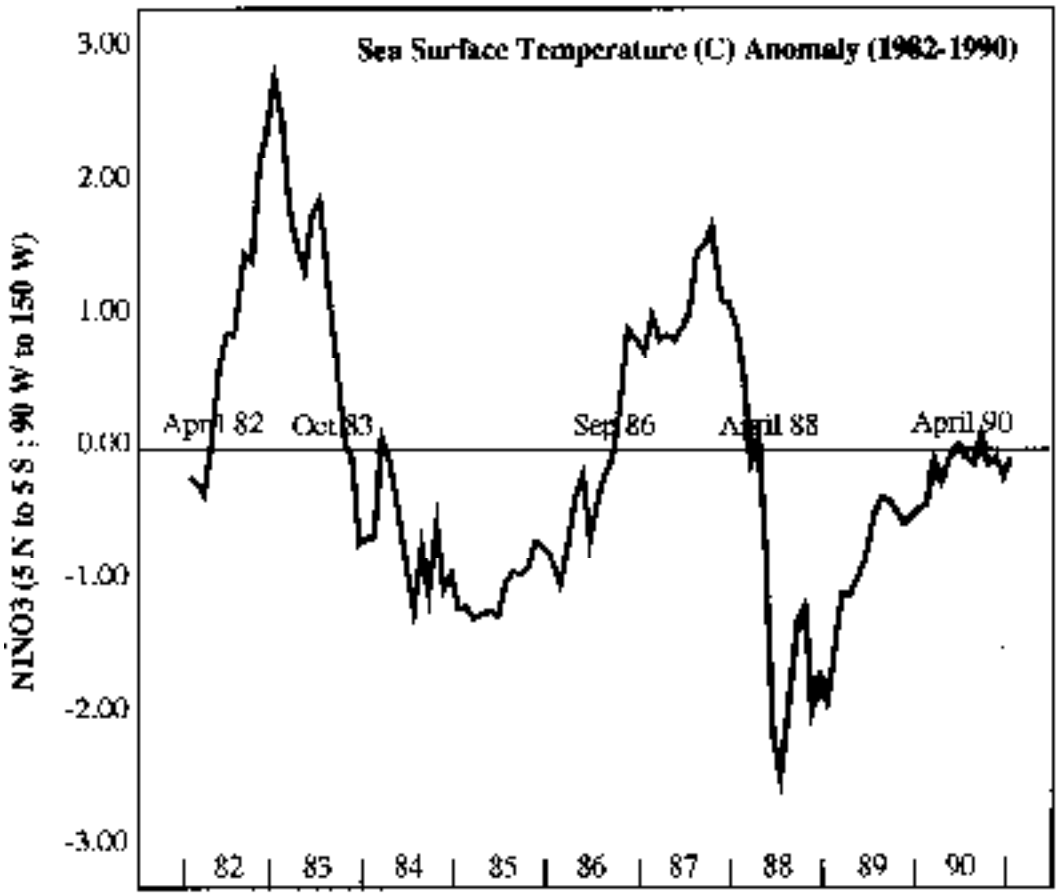

Figure 9.1
1980-1990 Nino3 SST anomalies

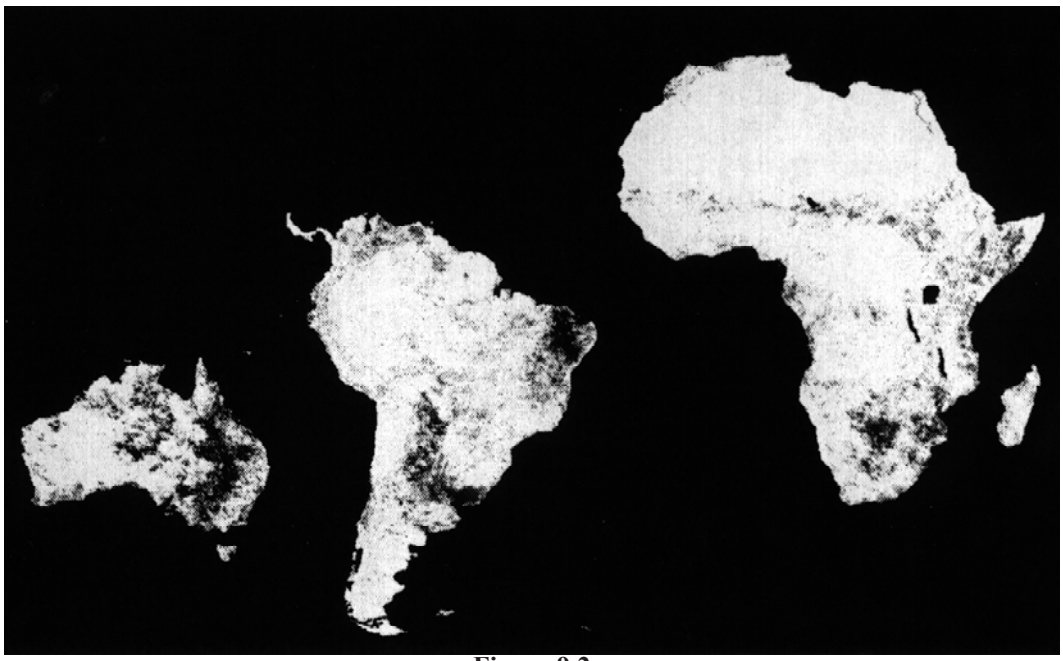

Figure 9.2
Summary of the areas of highest NDVI-SST anomaly occurrence for the 1982-1990 time period.

	ENSO Cycle Sea Surface Warming				ENSO Cycle Sea Surface Cooling			
Region	**May 1982 to** (+) ve NDVI Anomalies	**Apr 1983** (-) ve NDVI Anomalies	**Mar 1987 to** (+) ve NDVI Anomalies	**Feb 1988** (-) ve NDVI Anomalies	**Mar 1985 to** (+) ve NDVI Anomalies	**Feb 1986** (-) ve NDVI Anomalies	**May 1988 to** (+) ve NDVI Anomalies	**Apr 1989** (-) ve NDVI Anomalies
Northeastern Brazil	83,200	498,600	75,000	360,700	1,001,700	26,500	557,000	82,600
SE South America	485,000	144,300	406,200	285,200	996,600	105,200	16,500	1,665,800
Eastern Australia	1,000	1,743,500	106,400	499,100	173,100	744,400	201,300	549,900
Central Australia	62,500	39,700	67,800	313,400	16,800	670,400	256,800	307,300
East Africa and Horn	555,200	4,900	245,900	260,200	73,300	83,700	20,900	100,300
Southeastern Africa	34,800	391,000	137,500	170,900	373,900	8,600	72,900	25,700
Central S Africa	125,600	60,700	34,200	212,300	93,400	406,800	759,800	19,500

Table 9.1
Areas of Africa, Australia and South America where linked tropical Pacific SST and NDVI anomalies were determined from 1982 to 1990. The areas in this table are the areas where time series correlation coefficients are greater than /0.5/ and where the cumulative twelve month NDVI anomaly was greater that 0.3 or less than -0.3.

Six biome types are defined by the fact that structure is what effects radiative transfer.

Calculation of the areas affected by the NDVI-ENSO cycle anomalies revealed that sizable areas were affected by the 4 SST anomalies during the 1982-1990 time period (Table 9.1). These included areas of Northeastern Brazil which ranged in area from 360,000 to 1,000,000 km2; an area of 1,700,000 km2 in Southeastern South America which was strongly affected by the 1988 SST cooling; and an area of 1,700000 km 2 in Australia which was heavily affected in the 1982-1983 ENSO cycle SST warming. These results are indicative of the magnitude of impacts natural forcings can have on the global climate system through SST-related precipitation anomalies.

While the areas affected by the ENSO cycle precipitation anomalies always recover within several years following the anomaly, severe drought in Northeastern Brazil is reported to have caused the migration of up to 500,000 people into the Amazon Basin of Brazil. Once in Amazonia, these recent immigrants were responsible for increasing tropical deforestation. Thus, climatic variation in arid and semi-arid areas can indirectly influence human alteration of the natural environment.

This analysis will be extended from 1991-1995 when the processed satellite data become available. At the moment, there is a great deal of confusion in the ENSO cycle modeling community as none of the models can explain what is happening with ENSO cycle anomalies in the 1990s.

The land cover classification described by Myneni is based on radiative transfer theory. Six biome types are defined by the fact that structure is what effects radiation. The biomes are: grasses and cereal crops, broadleaf crops, shrub-desert, savanna, leaf forest, and needle forest. The characteristics of these biomes are as follows:

Biome 1 / grasses and cereal crops

* vertical and lateral homogeneity, vegetation ground cover ~100%
* background brightness intermediate
* erect leaf inclination

Biome 2 / shrublands

* lateral heterogeneity, low to intermediate ground cover of vegetation
* bright backgrounds
* small leaves

Biome 3 / broadleaf crops

* lateral heterogeneity minimal, vegetation ground cover ~80%
* dark backgrounds
* regular leaf spatial dispersion
* photosynthetically active, i. e., green, stems

Biome 4 / Savanna (grass cover with tree cover)

* 2 distinct vertical layers
* understory is grass (Biome 1)
* low ground cover of overstory trees
* canopy optics and structures differ accordingly

Biome 5 / Leaf forests

* vertical and lateral heterogeneity, ground cover 100%
* green understory, crown mutual shadowing, foliage clumping
* trunks/branches
* canopy structure and optics differ accordingly

Biome 6 / Needle forests

* needle clumping on shoots, severe shoot clumping
* dark vertical trunks, sparse green understory
* crown mutual shadowing

A combination of red, near infrared, and NDVI measurements from ±40 degrees can be used to spectrally separate the 6 proposed "radiative transfer biomes."

Natural Disturbance and Change in the Brazilian Amazon

Bruce Nelson

INPA - Instituto Nacional de Pesquisas da Amazonia
Manous, Brazil

Much of the rain which falls on the central and western Amazon is derived from water vapor recycled back to the atmosphere by forests in the eastern Amazon. Therefore, rainfall in the central Amazon could be reduced by deforestation in the eastern Amazon.

Nelson discussed documented and postulated effects of recent "modern" deforestation in the Brazilian Amazon region on rainfall downwind of deforested areas, on local nutrient stocks and on global greenhouse gas emissions. He also discussed naturally disturbed and naturally changing vegetation types which may create spectral background noise which impedes the detection and/or quantification of increased deciduousness caused by anthropogenically decreased rainfall and/or fire penetration as a result of logging activities.

Modern Deforestation

The Brazilian "Legal" Amazon is a collection of political units covering about five million square kilometers (km2). About 75-80% of this area was originally covered by Amazon forest and by closed-canopy woodland, the remainder being natural Amazon savannas or natural woodlands with discontinuous tree canopies ("cerrado").

American and Brazilian scientists have measured modern deforestation using wall-to -wall Landsat Thematic Mapper (TM) images. Estimates of the total area deforested as of 1991 range from about 320,000 to 426,000 km2. This includes all anthropogenic secondary forests spectrally recognizable as such (usually less than 25 years old) as well as dry bare soil, charred grasses or slash, and dry non-photosynthetic vegetation (NPV). These three materials dominate agricultural and pastoral landscapes in the dry season, when the images are acquired. Most of the modern deforestation is concentrated along the eastern and southern flanks of the Brazilian Amazon; very little has taken place in the central and western portions of the region.

These are at least three deleterious effects of modern deforestation:

1. Reduction in rainfall over forests in the central Amazon;

2. Loss of nutrients originally stored in biomass of the primary forest;

3. Amazonian contribution to the green house effect.

Reduction in rainfall

All water vapor which condenses over the Amazon basin is brought in from the Atlantic Ocean by easterly trade winds. Over half of the rain which falls on the forest is recycled back to the atmosphere, either by evaporation from wetted leaves and wood, or by root uptake followed by

leaf transpiration of water which reached the soil. This means that much of the rain which falls on the central and western Amazon is derived from water vapor which was recycled back to the atmosphere by forests in the eastern Amazon. It is therefore conceivable that rainfall in the central Amazon would be reduced if deforestation of the eastern Amazon is complete.

The effect of just a 15% decrease in rainfall near Manaus with proportionate lengthening of the dry season could be disastrous. A natural experiment exists to indicate what could happen. Rainfall near Manaus is about 2100 mm/year. Dense forest dominates the landscape, which is spectrally homogeneous on TM images, even over sandy soils. A single hectare of dense forest near Manaus supports about 220 different tree species. Species-abundance curves probably exceed 1000 tree species before leveling off.

Further east, near to Santarem or Obidos, rainfall is about 1750 mm/year. TM images of this region are spectrally more heterogeneous than the Manaus area, due to the extensive non-forest vegetation and semi-deciduous forests, particularly on sandy soils. On the clay soils, a homogeneous dense forest predominates but the diversity is much reduced: species-abundance curves flatten at about 200 tree species. Just six dominant species account for more than half of the trees in one study area.

With each cut and burn cycle, more of the original nutrient capital is lost to leaching. Thus the system eventually becomes depauperate with successively diminishing crop yields, the fallow cycles must be much longer, and the growth rate of the secondary forests is much diminished.

Whether or not this unsettling scenario comes to pass depends largely on the type of land cover which will predominate in the deforested eastern Amazon. Four to five year old secondary forests attain a leaf area index (LAI) of about 5.0, close to the 5.7 measured for dense forests near Manaus. These secondary forests will presumably be good at recycling rainfall by both evaporation and transpiration. Since the fallow stage occupies at least 65% of a swidden/fallow time cycle (i. e. just 2-3 years of crops followed by a minimum of 4-5 years fallow), most of the agricultural landscape will be in fallow stage with high LAI at any one point in time.

If on the other hand, pastoral landscapes dominate the eastern Amazon, one can expect decreased transpiration, decreased rainfall interception and resultant decreases in rainfall downwind. Though ungrazed grasses may obtain a respectable LAI, pastures in the Amazon are often overgrazed, there is much bare soil exposed by the trampling of cattle and the grasses largely die back during the dry season in some areas.

Loss of nutrients stored in biomass

Several studies have shown that most of the upland (terra firme) Amazon is covered by sandy or clay soils with very low nutrient stores, high acidity and low cation exchange capacity. (Cation exchange capacity is a measure of the capacity of soil to hold charged positive ions against negatively charged soil molecules or crystalline surfaces. Positively charged nutrient ions are available in the soil solution, and the soil holds them tight by electrostatic force and "exchanges" them with plant roots. The plant gives up a positively charged hydrogen ion [a proton] in exchange for positively charged nutrient ions, such as those of Mg or Ca. Organic material in soils and certain types of clay, such as montmorillonite, have a high cation exchange capacity and can therefore hold onto some dissolved mineral nutrients, keeping them from being leached away and making them available to plant roots for exchange. Weathered Amazon soils generally have a low cation exchange capacity, as they are composed largely of silica, kaolin clay, iron oxides and aluminum oxides, with little or no organic material.)

Near Manaus, about 90% of the calcium and 90% of the potassium stocks are held in the living biomass of the forest. Most of the remaining 10% is found in a rapidly decaying thin

layer of litter. These nutrients are made available to crops by cutting and burning the forest. Ashes from the burn also increase the pH of the soil, making phosphorous available to corn and manioc.

Within 2-3 years, the pH drops and the plot is abandoned, to be quickly overgrown by secondary forests species which can access phosphorous at low pH. By the time of abandonment, about 50% of the soluble nutrients have been lost from the system. The secondary forest is allowed to grow and a new cut and burn cycle can be started after five or more years. But with each cycle, more of the original nutrient capital is lost to leaching. Thus the system eventually becomes depauperate with successively diminishing crop yields, the fallow cycles must be much longer, and the growth rate of the secondary forests is much diminished. Some sites east of Belem have undergone about ten cycles of slash and burn, but these are located over calcium carbonate deposits. Nonetheless, they have very slow secondary forest growth rates during the fallow stage.

Amazonian contribution to the global increase in the greenhouse effect

According to a review conducted by Philip Fearnside, Brazil contributes about 5% of the total global anthropogenic greenhouse gas emissions. Most of this (4 of the 5%) is due to deforestation of the Amazon, the remainder being caused by burning of fossil fuels in that country. Another way of putting the Amazonian contribution in perspective is to state that about one decade of fossil fuel burning (1975-1985) worldwide is equivalent to complete combustion of the entire Amazon forest, insofar as the production of carbon dioxide is concerned.

Carbon dioxide is removed from the atmosphere by secondary forests in the "deforested" parts of the Amazon. According to recent measurements by the University of New Hampshire, young secondary forests cover fully 30% of the area deforested by non -indigenous people in the Brazilian Amazon. No quantification has yet been done of the role of these secondary forests in partially reversing the effects of deforestation, by absorbing carbon dioxide.

Naturally Disturbed And Naturally Changing Vegetation Types

Natural changes in the Amazon are far more subtle than the deforestation caused by the modern human activities of non-indigenous people. (Included among these "natural" changes are the deleterious effects of some land-use practices of indigenous peoples.) These natural changes have also occurred over a much longer time period. Their environmental consequences are less drastic than the deforestation by modern man, but they are nonetheless very extensive in area, and are certainly very interesting.

These natural changes and disturbances were detected in the same satellite images used for a study by INPE (Brazil's Space Institute) of Amazon deforestation caused by ranchers, agriculturalists and loggers. The study utilized Landsat Thematic Mapper (TM) images which are color composites of three "digital photographs," one sensitive to the red portion of visible light and the other two sensitive to different infrared wavelength bands. The images were studied at a scale of 1:250,000. About 140 different images were studied, each measuring 185 km on a side. The images cover the 4,000,000 km 2 of landscape originally covered by forest in the Bra zilian Legal Amazon.

Natural changes in the Amazon are far more subtle than the deforestation caused by the modern human activities of non-indigenous people.

The natural change features detected are:

1. Forests which have undergone fire penetration (whether of anthropogenic or natural origin). Most Amazon forests are not expected to burn unless they are first cut and allowed to dry out, because of the high water content of the biomass and dampness of the litter layer. Tens of thousands of km2 of standing forest were burned on periodically flooded forests over sandy soil during the 1925 drought. At least 1,500 km 2 of terra firme forest on clay soils near Santarem burned during the 1983 drought, though in that case the burning was catalyzed by mechanized selective logging, which leads to accumulation of dry combustible slash.

2. Fields of parabolic dunes reactivated at different times in the past, probably in conjunction with fires. These are found along the lower course of the Rio Branco in the states of Roraima and Amazonas. The total area affected by aeolian reactivation in the last few thousand years is very large, but the two dune fields most recently reactivated (tens to hundreds of years ago?) cover just 1,500 km2.

Most Amazon forests are not expected to burn unless they are first cut and allowed to dry out, because of the high water content of the biomass and dampness of the litter layer.

3. Sandstone table mountains, also susceptible to fires during very dry years. These cover a few hundreds of km 2 in the northern part of the Brazilian Amazon.

4. Granitic and laterite (canga) hilltops, also susceptible to fire penetration during dry years. The most extensive example is occupied by a fern-savanna fire climax (southern braken fern) and is burned frequently by Yanomami Indians. The fern savannas cover 600 km2.

5. Mortality of “terra firme “ forest caused by ponding and waterlogging of very small depressions, during a year of unusually high rainfall. This affected 2 to 2.5% of the forest in one area north of Manaus in 1989.

6. Synchronous mortality of forests dominated by arborescent bamboos. These sites may be susceptible to fire penetration if mortality coincides with a very strong dry season. Bamboo dominated forests which undergo synchronous mortality cover 92,000 km 2 in the SW Brazilian Amazon, and over 122,000 km2 when Peruvian and Bolivian forests are included.

7. Expansion of bamboo forest patches either by successful competition or by allelopathic means. This is indicated by the rounded edges of the bamboo/mixed-forest contact line as seen on satellite images.

8. Vine forests, which are a mix of sparse tall forest trees interspersed with dense mats of heavy woody vines; vines topple the trees and keep the forest in a late successional stage floristically. Vine forests cover about 100,000 km2 in the eastern Amazon, and additional areas in the southwestern state of Acre, as well as Bolivia.

9. Extensive patches of forest dominated by babassu palm. The patches have a spatial pattern suggesting that they occupy sites of pre-modern swidden agriculture (slash and burn). The babassu palm is know to increase its numbers when sites are repeatedly burned, but can also maintain these high densities once the fires are eliminated. Spectrally recognizable dark palm forests cover at least 20,000 km2 in the SE Brazilian Amazon.

10. Dozens of circular patches 2-13 km in diameter, in the upper Xingu Basin, which are apparent fire scars and cover over 1,000 km2.

11. Blowdowns caused by convective winds. These cover a total of 900 km2, based on summing the areas of 330 features over 30 hectares each in size. The largest blowdowns exceed 2,000 hectares each in size. Blowdowns are concentrated along a zone traversing the Amazon from southern Venezuela to northern Bolivia.

Discussion On Modern Deforestation

As of 1985/86, according to the latest figures of Tucker and colleagues, about 320-330,000 km2 of the Amazon forest had been deforested, that is, converted to urban areas, pastures, crops, or young secondary forests. This is less than 10% of the original forest present in the region. Though 10% seems small, this has occurred over a very short time. Furthermore, wherever good roads provide access, the local deforestation percentage is much higher than 10%. Most of the untouched parts of the Amazon are economically inaccessible to loggers, ranchers and farmers. As such, Nelson remarked, for a rancher or logger, most of Amazonia might as well be lunar real estate. So the 10% figure is misleading. It does not reflect a national conservation policy, but rather the difficulty, so far, of opening up remote areas with good roads. It is true, however, that some government policies which encouraged deforestation, including the building of roads into remote areas, are no longer being implemented. This is due to both domestic and international pressure during the late 1980s and early 1990s.

Some government policies which encouraged deforestation, including the building of roads into remote areas, are no longer being implemented. This is due to both domestic and international pressure during the late 1980s and early 1990s.

Discussion on Natural Disturbances

Natural disturbances such as fires, drought and mortality from waterlogging can be very important catastrophic setbacks to forest succession. They may cause most primary forests to be in a state of carbon absorption for long periods, intercalated with brief periods of net carbon release. Thus, eddy correlation measures may artificially suggest that the Amazon forest is a carbon sink, since these measurements are made over short time periods.

Even studies which have long time lines of data are subject to misinterpretation if they ignore the role of catastrophic drought. A study by Philips and Gentry published in Science, 18 Feb. 1994, showed an increase in turnover rates of tree species in forests throughout the world's tropics, occurring in the 1980s. This may simply be the effect of increased mortality and increased subsequent recruitment after the drought of 1982/83. Data from Borneo and from Barro Colorado Island in Panama support this view. Philips and Gentry suggested that the increase in turnover was the result of carbon fertilization from increased concentrations of atmospheric carbon dioxide.

CO2 and Temperature Effects on Grassland Ecosystems Land Use Practices and Mitigation Strategies

Ivan Nijs

University of Antwerp, Department of Biology
Laboratory of Plant Ecology
Wilrijk, Belgium

Leaf thickness increased by CO2 enrichment could reduce the dose of UV-B plants receive in sensitive areas. Conversely, ecosystems exposed to higher temperatures typically yield thinner leaves, which could make them more susceptible to UV-B.

In the context of global climatic change, Nijs and colleagues have undertaken a series of experiments aimed at increasing understanding of the effects of increased carbon dioxide and temperature on grassland vegetation. Goals include a better assessment of the risks and opportunities for agricultural production as well as improved knowledge of ecosystem functioning. Their focus is on grasslands in natural and agroecosystems because grasslands make up 50% of agricultural land in Belgium, constitute a major carbon pool of the global carbon cycle, are a stabilizing factor in soils, and are a major pool of biodiversity. The scale of focus in this work ranges from the sub-cellular to the ecosystem level. The work is primarily experimental but also includes some modeling.

Overview of Ongoing and Past Research

The first approach, in 1986, was to set up ecosystems in enclosed sunlit chambers and use these to estimate carbon balance over minutes, days, weeks, seasons, and years. The enclosures were contained in a greenhouse. Control temperatures were designed to recreate ambient conditions in Antwerp and CO2 levels were ambient or enriched. A switching system enabled the researchers to sample the different chambers. They obtained daily profiles of carbon flux density and CO2 exchange rates, and evapotranspiration rates for the whole system. Drought stress experiments were also being conducted to see if plants grown in elevated CO2 conditions are more susceptible to prolonged drought conditions.

In a more recent system, built in 1991, the simulations of climatic change involve exposing test plots to:

* 350 ppm CO2 and 700 ppm CO2
* ambient air temperature and +4° C
* natural illumination (includes UV-A and UV-B)

Criteria for the exposure system include:

* reproduction of field temperature
* supply ambient or CO2-enriched air
* large area of plant material sunlit
* UV transmissible
* low inside-treatment variability
* low cost

In this system, six grass species/cultivars were being studied for effects on:

* dry matter production and content
* leaf area index
* dry matter allocation (distribution over roots, stubble, leaves, and stems)
* canopy architecture (height, vertical distribution of leaf area)
* tiller development
* light profile in the canopy
* leaf transmission
* leaf area to leaf mass ratio
* leaf assimilation (light, CO2, acclimation)
* stomatal functioning

Free air CO2 enrichment experiments (FACE) are now gaining in popularity over enclosed systems. In such a system, emission points for CO2-enriched air flood the vegetation under study. There are grassland FACE experiments underway (Zürich, Switzerland), but one key problem with FACE is that air temperature cannot be controlled. In a newly developed technique at the University of Antwerp, infrared lamps are used to raise ambient canopy temperatures. They can then be compared to controls using thermocouples shielded from sunlight, yielding a 2.5°C rise. Infrared thermometers would be even better.

A new project will study interactions between UV-B rise due to ozone depletion, CO2 enrichment, and temperature rise, in an effort to uncover synergisms that might emerge. One possible interaction mechanism is that leaf thickness increased by CO2 enrichment could alter the dose of UV-B plants receive in sensitive areas. The thickening caused by CO2 enhancement is either an increase in density or in number of cell layers. Conversely, ecosystems exposed to higher temperatures typically yield thinner leaves, which could make them more susceptible to UV-B.

A key question in recent experiments was "Is N availability a limiting factor for the response to CO2?" This is relevant because N inputs are high in agriculture and low in natural systems. The answer, from these experiments on cool-temperate grasses, may have relevance to current European Union thinking that there is too much land in agricultural use and that this is causing undue environmental stress (such as increase in environmental nitrates). It could influence policy towards altering heavily used agricultural land into more extensively managed lands, depending on their future CO2 response.

Further, there are questions about how complex the ecosystem needs to be in order to get accurate results. Plants grow naturally in complex stands so it doesn't make sense to eliminate competition in the experiments. Also, plants' reactions may change with different neighbors. A series of experiments focusing on two species interactions is presently being conducted at the University of Antwerp (UA) to derive general principles on how CO2 and temperature influence resource acquisition (nutrients, light, space, and water). First results show that modification of resource capture and its dynamics can potentially explain shifts in species composition within grasslands.

Experiments on temporal variability reveal that CO2 and temperature effects change during the growing season. In early Spring, for example, high temperature increased productivity; this response then reversed in summer when it severely depressed productivity.

Results and Their Implications

Within a group of six species, examined at UA in a screening experiment, the response to either CO2 or temperature was generally the same in sign (whether positive or negative) for a great number of plant or stand features. This demonstrates that there is a functional type for cool-temperate species, in the sense that they all respond in basically the same way to the stimuli. Figure 11.1 summarizes the response of the major characteristics to elevated CO2 and elevated temperature. For many of those characteristics, CO2 and temperature effects were opposite.

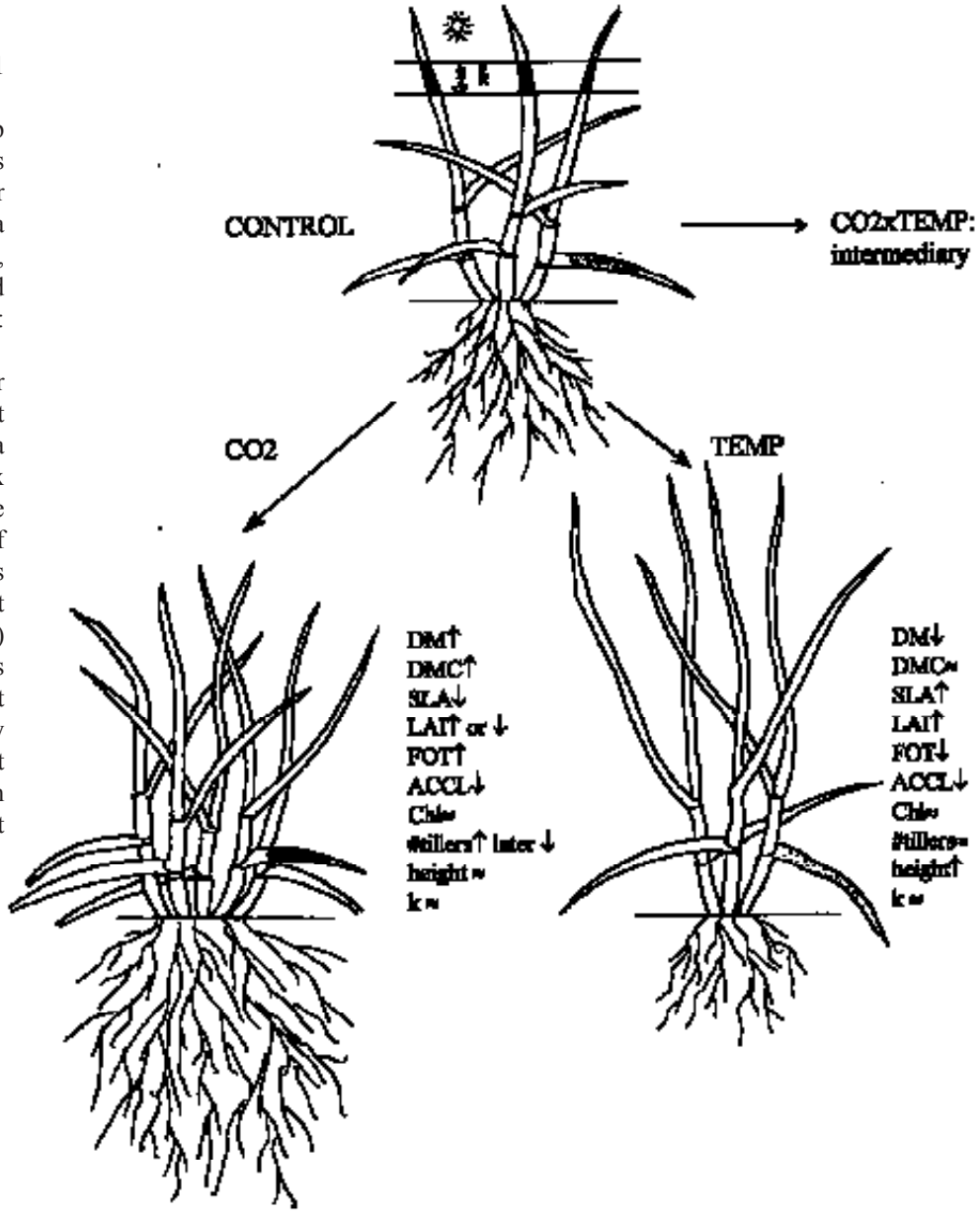

Figure 11.1

Summarized response of a group of six cool-temper ate grasses to elevated CO2, increased air temperature, or the simulta neous combination of both, on a number of leaf and stand characteristics:

DM Dry Matter
DMC Dry Matter Content
SLA Specific Leaf Area
LAI Leaf Area Index
***FOT** Assimilation Rate
ACCL Acclimation of Photosynthesis
Chl Chlorophyll Content (Weight Basis)
 # tillers Number of Tillers (Shoots) Per Plant
height Maximum Canopy Height
k Canopy Extinction Coefficient

Experiments on temporal variability reveal that CO2 and temperature effects change during the growing season. In early Spring, for example, high temperature increased productivity; this response then reversed in summer when it severely depressed productivity. This emphasizes the need to examine results over the full growing season.

CO2 and temperature both affect assimilation capacity which is in turn highly determined by the leaf nitrogen status. Examining the relationship between photosynthetic productivity and nitrogen provides a connection to a number of issues, such as eutrophication, excess fertilization, atmospheric nitrogen deposition, and the control function of nitrogen in the plant. It further allows an assessment of whether limited nutrient availability can reduce the response to CO2.

The procedure to approach assimilation used here was based on a separation of the biophysical and biochemical components of photosynthesis. This was achieved by combining several models including the model of Farquhar (1980) and the model of Ball (1987). This allows an investigation of whether the photosynthesis-nitrogen relationship is universal for different species and different growth conditions which would allow the modeling of carbon uptake as a function of the nitrogen status of the ecosystem.

Both long-term exposure to elevated CO2 or increased air temperature reduced the photosynthetic efficiency of leaf nitrogen.

Results from several species show that this was not the case; both long-term exposure to elevated CO2 or increased air temperature reduced the photosynthetic efficiency of leaf nitrogen. The actual leaf nitrogen efficiency in elevated CO2 increased though, due to the direct CO2 effect, which compensated for the long-term acclimation. It was also shown that exposure to the global change treatments used here induced an internal reorganization within the leaf in the sense that the investment of nitrogen in different processes was altered to maintain optimal functioning. Prior to further extrapolations, the model results were compared with independently measured data, which assured a sufficient predictive capability.

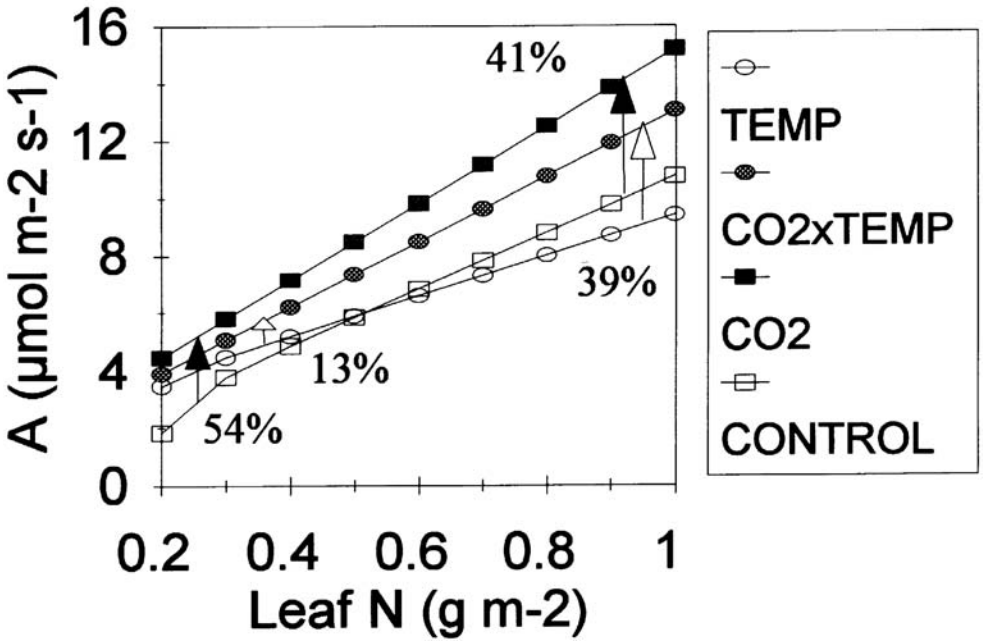

Figure 11.2

Leaf assimilation rate as a function of leaf nitrogen content in perennial rye grass grown in ambient conditions (Control), elevated CO2 levels (CO2), increased temperature (Temp), or the combination of elevated CO2 and increased temperature (CO 2x Temp). Model responses for plants grown in optimal to deficient N supply. Arrows indicate % change due to treatments.

Subsequent model results provided an answer to the principle question of this project, namely, whether nutrient deficient ecosystems will still be able to respond to elevated CO2. Figure 11.2 shows that the model predicts no attenuation in the response to CO2 when the leaf nutrient status deteriorates, even up to the point of complete N-deficiency. This result was confirmed by harvests of both above-ground and total stand dry matter in different species. The response to warming, on the other hand, does depend on nutrient availability. In a nutrient-rich environment, the effect of +4°C is predominantly negative, but this is reversed to a positive effect when the N status of the leaf becomes more deficient. Long-term modeling from other studies (Parton, 1995) suggests that some of the effects found here would decline, but not disappear, over time.

The experimental and modeling results produced by this study provide an underpinning for agricultural management policy and land use planning. They predict consequences of certain land use decisions, particularly with respect to fertilizer inputs. Damage from high temperature, for example, can predominantly be expected in agroecosystems while natural or extensively managed ecosystems can better withstand future temperature increases which will make them become relatively more important as carbon reservoirs. There is little potential for manipulation in this however as a lower N input into grasslands would reduce productivity more than it would alleviate the temperature stress.

The results from this study of grassland ecosystems suggest that non-CO2 greenhouse gas emissions should be preferentially reduced. While the direct fertilization effects of CO2 will compensate for its negative warming effects on productivity, methane, NOX and CFCs have no such compensating effects.

Concerning the seasonal dynamics of productivity, the results indicate that the difference between Spring and Summer productivity will increase in a future climate. In addition to this, an increased sensitivity to extreme weather events (e. g. high temperatures) is expected to further exacerbate this trend in seasonal dynamics.

With respect to greenhouse gas reduction strategies, the results from this study of grass land ecosystems suggest that non-CO2 greenhouse gas emissions should be preferentially reduced. While the direct fertilization effects of CO2 will compensate for its negative warming effects on productivity, methane, NOX and CFCs have no such compensating effects. A full analysis of this however, will have to include a similar investigation for the other major ecosystem types of the world, as well as the specific emission reduction costs of each of these atmospheric components.

Assessing Impacts of Land Use Changes on Ecosystem Properties with In Situ Methods Compared with Remote Sensing

Dennis Ojima

Natural Resources Ecology Laboratory
Colorado State University
Fort Collins, Colorado

Work on a variety of spatial scales is needed to analyze structural and functional properties of ecosystems and detect change. The methodologies involve field studies at the meter scale or less, use of models, remote sensing, and spatial and temporal analyses. Research begins at the single plant level and continues up to the patch scale to understand biogeochemical and physiological change. At the watershed to landscape level, influences on soil properties, biogeochemical cycles, distribution of plants, and trace gas fluxes be come relevant. Patch scale and regional scale changes in ecosystem properties can then be incorporated into couplings with atmospheric models, and, at the global scale, issues such as net primary productivity (NPP) are relevant to a variety of models.

Work on a variety of spatial scales is needed to analyze structural and functional properties of ecosystems and detect change.

A series of databases is developed into a modeling system for vegetation, soils, elevation, etc., and incorporated in nested way coupled through a series of models (see Figure 12.1). This information can then be useful in dealing with proximate causes of change that influence gain or loss of ecosystem or biome types. For example, it can provide information for reforestation or conservation research programs, such as those that return agricultural lands to grasslands.

Natural succession and change need to be incorporated in assessment frameworks as well. Coupling of ecosystem processes related to change includes deposition and inputs of nitrogen (N), changes in acidity (pH) of rainfall, other inputs to the system, and biogeochemical and hydrological cycles of the ecosystem. Changing land cover modifies a number of ecosystem properties.

Land Use Change Impacts:

* Land surface impacts, such as changes in albedo and roughness
* Hydrological impacts like rerouting of water, depletion of aquifers, erosion losses
* Trace gas fluxes (N2O, CH4, aerosols, biogeochemistry altered)
* Biological impacts (plant competition changes, soil carbon potentially lost, microbial populations altered, nutrient cycling patterns altered, biodiversity issues, habitat fragmentation, latent and sensible heat fluxes)

An example of some of these changes in ecosystem properties occurred in Texas with the expansion of mesquite at the time of European settlement. A succession from subtropical grassland areas to open savanna resulted from alterations in the grazing pattern and subsequent fire regime modification. This led to a number of changes in the ecosystem involving allocation of carbon, structure, albedo, energy balance, and fertility (mesquite is a nitrogen fixer so islands of fertility developed). Nitrogen trace gas fluxes were greatly altered; there were low N fluxes compared to tree and woodland areas.

Pristine grassland areas worldwide, especially in Asia, are changing from species-rich ecosystems with the ability to respond to changes to monocultural systems characterized by in creases in soil respiration, erosional losses, and changes in secondary productivity related to domestic animals.

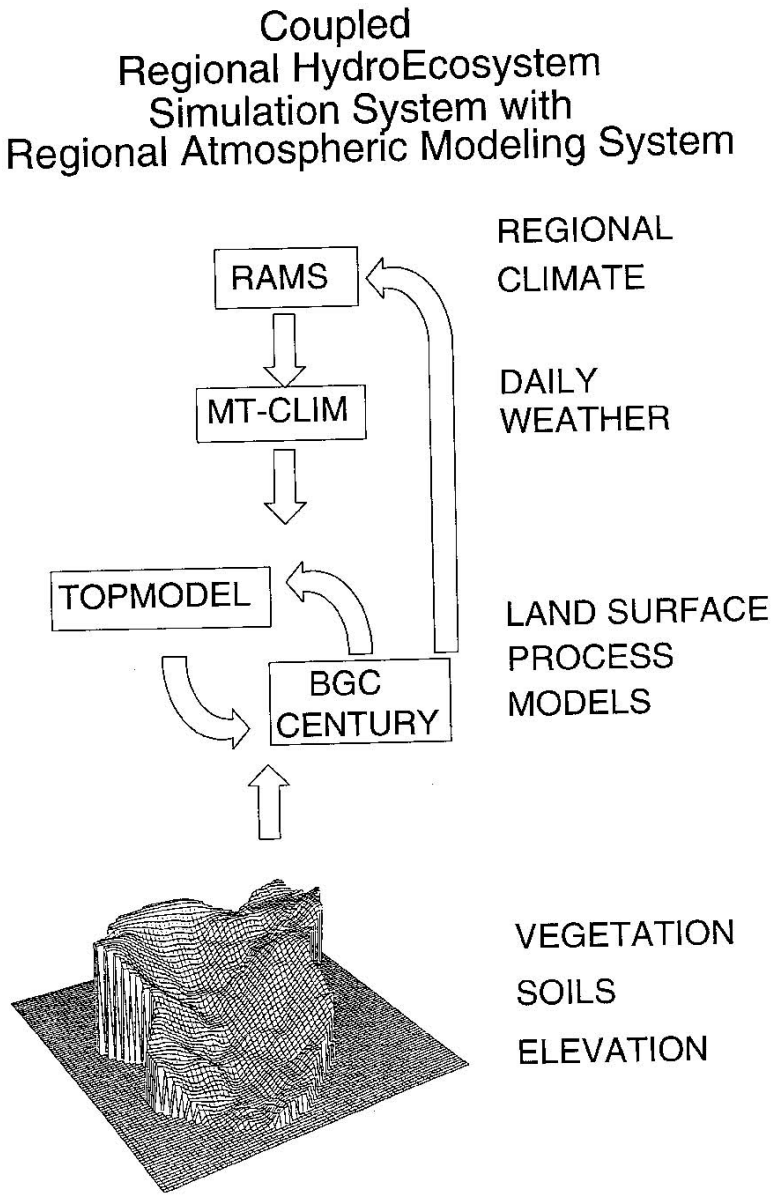

Figure 12.1

Integrated framework to link climate, soil and vegetation processes.

Structural change can also have a great influence on hydrological cycles. Without forest cover, rainfall over the annual cycle is reduced by approximately 60%. Other hydrological effects include albedo changes, evapotranspiration changes, increased runoff, erosion, and changes in the amount of water available in the region.

An illustration of dramatic change brought about by land cover change occurs on the Oklahoma panhandle (Roger Pielke, personal communication). Under current land use practices, native rangeland vegetation has been largely replaced with irrigated land, urban area, and dryland agriculture. Even in this semi-arid system, humans have impacted land cover quite significantly. Figure 12.2a shows a native vegetation land surface parameterization for a 70 km x 100 km region. The simulated results show the pattern of clouds and convective storm activity under the native vegetation regime. Figure 12.2b repeats the simulation but with current land cover conditions for the same date. The dramatic build up in mesoscale climate activity in the region is apparent. Observed meteorological results were very similar to modeled change.

It is hypothesized that the change in land cover is responsible for creating the observed significant variation in natural weather patterns with dramatic implications. If this hypothesis is correct, then changes in landscape patterns over the past 100 years have caused meso-meteorological effects, and may have contributed to altered climatology of the region. In addition to these rapid changes, there are biogeochemical changes in allocation patterns of nutrients, and other less obvious changes.

Pristine grassland areas worldwide, especially in Asia, are changing from species-rich ecosystems with the ability to respond to changes to monocultural systems characterized by increases in soil respiration, erosional losses, and changes in secondary productivity related to domestic animals. Intensity and time of grazing impact semi-arid areas in a number of ways. Changes in fire regime cause major changes in the structure of an ecosystem, as well as its biogeochemical and hydrological cycle.

The CENTURY model can be used to study the impacts of climate change on ecosystem processes. Figure 12.3 demonstrates how the model integrates a water budget model, a grass/crop model, a soil organic model, and a forest model. Management practices such as irrigation, harvesting variables, input of plant residues, tillage, nutrient enhancement, modification of fertilizer rates, etc., are incorporated into the CENTURY model as well, and manipulations can reflect common land use changes.

It is hypothesized that the change in land cover is responsible for creating the observed significant variation in natural weather patterns with dramatic implications.

The CENTURY model can be regionalized by parameterizing, validating for the site-specific parameterization, and incorporating regional information including remote sensing data. Remote sensing data is used as input but also to look at validation of model output for the region by looking at changes in NDVI or greenness for the growing season. This is a critical factor in assessment. It is also necessary to track results through several years to capture interannual variability.

It is possible to predict net primary productivity (NPP) and biomass against NDVI signa tures using AVHRR data. Using regional aggregation satellite data to provide NDVI and biomass provides a way to look at large grassland areas, and bring results up to the regional scale.

Microbial processes can be studied at the soil level and aggregated up to the patch and global levels. At the soil surface there are microbial changes such as growth of blue-green f-fixing algae after a burn. These are a nitrogen-fixing set of organisms that replace N into the system. After burning, there is an enhancement of N inputs through this process.

Chamber techniques are being used to look at fluxes of trace gases over a 15-year observation period. Tower techniques are being used to study CO2 and energy at the FIFE site (Manhattan, Kansas) and ammonia fluxes in burned areas of tall grass prairie. Smaller towers are being used to study methane fluxes in the boreal forest.

There has been a dramatic change in methane uptake between areas of native grassland and current wheat crop systems. The resulting reduction in the sink strength can contribute to the increase in methane in the atmosphere.

Management practices such as irrigation, harvesting variables, input of plant residues, tillage, nutrient enhancement, modification of fertilizer rates, etc., are incorporated into the CENTURY model, and manipulations can reflect common land use changes.

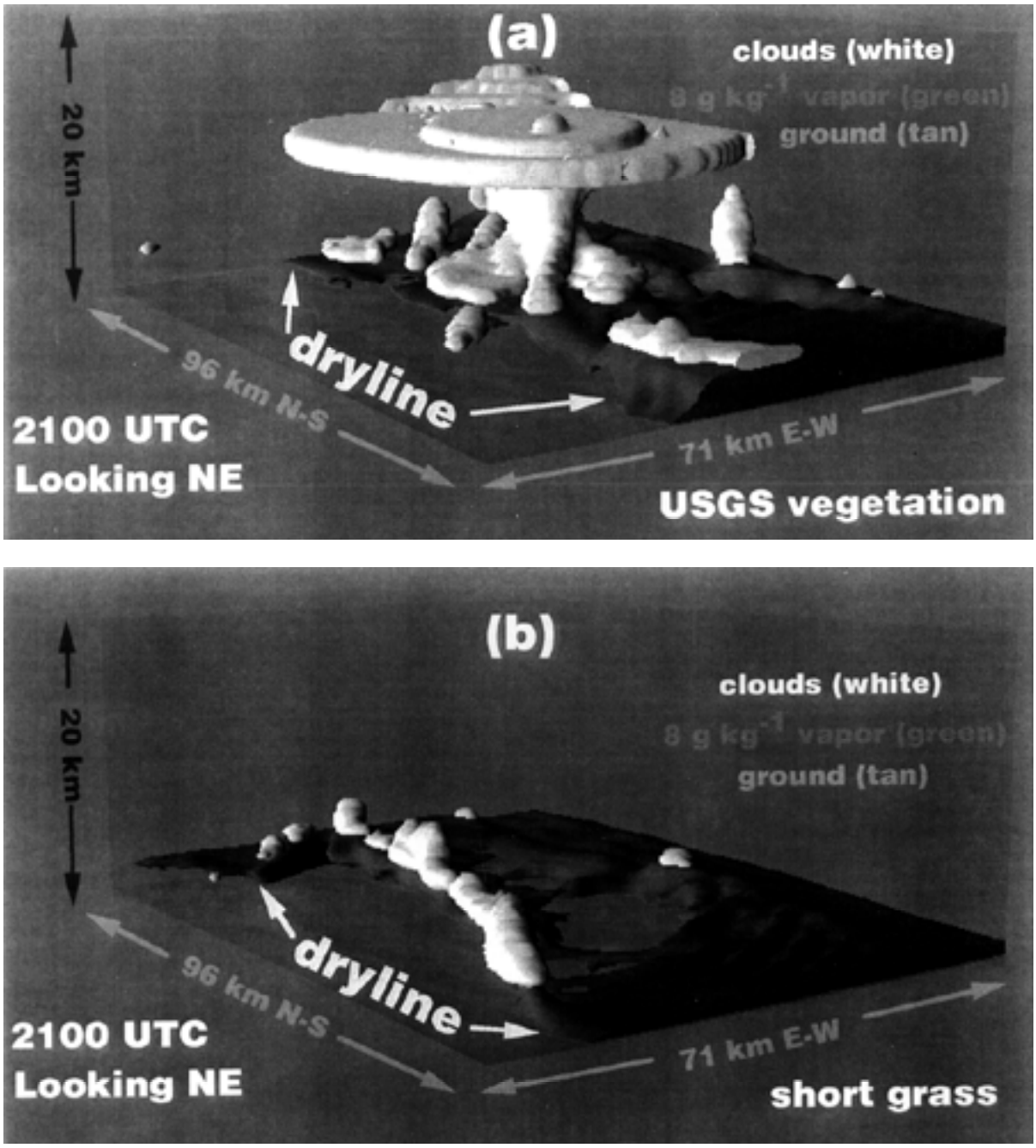

Figure 12.2

Model output cloud and vapor mixing ratio field on grid 4 at 2100 UTC on 15 May 1991. Figure (a) shows convective storm development with "actual" land cover derived from USGS data. Figure (b) shows convective storm development treating the land surface as shortgrass steppe. (from Pielke, R. A., T. J. Lee, J. H. Copeland, J. L. Eastman, C. L. Ziegler, and C. A. Finley, 1995. "Use of USGS-provided data to improve weather and climate simulations," Ecological Applications, in press.)

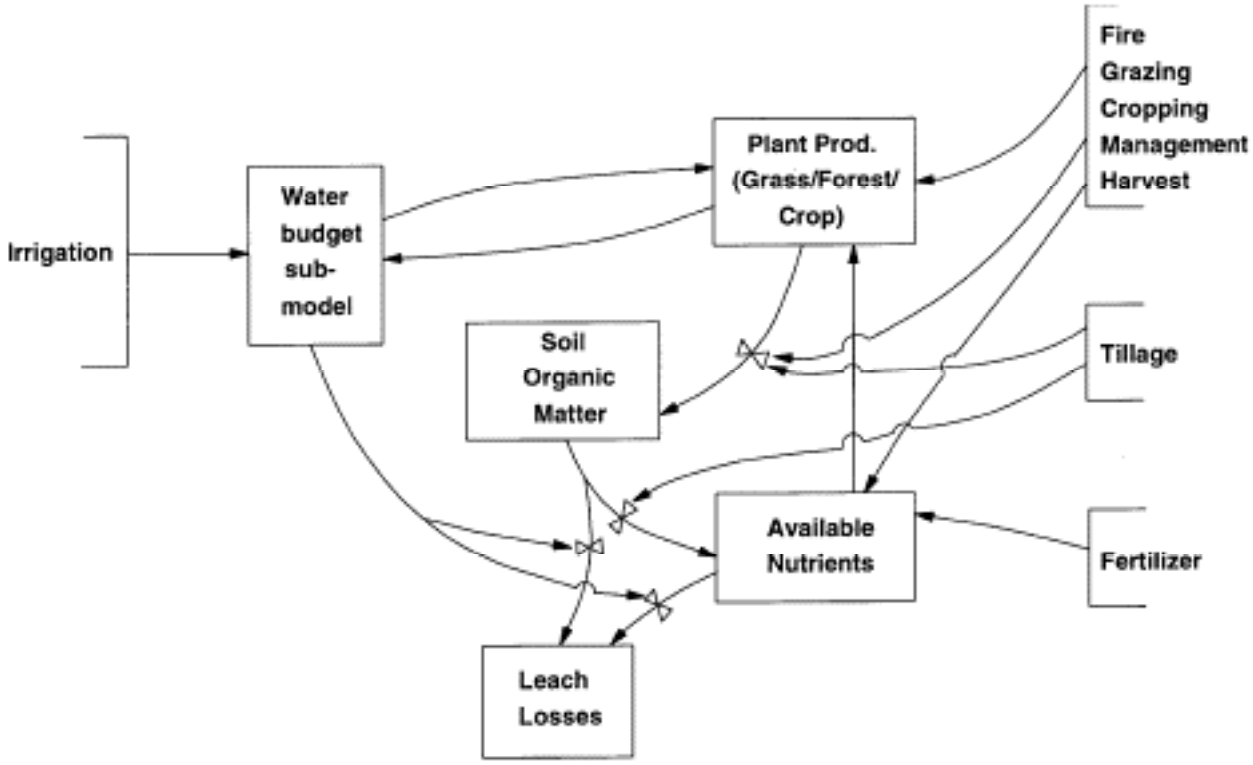

Figure 12.3

Simplified representation of the CENTURY Model

Vegetation Modeling

Bill Parton

Natural Resource Ecology Lab
Colorado State University
Fort Collins, Colorado

The major goal of the linked biogeochemistry and general circulation models is to simulate the interactive impact of climate and vegetation changes on trace gas production (CO2, CH4 and N2O) and atmospheric circulation patterns.

Parton gave an overview of the different types of vegetation models, presented results from recent model comparisons and other research activities, and discussed how land use/land cover data are being incorporated into ecosystem models.

The three major types of vegetation models include vegetation distribution models, plant physiology models and ecosystem models. Vegetation distribution models fall into two general types: climate-based models and optimum water use models. The climatic vegetation distribution models are based on empirical correlation of patterns in climatic variables (e.g., precipitation, minimum and maximum air temperature, potential evapotranspiration [PET] and the ratio of rainfall to PET) to observed vegetation distributions. Optimum water use models calculate the optimum leaf area index (LAI) as a function of the environmental conditions. These models assume that plant LAI will be optimized as a function of water stress with lower LAI values for arid environments. The optimum water use models also use climatic factors such as maximum and minimum air temperatures to classify vegetation distributions.

Detailed plant growth models have been developed for a large number of crops (e.g., corn, wheat, alfalfa) and natural systems (grasslands, coniferous forests, deciduous forests, and savannas). These models are designed to simulate the mechanisms that control plant growth as a function of the environmental conditions. The models use mechanistic representations of plant processes such as photosynthesis, root and shoot respiration, carbon allocation, and growth of the different plant parts. The driving variables for the models are daily or hourly microclimatic variables such as soil and air temperature, solar radiation, relative humidity, and wind speed. These models are primarily used at selected sites where detailed soils and microclimatic data are available and are difficult to use at regional scales because of the lack of sufficient data to run the models. Many of the detailed plant growth models do not consider the limitations of nutrients on plant growth.

Ecosystem models have been developed for all of the major natural ecosystems in the world and many of the major cropping systems. Ecosystem models include plant growth, nutrient cycling, soil organic matter cycling and water and temperature submodels. They generally represent all of the major components of the systems that are being modeled and use more simplified representations as compared to the detailed mechanistic process models. Most ecosystem models are designed to run at different sites and use data available at the regional and global scales. Many of the ecosystem models are now being combined with vegetation distribution models. The combined models will be able to simulate response of ecosystems variables and vegetation distributions to environmental changes. There is substantial interest in combining ecosystem biogeochemistry models with atmospheric circulation models. Figure

13.1 shows the major links of ecosystem models to atmospheric circulation models. The major goal of the linked biogeochemistry and general circulation models is to simulate the interactive impact of climate and vegetation changes on trace gas production (CO2, CH4 and N2O) and atmospheric circulation patterns.

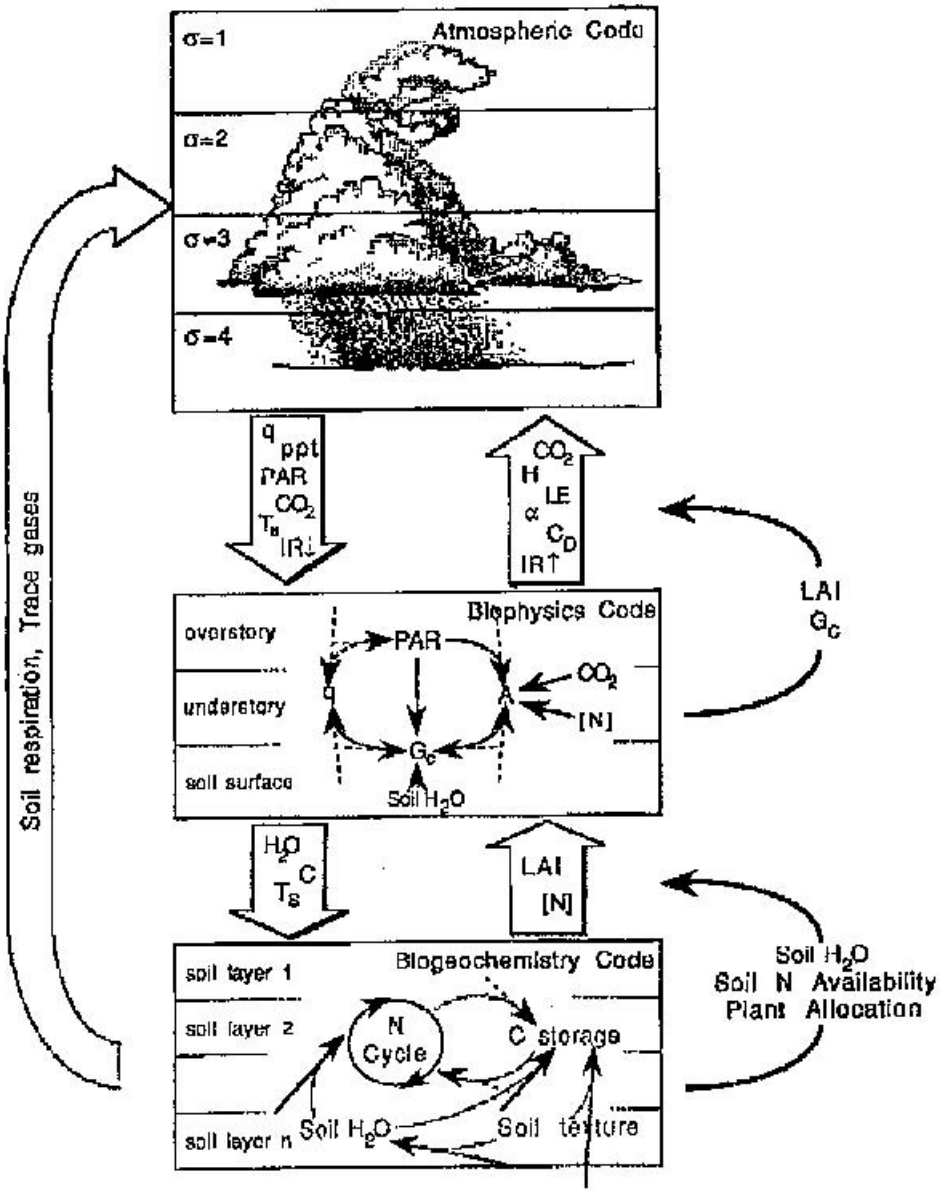

All of the models showed some response to increased atmospheric CO2 and the combined impact of changing climate and increased CO2 was to reduce the divergence between the models.

Figure 13.1
Flow diagram of the major atmospheric-biospheric interactions.

Model Comparisons

Recently there has been substantial interest in the comparison of process and ecosystem models. Some of the reasons for model comparisons include: 1) improving scientific understanding, 2) providing error bars on climatic change predictions, 3) development of

community models, and 4) selection of the specific models for environmental assessment activities. Parton presented results from process-oriented decomposition model comparisons and comparison of ecosystem models used in climatic change assessment. The major goal of process-oriented model comparisons is to improve scientific understanding about specific processes. A decomposition model comparison was set up to compare the processes that control decomposition of surface litter. The models used a common data set to test and parameterize the models and an independent data set was used to validate and compare model predictions. The model comparison showed that all of the models simulated observed carbon dynamics well. None of the models, however, simulated the nitrogen dynamics with good accuracy, and this illustrates the lack of understanding about the dynamics of N in surface litter.

Parton discussed the results from ecosystem model comparisons from two projects which had the objective of using model comparisons to provide error bars on environmental change predictions. The forest model comparison was designed to compare eight forest growth models for coniferous forest sites in Sweden and Australia. A common data set was used to tune the models for the specific sites and then the model predictions of climatic change impacts were compared. There was a formal comparison of the model results with the observed data sets and the climatic change predictions. The results showed that there were large uncertainties in the model responses to changes in temperature, atmospheric CO2 levels and the interactions between plant and soil systems, and the long-term response to increased atmospheric CO2 levels.

The CENTURY model is one of the few global ecosystem models that have been set up to include the impact of land use practices on ecosystem dynamics at the site, regional and global scale.

The VEMAP model comparison considered three biogeochemistry models and three biogeography models. The models were all compared under contemporary conditions for sensitivity to increased CO2 and climatic change. The models simulated dynamics of all the ecosystems in the U. S. at .5 degree resolution and used the same data bases for current climate, soils, vegetation and climatic change scenarios. The comparison of the biogeography models under contemporary climate shows that the models agree fairly well for the geographic distribution of the major vegetation types. All of the models showed some response to increased atmospheric CO2 and the combined impact of changing climate and increased CO2 was to reduce the divergence between the models.

The contemporary climate comparisons of the biogeochemistry models for NPP, total actual evapotranspiration and total storage of C showed substantial agreement among the models. The CENTURY and TEM models showed that increasing temperature resulted in increased decomposition, N availability and higher NPP. For BIOME-BGC, increasing temperature resulted in increased drought stress, decreased NPP and decreased total C storage. The differences among the models are most pronounced for the combined impact of increasing CO2 and climatic change. With the CENTURY and TEM models, nutrient availability is the primary control on plant production, while BIOME-BGC is less controlled by nutrient dynamics and more controlled by water stress. This reflects the different conceptual frameworks used to develop the models.

Incorporation of Land Use in Ecosystem Models

Most of the global ecosystem models have focused on simulating the dynamics of natural ecosystems. Human land use has substantially altered natural ecosystems in the both developed and less developed counties. Land use practices such as forest clear cutting, planting of crops, and animal grazing have altered many of the natural ecosystems in the world, along with the

global carbon, nutrient and water budgets. The CENTURY model (see Figure 13.2) is one of the few global ecosystem models that have been set up to include the impact of land use practices on ecosystem dynamics at the site, regional and global scale. The model has been set up to simulate all of the major land use systems and includes management practices such as cultivation, fertilization, irrigation, and grazing.

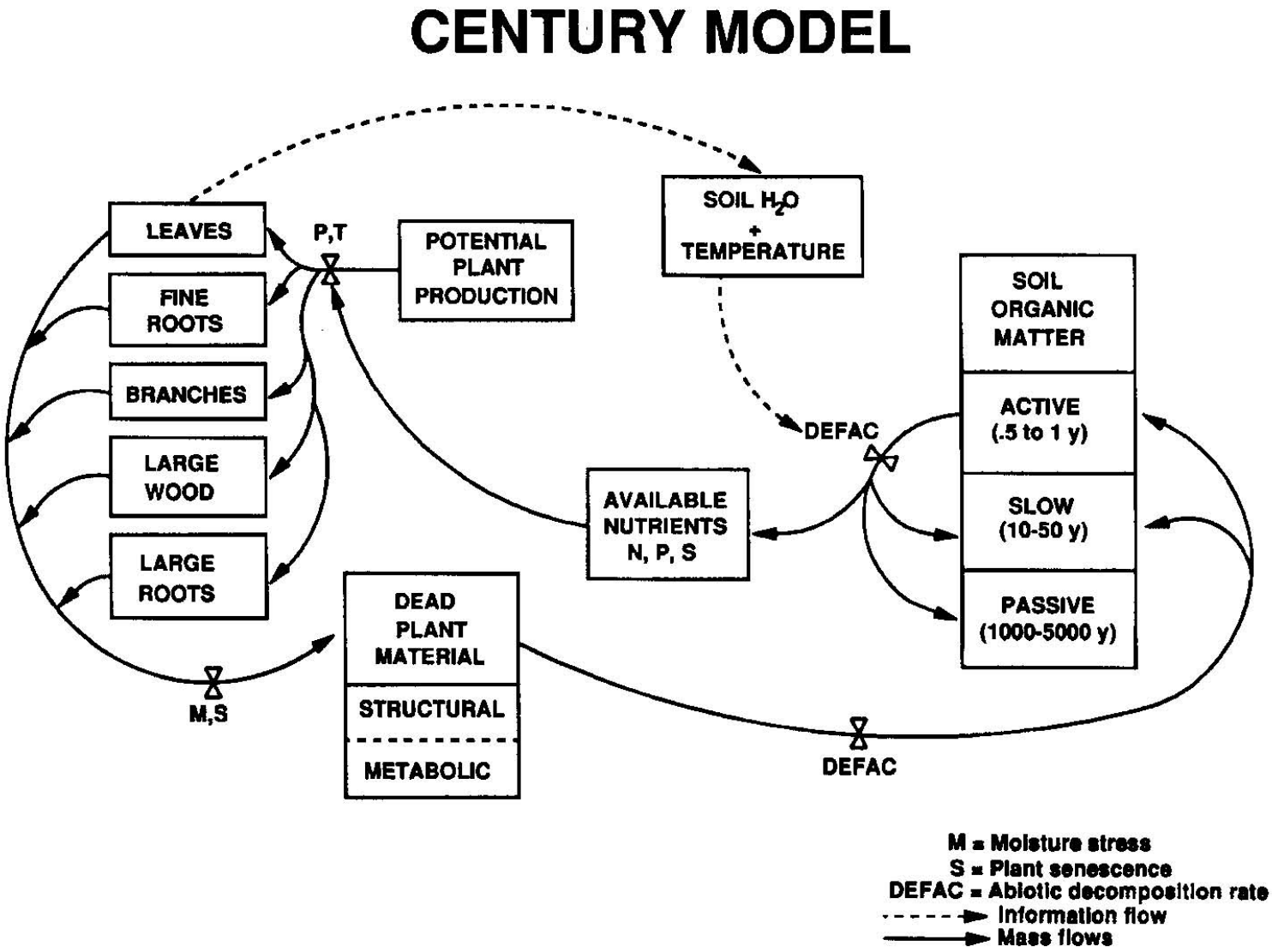

Figure 13.2
Flow diagram of the CENTURY model

Figure 13.3 shows the simulation of winter wheat crop yields from 1920 to 1990 for Weld County in eastern Colorado. The model included the change in cultivation practices, crop varieties, and fertilization levels in order to simulate the changes in crop yields during that time period. This model allows the tracking of long term changes in soil organic matter and nutrient cycling, and projections of the impact of new land use practices such as the Conservation Reserve Program on agroecosystem dynamics. Most of the current global ecosystem models are in the process of being modified to incorporate the effect of land use practices on natural and managed ecosystems.

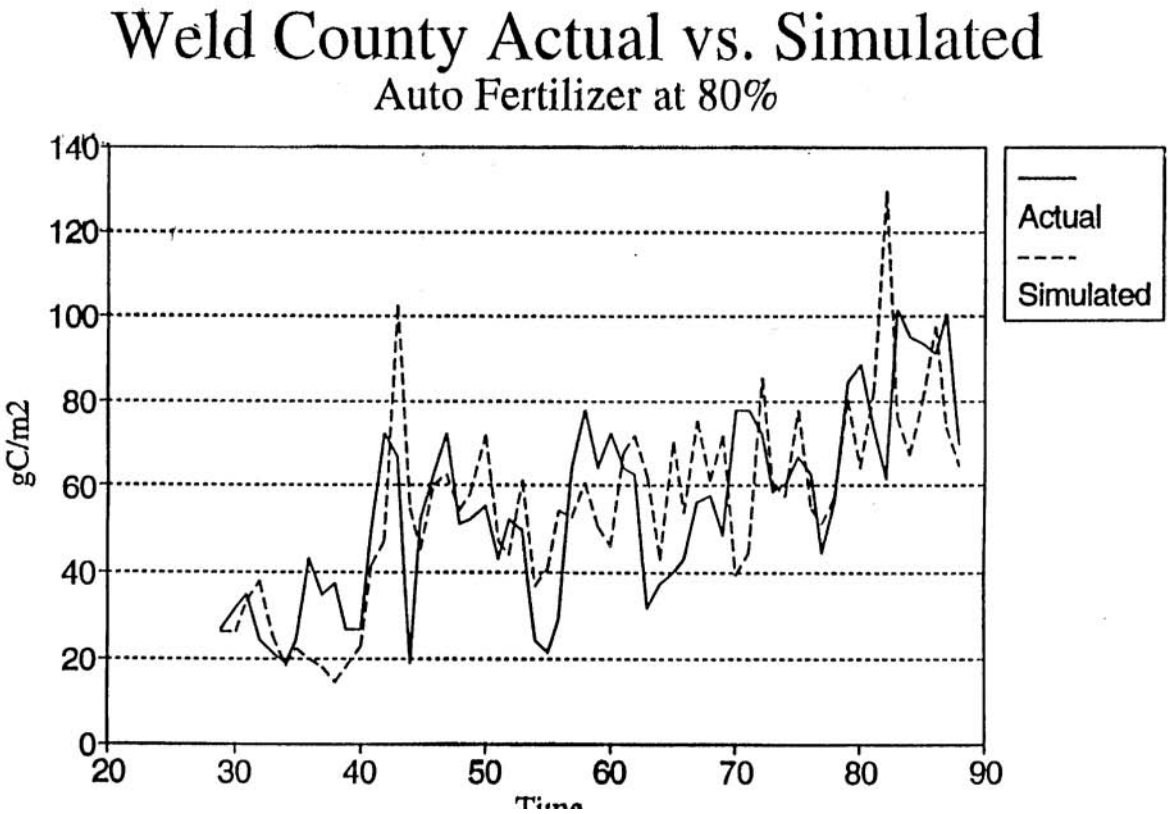

Figure 13.3
CENTURY-simulated versus observed winter wheat yield for Weld County, Colorado from 1930 through 1990.

Uses of a Bidirectional Reflectance Model with Satellite Remote Sensing Data

Jeffrey L. Privette

Department of Geography, University of Maryland
College Park, Maryland

Privette initially discussed the bidirectional reflectance model and some results from combining vegetation indices with bidirectional reflectance characteristics. Next, he discussed the inversion of a bidirectional reflectance distribution function (BRDF) model. Investigations on the invertibility of the model are followed by results using ground-based reflectance data from the First ISLSCP Field Experiment (FIFE). Privette also discussed results from inversions with satellite reflectance data collected over the FIFE site.

This study was limited to grassland applications. Grasslands cover approximately 16% of Earth's land surface and account for nearly 10% of its net productivity. In addition, some results suggest grasslands are one of the most climatologically sensitive earth covers. Thus, grasslands may be early indicators of a changing climate.

Grasslands cover approximately 16% of Earth's land surface and account for nearly 10% of its net productivity. In addition, some results suggest grasslands are one of the most climatologically sensitive earth covers.

The bidirectional reflectance of a vegetated surface is a function of the irradiance field, the spectral properties of the plant organs and soil particulates, and the structure of the vegetation, litter and soil. Although soil and atmosphere scattering is modeled relatively easily, scattering from vegetation is more difficult due to the finite size scatterers at fixed positions. To make the problem more amenable to mathematical solution, we invoke the turbid medium approximation whereby we consider the leaves ground up into infinitesimal leaflets and redistributed between the atmosphere and soil in the same orientation as the original plant leaves. The DISORD model from Ranga Myneni is perhaps the most accurate vegetation turbid medium model available. It is based on the radiative transfer equation, uses discrete ordinates to solve the multiple scattering problem, and has been validated against a series of canopies. It is a function of leaf area index (LAI), leaf angle distribution, leaf optical properties, soil reflectance (Lambertian or anisotropic), leaf specular reflectance, a hot spot parameter and the ratio of direct-to-total irradiance. This model was used throughout this study.

Vegetation Indices

A grassland reflectance distribution in the red and near-infrared (NIR) bands shows strong anisotropy. Since the NIR angular distribution is not a constant multiple of the red distribution, vegetation indices must depend on the view and solar geometry. To compensate for this, we often attempt to use near-nadir view geometries. While convenient, nadir views may not be best. Indeed, samples at other geometries may be more sensitive to the desired vegetation parameters. For example, many have reported the near-linear relationship between fAPAR and NDVI. To find a geometry where this relationship is most linear, NDVI was modeled for canopies of LAI=1, 3 and 5 and erectophile and planophile leaf distributions for 12 solar zenith angles. All view angles in the upper hemisphere were considered. At 75 degrees forward scattering, the

squared linear correlation coefficient for the fAPAR-NDVI relationship was 0.247. However, at other angles, very encouraging results were possible. At 30 degrees backscatter, off the principal plane, r^2=0.928. The sensitivity of NDVI to fAPAR (the slope of the regression line) is also highest at medium backscatter angles. A comparison of NDVI with LAI suggests, however, that this correlation is greatest at higher view zenith angles in the backscatter direction.

The effects of using different angles for red and NIR reflectances in the construction of NDVI were also considered. Using principal plane data, one can see that an index formed with forward scattered red reflectance and near-nadir NIR reflectance has the highest correlation with fAPAR. Sensitivity to fAPAR is greatest with an index formed from red reflectance in the middle backscatter region and NIR reflectance in the middle forward scatter region. Such indices could be formed from a single pass of EOS MISR or multiple passes from AVHRR or EOS MODIS. In conclusion, the knowledgeable combination of BRDF effects and vegetation indices can significantly improve the accuracy of retrieved biophysical parameters from indices.

The angular distribution of radiation scattered by the Earth's surface contains information on the structural and optical properties of the surface.

The inversion problem

As stated above, the angular distribution of radiation scattered by the Earth's surface contains information on the structural and optical properties of the surface. Potentially, this information may be retrieved through the inversion of surface bidirectional reflectance distribution function (BRDF) models. An inversion requires the adjustment of a set of model parameters until the model-predicted reflectance best matches a set of empirical reflectance data. Once this occurs, the set of parameters leading to the best match is considered the best estimate of surface conditions at the time of the data sampling.

Only model parameters most affecting the canopy reflectance can be retrieved. In this study, the sensitivity of a top of canopy (TOC) reflectance was determined for canopies of arbitrary optical depth. In general, the TOC reflectance was primarily sensitive to soil reflectance and LAI for LAI < 1. For canopies of LAI > 1.5, reflectance was primarily sensitive to leaf optical properties.

The invertibility of the discrete ordinates model was shown for typical conditions us ing synthetic, noise-free data. In general, solutions were reasonably accurate except for cases of high LAI, low solar zenith angle (SZA) and incorrect leaf angle distribution (LAD) specification. Even for cases with incorrect inversion solutions, however, estimates of spectral albedo, absorbed radiation and canopy photosynthetic efficiency were accurate. These were determined from forward modeling using the retrieved canopy parameters. Inversions using data collected under satellite sampling schemes (AVHRR and MISR) were reasonably accurate in most cases. The only exception was the case of orthogonal plane samples from MISR. Principal plane samples resulted in the most accurate solutions.

Effects of Gaussian noise in the empirical reflectance data were also tested. Parameters to which reflectance was most sensitive were retrieved with less than 10% relative error for noise of 10% relative variance. Surface state parameters remained accurate for all noise levels. These general experiments suggested the model could be inverted under many conditions. Thus, inversions with empirical reflectance data were tried.

Data from the FIFE experiment were used for the inversions described here. FIFE was a multi-year, international study of a grassland climate and ecosystem. The experiment was conducted on a 15 km x 15 km site near Manhattan, Kansas (39° 0' latitude, 96° 3' longitude).

The FIFE site consisted mostly of grazed and burned grassland. To a reasonable degree, the terrain was flat (±50 m elevation), had natural homogeneous vegetative cover, and had strong climatic forcing. FIFE included the coordinated measurement of soil, canopy and atmospheric parameters via ground, aircraft and space-borne detectors. Data was used from a site that underwent a prescribed burning in the spring of 1989 to eliminate dead vegetation from previous years. This resulted in a comparatively dense canopy over the summer months. The predominate vegetation included three C4 grasses: little bluestem (Andropogon scoparius Michx), big bluestem (Andropogon gerardii Vitmin), and indian grass (Sorghastrum nutan L. Nash). The site was not grazed or cultivated.

Before inversions were attempted, a decision on the use of a Lambertian or anisotropic soil background was necessary. Simulations with Lambertian and anisotropic backgrounds revealed that soil anisotropy affects TOC reflectance for relatively thick (LAI < 8) canopies. Thus, an anisotropic soil model was deemed necessary for FIFE. Inversions were conducted with FIFE soil data. A relatively invariant solution was determined using data represent ing a wide range of spectral, SZA and soil moisture conditions. In this case, the mean of the absolute values of reflectance errors was 0.006 (3.5%).

The accuracy of the retrieved LAI depended on the accuracy of the retrieved leaf optical properties and vice-versa.

Next, inversions were conducted with field measured canopy reflectance data. FIFE data from a ground-based MMR instrument was chosen for model inversions. The MMR had seven bands in the visible and NIR wavelengths. Results were binned according to SZA (above or below 40°). Only LAI results were shown since this is the parameter generally of greatest interest. LAI was most accurately determined at low SZA with NIR data. Shortwave albedo agreed well with pyranometer-measured values, however fAPAR was overestimated in all cases. Nevertheless, there was significant variability in measured fAPAR data. It is expected that results will improve with more accurate validation data.

Finally, inversions with satellite data were attempted. Based on its wide range of sampling geometries, global coverage, and high temporal resolution, AVHRR data was used. Since satellite data has more noise in it than ground radiometer data, the number of model parameters was reduced. The model was configured for inversion by fixing LAD with the site-wide value. Moreover, leaf transmittance was coupled to leaf reflectance using a regression equation determined from empirical spectrometer data. LAI and leaf reflectance/transmittance remained variable.

To improve the accuracy and efficiency of model inversions, a scheme was developed for differentially weighting the empirical data. The scheme is based on the sensitivity of TOC reflectance at a given sun-target-sample geometry to model parameters. For example, the sensitivity to a 10% reduction in LAI is shown in Figure 14.1. Directions for which reflectance is more sensitive to a given parameter have a larger weight than directions for which reflectance is less sensitive. Simulations with synthetic data verified that merit function gradients increased when this weighting scheme was applied (see Figure 14.2). Steeper gradients were found to improve optimization accuracy and efficiency.

To validate the model, mean parameter values were determined over the entire FIFE site via various averaging schemes. Using atmospherically corrected AVHRR data from 1987, model estimates were compared to AVHRR data. Model estimates agreed reasonably well with empirical data from mid-June through mid-August. Errors in data gathered before mid-June and after mid-August were attributed to non-green surface conditions (burned and senescent canopies, respectively).

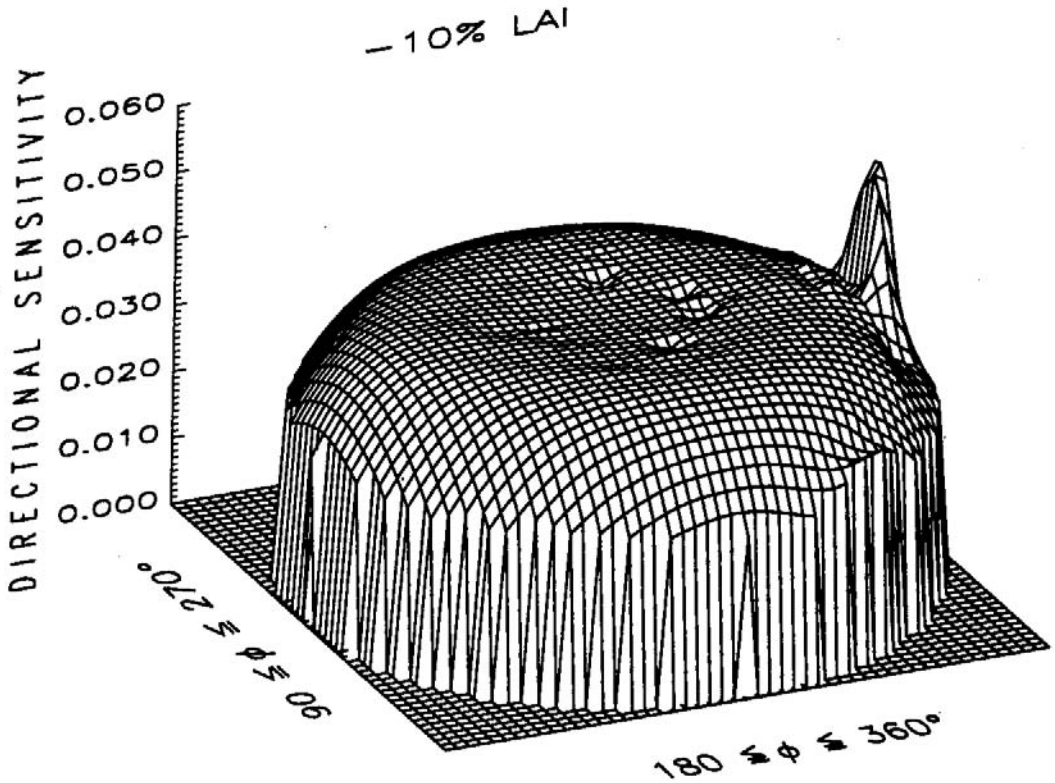

Figure 14.1
Polar plot of directional sensitivity (change in BRDF) for 10% decrease in LAI.

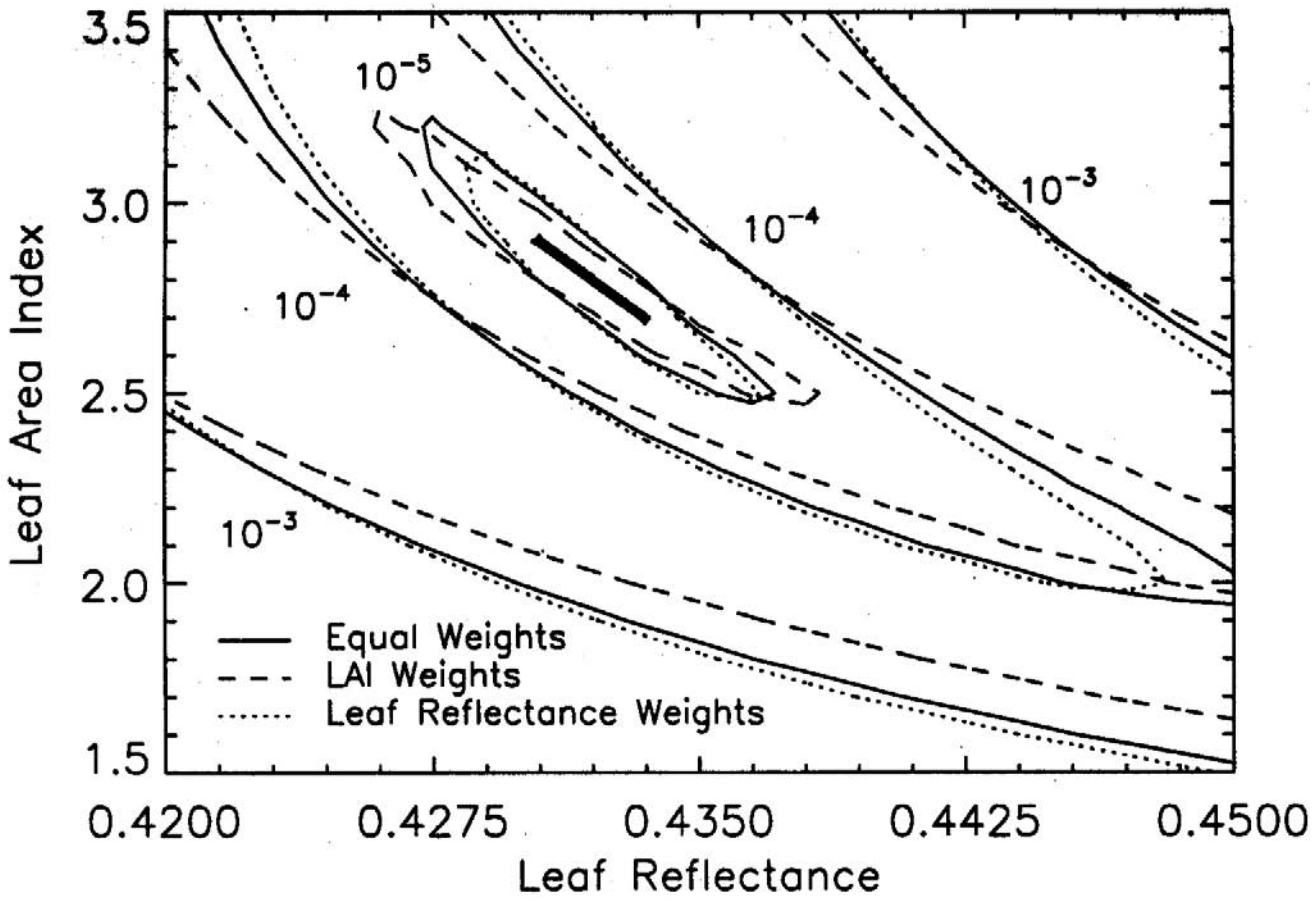

Figure 14.2
Variation in merit function due to directional sensitivity weights from different parameters.

The weighting scheme was used to select promising 11-day subsets of AVHRR data for inversions. Using the LAI and leaf reflectance/transmittance weighting schemes, site-wide LAI and leaf optical properties were accurately retrieved in one parameter inversions (see Figure 14.3). Solutions from inversions with two adjustable parameters were less accurate, but were acceptable in some cases. Specifically, the accuracy of the retrieved LAI depended on the accuracy of the retrieved leaf optical properties. When one was accurately retrieved, so was the other. Where there were large errors in one, there were large errors in the other.

Conclusions from this study are:

* 2-3 parameters (LAI, leaf optical properties, soil single scattering albedo) could be estimated from AVHRR (MODIS) data collected over grasslands. This requires reasonably accurate estimates of other model parameters, however.

2-3 parameters (LAI, leaf optical properties, soil single scattering albedo) could be estimated from AVHRR (MODIS) data collected over grasslands.

* MISR sampling geometry should allow the accurate retrieval of the same parameters when the ground track is close to the principal plane.

* Retrieval accuracy for LAI depends on the accuracy in leaf optical property estimates, and vice-versa.

* LAI and soil properties can be accurately estimated only for thin canopy (LAI < 3) cases.

* Leaf optical properties can only be estimated accurately for canopies of LAI > 1.

* NIR bands are superior for the determination of spectrally independent parameters of grasslands. At very low LAI (<1), red bands may be superior.

* LAI, soil properties and LAD are most accurately estimated with low SZA and view zenith angle (VZA). SZA should not be less than 10°, however, or azimuthal asymme try is lost.

* Leaf optical properties are most accurately estimated at high SZA and VZA.

* Surface state parameters (fAPAR, albedo, etc.) may be accurately estimated for the time of sampling even if moderate errors occur in the retrieved soil and canopy parameters.

* Surface state parameters can only be accurately estimated at other times if errors are small in the retrieved soil and canopy parameters.

* An anisotropic soil model is required to accurately model relatively thick canopies (LAI < 8), especially if reflectance near the hot spot is estimated. Inversions of the model of Jacquemoud et al. [1992] requires data from multiple spectral bands, at multiple VZA and SZA, and in multiple azimuthal planes to produce invariant es timates of roughness and phase function parameters.

* Optimization routines work best when the merit function surface is steep and does not contain local minima. The slope of the merit function around the minimizer can be steepened via weighting the merit function terms by the partial derivative of directional reflectance with respect to model parameters. This increases the efficiency and accuracy of the inversion.

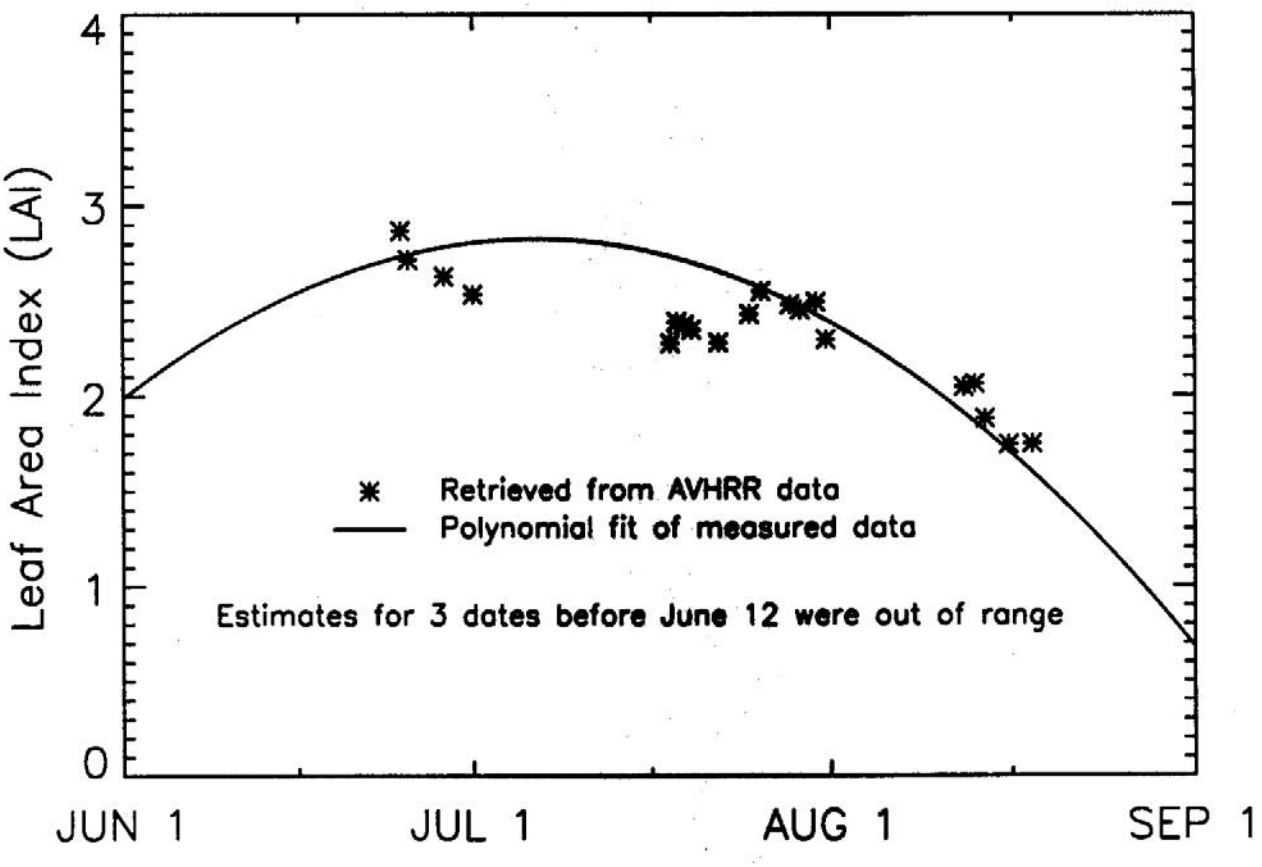

Figure 14.3
Comparison of AVHRR-retrieved and measured LAI over FIFE during 1987. BRDF model was inverted for one parameter.

LAI and soil properties can be accurately estimated only for thin canopy (LAI < 3) cases. Leaf optical properties can only be estimated accurately for canopies of LAI > 1.

Wetlands, Global Climate Change, and Remote Sensing

Elijah W. Ramsey III

National Biological Service, Southern Science Center
Lafayette, Louisiana

Wetlands help mitigate flooding and provide important habitats. They are transitional between terrestrial and aquatic systems and have one of the three following characteristics: 1) the land supports hydrophytes, at least periodically, 2) the substrate is predominately undrained hydric soil, and 3) the substrate is saturated or covered with water sometime during the growing season. From colonial times to the mid-1980s, the lower 48 states of the U. S. lost over 100 million of the more than 200 million acres of wetlands (>404,700 km of the >809,400 km). Primarily, these losses resulted from wetland drainage and conversion to agriculture. Wetlands are still being lost to conversion, however, loss of coastal wetlands is aggravated by salt water intrusion and water logging.

From colonial times to the mid-1980s, the lower 48 states of the U. S. lost about half of their wetlands. Primarily, these losses resulted from wetland drainage and conversion to agriculture.

Generally, wetlands can be grouped into swamps and marshes. Swamps include either inland or coastal bottomland hardwood and cypress/tupelo freshwater forests and coastal saline mangrove forests. Cypress/tupelo forests are permanently flooded, while bottom land hardwood forests are intermittently flooded. Of the original estimated 25 million acres of bottomland hardwood forests, only about 5 million acres now exist (20,235 km2 of the original 101,175 km2).

Marshes are intermittently flooded coastal and inland grasslands that can be fresh or saline. Coastal marshes continuously undergo compaction. To maintain an elevation equilibrium, compaction must be offset by sediment or detritus input. Canal building and channelization can disrupt the flow of sediment into the marsh. For example, channelization of the Mississippi River in the mid-1950's severely reduced the flow of fresh water and sediments to the coastal Louisiana marshes. By the mid-1970s, this disruption, and others, resulted in losing nearly half the coastal Louisiana marshes.

The following examples illustrate three important aspects related to remote sensing of coastal wetlands threatened by global climate change influences; marsh loss detection, flood detection and monitoring, and management practices affecting the utility of remote sensing in detecting marsh loss.

Detecting wetland change: Hurricane Andrew (August 26, 1992) Impacts to the Coastal Louisiana Marshes

Marsh loss due to the hurricane impact was examined by using November 1990, March 1991, October 1992, and January 1993 Landsat Thematic Mapper (TM) images. TM images were separated into pre- and post-hurricane image sets and progressive clustering used to classify each image set into marsh and water. The pre and post classified images were differenced to

produce a marsh loss map. To evaluate the accuracy of the classified and change maps generated from TM images, pre- and post-hurricane color infrared photographic images (about 1 m spatial resolution, October 1991 and 1992) were similarly classified. Results of the comparison indicated that in both the pre- and post-hurricane classifications, the TM marsh class was over estimated. The over estimation was attributed primarily to two causes. First, small gaps (<3m) containing water or floating vegetation in the otherwise continuous marsh canopy were misclassified as marsh. Second, more continuous areas containing mixtures of marsh, floating vegetation, and mud within the 30m spatial resolution of the TM sensor were predominantly classified as marsh.

The over estimation of marsh extent in the pre- and post-hurricane TM classifications resulted in about a 50% over estimation of marsh loss. The TM change analysis missed small areas of marsh change, critical to detecting the initiation of marsh loss. Further, larger areas of marsh loss were mostly located correctly in the TM analysis, but were spatially too extensive, causing an over estimation of marsh loss. Finally, higher spectral resolution of the TM sensor was not as important as the high spatial resolution of the photography in detecting marsh loss.

Sea level rise poses one of the greatest threats to the long-term health and stability of coastal wetlands.

Sea Level Rise: Associating Marsh Flooding With Marsh Type and Biomass

Sea level rise poses one of the greatest threats to the long-term health and stability of coastal wetlands. This susceptibility is primarily an effect of the low shore-normal topographic gradient of coastal marshes (around 12 to 30 cm/km). To predict the possible consequences of sea level rise on a coastal marsh, the relationship between flooding extent, frequency, depth, and duration

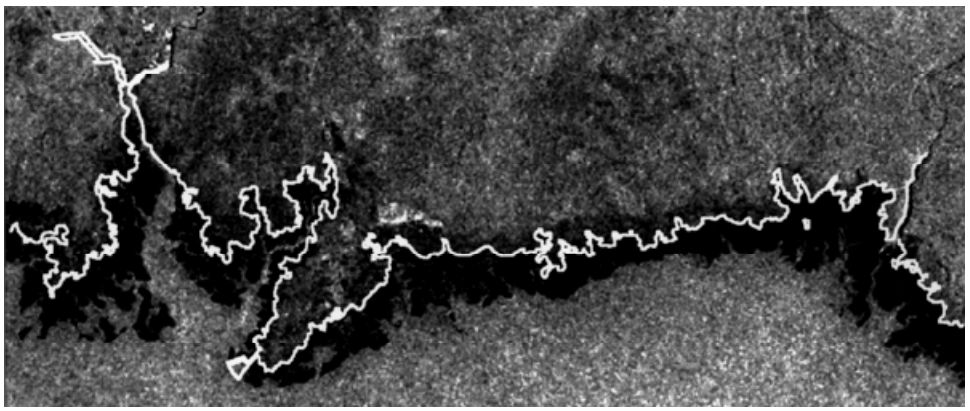

13 September 1993; flooded (above)

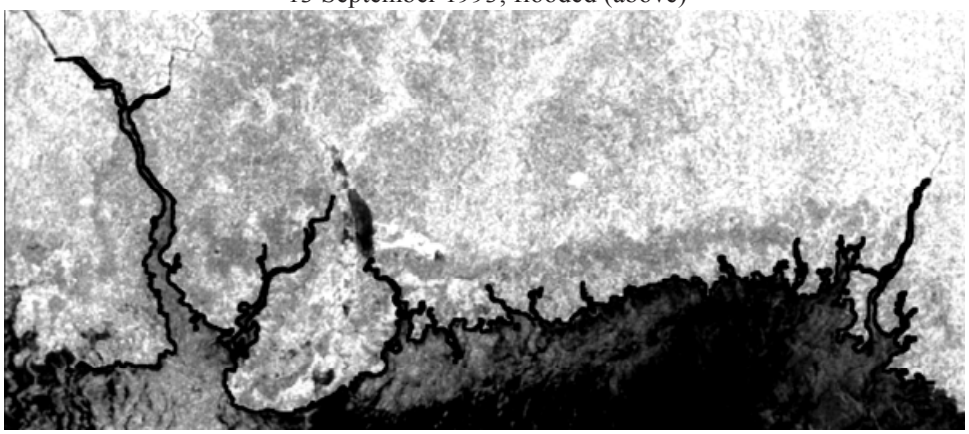

18 October 1993; non-flooded

Figure 15.1

ERS-1 SAR images acquired on September 13, 1993 (flooded) and October 18, 1993 (nonflooded) of a black needlerush marsh in the Big Bend area of coastal Florida.

and marsh type and biomass is being examined in the Big Bend area of coastal Florida. To support this effort, at five marsh field sites, near-continuous recording of flood depth were collected. Concurrently, six consecutive ERS-1 SAR satellite images were collected of the marsh. Comparison of recorded flood depths at the times of the ERS-1 satellite collections, showed SAR returns from flooded marsh were attenuated in comparison to SAR returns from non-flooded marsh (Figure 15.1). Use of this finding allowed flood extent contours to be generated at the times of three ERS-1 SAR collections.

Next, an attempt will be made to convert these flood extent contours to topographic contours and from these generate a micro topographic surface of the marsh. Currently, only 150-cm topographic contours are available for the area. Recorded flood data will then be used to produce flood frequency, depth, and duration surfaces covering the marsh area; storm surge data will also be included where appropriate. If successful, the flood surfaces will be associated with marsh characteristics produced by using sets of optical data collected during the same time period. Ultimately, the connection between marsh and flooding characteristics will be used to simulate the consequences of a rising sea level on marsh type and biomass.

Burn Management Practices and Detecting Marsh Change with Remote Sensing

Large areas of marshes in the Gulf Coast are burned each year. To examine the effects of these burn practices in detecting marsh change, TM images and canopy reflectance spectra (400 to 900 nm with about 2.5 nm spectral bandwidths) of three sites were collected over an eight month period of a coastal Louisiana fresh marsh (about 12km by 12km). A December 1990 classified TM image was used to mask-out water and scrub shrub from all TM classifications.

By March 1991, large expanses of the study area had been burned. These burns were separated as old (January) and new (early March) burns. January reflectance spectra of the three in-situ field sites were spectrally non-distinct; however, reflectances of one site burned early in January were lower in magnitude. March canopy reflectance spectra of the three sites showed the beginnings of a red edge and nir plateau. The spectra associated with the previously burned site, however, was lower in amplitude with a more distinct red edge and nir plateau. Immediately after the March TM collection, another large area of marsh was burned. The extent of this burn was mapped by using the July 1991 TM image, however, most areas previously burned (January to March) were not detected. Inspection of the July canopy spectra from the three sites also indicated little spectral differences between the three sites. All canopy reflectance spectra had nearly the same magnitude and a well developed red edge and nir plateau.

Combining the March and July burn classifications allowed the generation of a burn history map for the area. The burn history map depicted marsh burned in January, in early March, and just after the March TM collection (Figure 15.2). In summary, TM imagery can be used to detect changes in a marsh subjected to burning. Even though advantageous to burn detection and recovery monitoring, these differences could lessen the utility of remote sensing techniques to detect marsh loss. Thus, remote sensing techniques should be developed that can discern changes in marsh canopy reflectance related to short-term management practices (e.g., burning) from longer term changes related to marsh loss.

Remote sensing techniques should be developed that can discern changes in marsh canopy reflectance related to short-term management practices (e.g., burning) from longer term changes related to marsh loss.

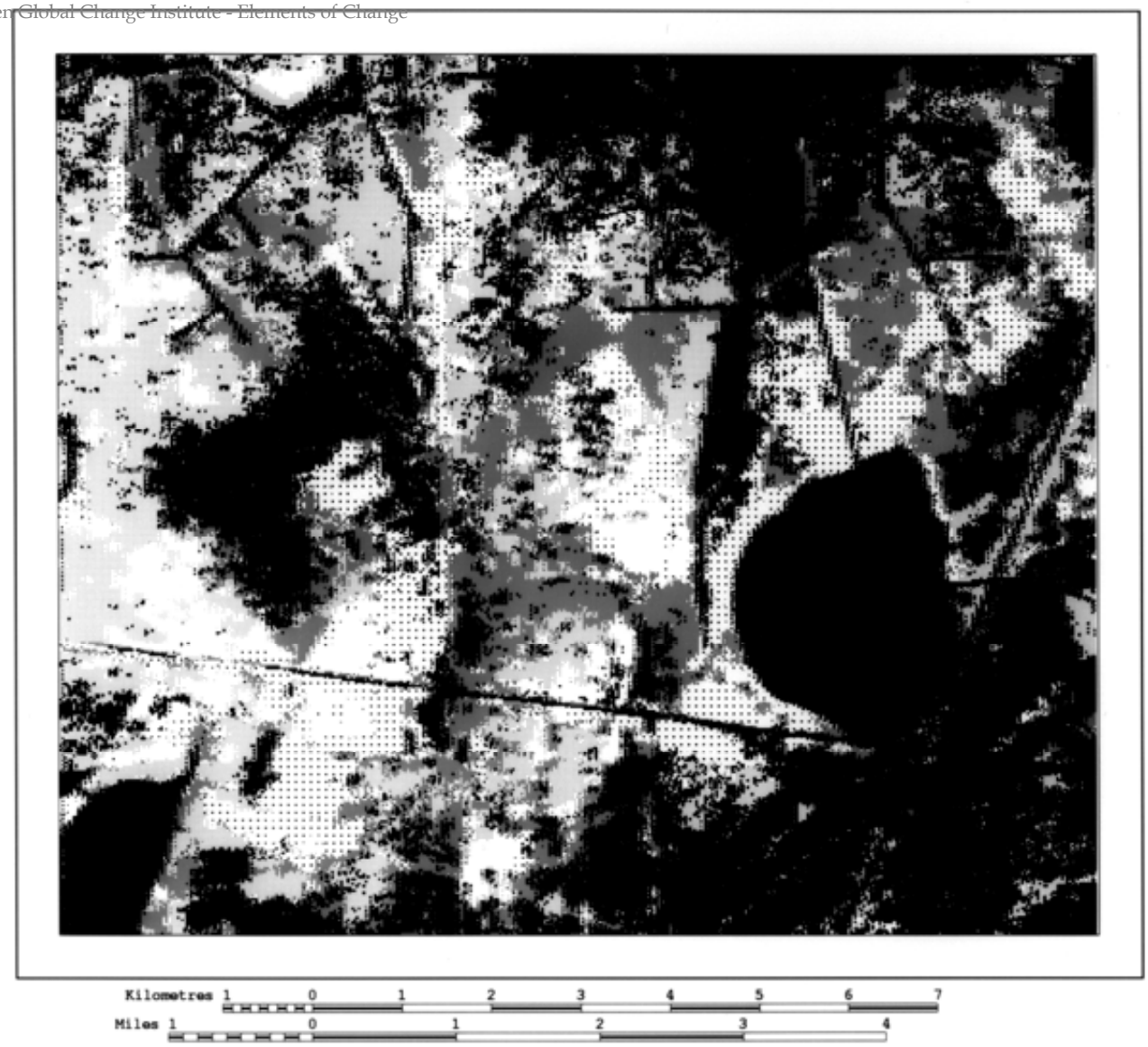

Figure 15.2

A burn history map of a fresh marsh area in south Louisiana. The map was generated by combining classified November 1990, March 1991, and July 1991 Thematic Mapper images. The burn history map details those marsh areas that were: 1 unburned between November 1990 and July 1991; 2 burned pre-March image and identifiable on the summer image (pre -Spring burns); 3 burned pre-Spring but non separable from unburned marsh in summer (non-detected burns); and 4 burned post-March image (post-Spring burns).

Remote Sensing of Land Cover and Phenology

Brad Reed

EROS Data Center, Science and Applications Branch
Sioux Falls, South Dakota

There is a strong co-dependence between global change models and the data that are nec essary to run them. Global change research is data limited and it is important to begin developing mechanisms to ensure that global change research can be properly supported by the necessary measurements and data sets. To that end, a research group at the U. S. Geological Survey's EROS Data Center (EDC) is working to produce products to support global change research, particularly global climate and ecosystem modeling efforts. Two of its contributions are 1) a land cover characteristics database, to which values of biophysical variables of importance to modelers can be assigned and 2) a seasonal characteristics database that describes the dynamics of the vegetated landscape.

Global change research is data limited and it is important to begin developing mechanisms to ensure that global change research can be properly supported by the necessary measurements and data sets.

The land cover needs of modelers vary in both their classification schemes and spatial scale. This is true for general circulation models (GCMs), ecosystem models, and mesoscale models. In developing the Land Cover Characteristics Database, EROS has taken into account the fact that data needs vary both within and between applications and that links must be made and compatibility strengthened with existing and future land cover classification systems. Flexibility and adaptability are the keys to the development of such a database. In order to ensure its use, the database must allow users to tailor it to their specific needs.

For the EDC Land Cover Characteristics Database, time series NDVI monthly maximum value composites taken from Advanced Very High Resolution Radiometer (AVHRR) satellite data are combined with digital Earth science information such as elevation, climate, and ecoregions, as well as with hard copy maps. Remote sensing data alone cannot separate land cover types sufficiently since distinct land cover types can have very similar spectral/temporal characteristics. Other information, such as spatial distribution and relationship to ecoregion, elevation, and climate, and coincidence to map information helps to distinguish these types and to assign labels to classes to differentiate regions with similar spectral characteristics.

The Land Cover Characteristics Database contains 159 distinct land cover regions. However, Reed points out, the product is more than a land cover map, it is a database. For each of the 159 classes there is AVHRR data, average biweekly NDVI, major land resource areas, elevation, and other environmental information. All of this information is supplied to users along with the land cover regions map so they have all the source information EROS used to create the database and can make adjustments to suit their own applications. Since many users have grown accustomed to working with particular land cover classification schemes, the 159 land cover types have been generalized into commonly used schemes such as the USGS Anderson Level 2 classes, those used for the Biosphere Atmosphere Transfer Scheme (BATS) and for the Simple Biosphere (SiB) model.

Now that the database is complete, a variety of operational applications are underway at various federal agencies. These include a national fire hazards assessment by the U. S. Forest Service, ecoregions mapping by the Environmental Protection Agency (EPA), water quality assessment by the U. S. Geological Survey, crop condition assessment by the U. S. Department of Agriculture, biogenic emissions modeling by the EPA, and weather forecasting by the National Weather Service.

On the whole, the results from model and operational applications are positive. The land cover database can be applied to a variety of models and has been shown to improve their results. The land cover characterization approach is a simple strategy based on how land cover data are used. It relates land cover to environmental functions and processes and is adaptable to a range of environmental modeling and assessment applications.

The key to defining seasonal characteristics is to identify the onset of the growing season.

The results from the U. S. prototype have encouraged modelers who are now anticipating the completion of a global land cover characteristics data set. The Global Pathfinder 1-km AVHRR data set will make this global land cover database possible. Over thirty countries have been cooperating on this project since April 1992 to assemble global 10-day 1-km AVHRR coverage. Though a challenge, this effort is progressing well. There are currently ten global 10-day composites that are complete for the globe. Thirty-six 10-day composites covering April, 1992 to March, 1993 are complete for North America and South America. This data is on-line at the following World Wide Web address: http://sun1.cr.usgs.gov/landdaac/landdaac.html

For the global land cover characterization, AVHRR data will be used one continent at a time, beginning with North America, then South America with priorities for other continents yet to be determined. Cooperating partners in this project include the University of Nebraska - Lincoln, EPA, U. S. Forest Service, National Aeronautics and Space Administration (NASA), United Nations Environment Programme (UNEP), the International Geosphere Biosphere Programme (IGBP), National Autonomous University of Mexico (UNAM), University of Cordoba, Argentina, and others. As the effort progresses, more collaborators are expected to join the project.

The North America land cover characterization based on one year of AVHRR data in 100 clusters is now in the preliminary labeling stage. A refining of these labels is underway, and new challenges seem to emerge all the time. One example is that in enlarging the scope from the conterminous U. S. to all of North America, the Yucatan region of Mexico appears as homogeneous because it has a higher NDVI than the rest of the continent. Such unexpected outcomes require new methods, such as applying an additional clustering procedure to that area. The North America land cover characteristics database is expected to be completed by the end of 1995 and the Western Hemisphere is expected to be completed by summer, 1996.

Another database developed at the EROS Data Center for use by the global modeling community is the prototype seasonal characteristics database for the conterminous United States. The objectives for this project are to:

1. develop a pixel-by-pixel seasonal vegetation characteristics database from time-series NDVI that is related to ecosystem dynamics;

2. define characteristics such that they are not dependent solely on NDVI values, but rather on NDVI time-series characteristics;

3. define characteristics that can be applied to a wide range of applications, including biodiversity analysis, ecosystem modeling, climate modeling, weather forecasting, and land cover characterization.

The source data for this database are the biweekly maximum value NDVI composites. Pre-processing issues include recoding very low values (to eliminate clouds and non-vegetated surfaces), and smoothing of the time series to correct for sub-pixel cloud contamination. An iterative median smoother is used to retain peaks and eliminate valleys of the temporal NDVI curve.

The key to defining seasonal characteristics is to identify the onset of the growing season. The method relied upon for this work is the calculation of a moving average, borrowed from market trend analysis and involves calculating the average of the previous ten biweekly periods and comparing that value to the observed value for a biweekly period. The moving average acts as a predictor; when observed NDVI values depart markedly from predicted values (i. e., when the true values do not follow the trend), the onset of the growing season is occurring.

The event we call the "onset of growing season" is a description of ecosystem-level changes (due to coarse 1-km satellite resolution) and is not necessarily related to conventional, field-measured phenological events. Once the onset of the growing season is identified, additional seasonal characteristics can be derived. There are basically three families of seasonal characteristics: temporal, NDVI value, and curve feature. Temporal characteristics are time of onset of growing season, time of end of growing season, time of maximum NDVI, and duration of growing season. NDVI value characteristics are NDVI value at onset of growing season, NDVI value at end of growing season, maximum NDVI value, and range of NDVI values. Curve feature characteristics are rate of greenup, rate of senescence, time-integrated NDVI, and modality of growing seasons.

Interesting results emerge from year-to-year comparisons. For example, 1993, a heavy precipitation year stands out from other years, due to large scale flooding in the Midwest. The difference in the response of natural (vigorous vegetative activity) vs. anthropogenic (seriously lowered vegetative activity) landscapes to the flooding are easily noted in these images. Another interesting result is the apparent "reverse green wave" in Great Plains grasslands where the more northern areas begin their growing season sooner than more southerly regions. This is caused by the different temperature requirements for growth by cool season C3 grasses in the north and warm season C4 grasses in the southern plains.

This seasonal characteristics database is currently being used by 10 university and government institutions to evaluate its utility in modeling applications. In addition, in a cooperative project involving Augustana College in Sioux Falls, South Dakota, EROS Data Center, and The Nature Conservancy has set up a network of ground observation sites in the Plains to assess the ground conditions that relate to the seasonal characteristics as observed by satellite. These two datasets represent examples of how data producers and providers are working closely with the modeling community. This helps assure that the data fit the needs of the modelers rather than forcing modelers to adapt their research to accommodate the data.

These datasets represent examples of how data producers and providers are working closely with the modeling community. This helps assure that the data fit the needs of the modelers rather than forcing modelers to adapt their research to accommodate the data.

Monitoring Land-Use Over Time Using Spectral Mixture Analysis

Donald E. Sabol Jr.

Remote Sensing Laboratory, Department of Geological Sciences
University of Washington
Seattle, Washington

Another approach to classifying/ monitoring land-use using multispectral images is based upon spectral mixture analysis. In this method, radiance is transformed into fractions of spectral endmembers (reflectance spectra of known materials in the image).

Mapping land-use has been an important application of remote sensing and has generally been accomplished using traditional classification techniques (i. e., supervised/unsupervised classifications.) When properly applied, these methods have been successful with individual image data sets. However, because of differential atmospheric, illumination, and instrumental effects, it is difficult to obtain consistent classes with these approaches between images taken at different times.

Another approach to classifying/monitoring land-use using multispectral images is based upon spectral mixture analysis (SMA). In this method, radiance is transformed into fractions of spectral endmembers (reflectance spectra of known materials in the image). Interpretation of these endmember-fractions (i. e. , green vegetation, soil, non-photosynthetic vegetation, shade) is more intuitive than radiance and lends itself to a physically-based image interpretation. These fractions can be used as a framework for classification and/or monitoring surface changes over time.

One application of SMA is for image classification where classes are defined as a domain of fractions that identify a type of land-use. An example of this application is a study to monitor land-use from 1988 through 1991 in an area north of Manaus, Brazil at two cattle ranches, Fazenda Dimona and Fazenda Esteio (Adams et al., 1995). These areas are dominated by primary forest that have been cleared at different times to create pasture. As a result, these areas contain large fields in various stages of regrowth.

Methods

A subset of four Thematic Mapper (TM) image data sets for this study area were used (1988, 1989, 1990, and 1991.) All four images were taken in August, the most cloud-free time of the year. The images were co-registered and then calibrated by: 1) calibrating the 1989 image using the spectral mixture analysis method (Smith et al., 1990), and then 2) intercalibrating the remaining images to the 1989 calibrated image. Spectral mixture analysis was applied to all four images using four reference endmember spectra that represented the 4 major surface components of natural environments: 1) green vegetation, 2) non-photosynthetic vegetation (i. e., bark, senescent grass, litter, twigs), 3) soil, and 4) shade (Gillespie et al., 1990.)

The data cluster of fractions for the 1989 data set were used to define class boundaries us ing an interactive computer display. The cluster of fractions were displayed on a modified tethedron that could be rotated to any projection. Each data point in the tethedron corresponded to a pixel in the image. Pixels highlighted in either the tethedron plot or image display, were

simultaneously highlighted in the other. In this way, the limits of different classes were initially identified by using areas of known land-use from field observations. The boundaries were then refined by testing the classification on the three remaining images.

Once all the images were classified, a pixel-by-pixel comparison of class changes over time was performed. In a few cases, unlikely class changes were observed. For example, it is highly improbable that an area of bare soil one year would become mature (terra firme) forest the following year. For these pixels, the class history was examined. An aberrant classification in a single year of a physically understandable regrowth trend would be reevaluated and reclassified. Tracking the pixel history was an effective tool for improving image classification.

Once all the images are classified, pixels with specific histories can be identified. For example, one can identify all of the pixels in an image that, at one time, were forest or regrowth and were subsequently cut.

Spectral mixture analysis is an intuitive, more interpretable framework for image analysis.

Results

The simple mixing model used in this study accounted for 95% + of the spectral variability in the four image data sets. However, because only 4 endmembers were used to model the image, (with only single representative green vegetation [GV] and non-photosynthesizing vegetation [NPV] spectra), spectral mimicking made certain classes inseparable. For example, dry pasture and slash, which both have high fractions of NPV, were spectrally indistinguishable. Therefore, to minimize confusion caused by applying inappropriate class names, the term "category" was used. Each category included one or more spectrally similar classes. In this study, 8 categories were identified:

1. primary forest/mature-regrowth forest,
2. closed-canopy regrowth/kudzu vine/crops,
3. open-canopy regrowth,
4. pasture/crops,
5. sparse pasture/partially cleared slash/partially burned slash,
6. dry pasture/slash,
7. bare soil/roads, and
8. terra firme forest.

Many of the pixels in the image were assigned unambiguous class names by monitoring the changes of the categories over time for each image pixel or by image context (i. e., long pixel-wide areas of category 7 [bare soil /roads], would be classified as a road.) Field work showed that the classification accuracy was consistently high.

In the study area, a trend of overall regrowth was identified. Many of the areas that were cut for pasture were subsequently allowed to evolve back to a secondary forest. Some pastures had been maintained through subsequent cutting/burning. Although the method was tested in the Amazon basin, the results suggest that endmember classification may be generally useful for comparing multispectral images in space and time.

The Jasper Ridge, California Example

The same approach to image classification was performed on the 2 June 1992 Airborne Visible/Infrared Imaging Spectrometer (AVIRIS) (224 spectral bands) image taken over the

Jasper Ridge Biological Reserve near Palo Alto, California. This area, with a Mediterranean climate, is covered with a variety of forest canopies and grasslands, including deciduous oak woodland, chaparral, evergreen forest, and forested wetland. The image was calibrated to reflectance using Green et al. (1993) and modeled using an appropriate set endmember spectra. Again, four endmembers were used representing the same four major surface components: green vegetation, NPV, soil, and shade. The same classification scheme was used as with the Brazil example, utilizing the same classification boundaries. The category names were changed to the appropriate land-cover names for this study area. A comparison of the resulting classified image to vegetation maps and subsequent field investigations showed a very high degree of classification accuracy. Although the method was tested in the Amazon basin, the results suggest that endmember classification may be generally useful for comparing multispectral images in space and time.

This approach is independent of imaging system and is generally applicable to multispectral images of natural environments.

Spectral Trajectories

Imbedded in the change in classification over time is the change in fractions. The temporal change in fractions can be useful in monitoring surface processes. Seasonal changes of forest canopies and grasslands have been detected in Jasper Ridge, California (Sabol et al., 1993) between June and October 1992. An increase in NPV at the expense of green vegetation from June through October was due to increasing exposure of bark and stems as deciduous trees drop their leaves. By understanding the seasonal spectral changes, one may be able to separate and identify subtle long-term ecological changes in forested areas.

The same approach has been used to map the status of forest regrowth in cut areas of the Gifford Pinchot National Forest in Washington and to establish fractional regrowth trends (Sabol et al., 1995). Recent clearcuts were characterized by high fractions of NPV and low fractions of GV and shade. With in creasing cover, stands had correspondingly higher fractions of GV and shade, along with a decrease in the fraction of NPV. Closed-canopy stands had low fractions of NPV (contributed by exposed branches) and intermediate values of shade. Older stands with increasingly complex canopies had higher fractions of shade.

Conclusion

Spectral mixture analysis is an intuitive, more interpretable framework for image analysis. Natural environments can be well modeled using the simple mixing model (with green vegetation, NPV, soil, and shade endmembers). The resulting fractions can then be used to identify (classify) different land-uses and/or regrowth states. When applied over a time series, surface processes can be monitored. This approach is independent of imaging system and is generally applicable to multispectral images of natural environments.

This approach is independent of imaging system and is generally applicable to multispectral images of natural environments.

References

Adams, J. B., Sabol, D. E., Kapos, V., Almeida, R. Filho, Roberts, D. A., Smith, M. O., Gillespie, A. R., Classification of multispectral images based on fractions of endmembers: Applications to land -use change in the Brazilian Amazon, submitted to Remote Sensing of Environment, in revision, 52:137-154, 1995.

Gillespie, A. R., Smith, M. O., Adams, J. B., Willis, S. C., Fischer, A. F. III, and Sabol, D. E., Interpretation of residual images: Spectral mixture analysis of AVIRIS images, Owens Valley, California, Proceedings Airborne Science Workshop: AVIRIS, Jet Propulsion Laboratory, Pasadena, CA, 4-5 June, 243-270, 1990.

Green, R. O., Conel, J. E., and Roberts, D. A., Es timation of aerosol optical depth and calculation of apparent reflectance from radiance measured by the Airborne Visible/Infrared Imaging Spectrometer (AVIRIS) using MODTRAN2a, Proceedings Airborne Science Workshop: AVIRIS, Jet Propulsion Laboratory, Pasadena, CA, 25-29 October, 73-77, 1993.

Sabol, D. E., Roberts, D. A., Adams, J. B., and Smith, M. O., Mapping and monitoring changes in vegetation communities of Jasper Ridge, CA, using spectral fractions derived from AVIRIS images, Proceedings Airborne Science Workshop. AVIRIS, Jet Propulsion Laboratory, Pasadena, CA, 25-29 October, 157-160, 1993.

Sabol, D. E., Smith, M. O., Adams, J. B., Zukin, J. H., Tucker, C. J., Roberts, D. A., and Gillespie, A. R., AVIRIS spectral trajectories for forested areas of the Gifford Pinchot National Forest (abstract), submitted for Fifth Annual JPL Airborne Earth Science Workshop, January 23-26, 1995, 133-136, 1995.

Smith, M. O., Ustin, S. L. Adams, J. R., and Gillespie, A. R., Vegetation in deserts: II Environmental influences on regional abundance, Remote Sens. Environ. 31:27-52, 1990.

Landsat Pathfinder Humid Tropical Forest Project

William Salas

Institute for the Study of Earth, Ocean, Space
University of New Hampshire
Durham, New Hampshire

The project aims at significantly improving the most important source of uncertainty in our understanding of the role of biota in the global carbon cycle.

Over the last two centuries, the concentration of carbon dioxide in the atmosphere has increased by more than 25%, from about 275 ppm in the eighteenth century to more than 350 ppm in 1989. Most of the increase is attributed to the combustion of fossil fuels, but up to a third is thought to have come from deforestation. Approximately 90% of the current annual net release of 1.8 x 1015 g of carbon is due to deforestation is from the tropics. Ten countries comprise two-thirds of the net release (Brazil, Columbia, Indonesia, Ivory Coast, Laos, Malaysia, Mexico, Peru, Thailand, and Zaire). At 0.6 x 10 15 g C per year, the net flux from Brazil was the largest single biotic source of biogenic carbon in 1988.

The amount of carbon held in terrestrial ecosystems is changed as a result of 1) direct human effects of land use, such as deforestation, and 2) indirect human effects on ecosystems, such as increased concentrations of atmospheric CO2 or climate change, which influence changes in ecosystem metabolism. At the present time, the net flux of carbon between the biota and atmosphere due to land use change (deforestation) can be calculated with more confidence than changes in carbon storage associated with large-scale changes in ecosystem metabolism. This is because of the large difference in biomass between forests and the agricultural systems which replace them, and because deforestation and reforestation can be readily documented and quantified, particularly if remote sensing data are utilized.

Changes in the stocks of carbon due to land use change cannot be measured directly for the Earth as a whole, or for an area the size of the Amazon Basin. Instead, the net flux of carbon must be modeled. Such an approach utilizes three types of data: 1) rates and geographic distribution of deforestation, 2) the fate of the deforested lands, and 3) changes in the stocks of carbon in biomass and soils as a result of disturbance and recovery over time.

Models developed with improved geographic and temporal data on deforestation rates, better parameterization of the dynamic nature of deforestation and reforestation, and improved data on above- and below-ground carbon response characteristics are needed.

Satellite remote sensing is the only means for resolving discrepancies or quantifying temporal and spatial variations in deforestation rates. There are no reasons why satellite-based techniques cannot be applied to a large area like the Amazon Basin, or a significant portion of the tropical forest belt, to resolve the aforementioned controversies and uncertainty, and thereby provide vastly improved forcing functions for global carbon models.

Project Objectives

The NASA Landsat Pathfinder Humid Tropical Forest (HTF) Project is a collaborative effort between the University of New Hampshire's Institute for the Study of Earth, Oceans and Space, University of Maryland's Geography Department, and NASA's Goddard Space Flight Center. The project has three major objectives:

1. Utilize Landsat data to map deforestation in closed tropical forests at sub-kilometer resolution for a base period (e.g., 1986);

2. Utilize Landsat data to quantify and map the rate of deforestation by mapping the change from other time periods (e.g., 1975, 1992); and

3. Create a Landsat data set and science products for distribution in a digital geographic information system (GIS) format, and de velop an information management system (IMS) to manage data orders, archiving and processing and distribution of products.

Through these objectives, the project aims at improving significantly the most important source of uncertainty in our understanding of the role of biota in the global carbon cycle. At the same time, the project will contribute significantly to improving the database for several international policy initiatives including the Framework Convention on Climate Change, the activities of the Intergovernmental Panel on Climate Change, national emission inventories, and many others which focus on the role of tropical forests. It is hoped that the results of this project will simultaneously fulfill the needs of the global change research community, the international policy community, and national-level forest resources and economic development programs. The project will focus on the three regions where most of the tropical deforestation in the world has occurred: (1) the Amazon Basin, (2) Central Africa, and (3) Southeast Asia. Mapping deforestation in these three regions will account for the majority of deforestation activities in closed tropical forests worldwide and will account for approximately 75-80% of the current net biotic flux of carbon.

Mapping deforestation in the Amazon Basin, Central Africa, and Southeast Asia will account for the majority of deforestation activities in closed tropical forests worldwide and will account for approximately 75 to 80% of the current net biotic flux of carbon.

As part of NASA's Pathfinder Program the project has two goals:

1. To utilize large amounts of existing satellite technologies and data in new ways to address important global change research questions in advance of, and leading toward, the launch of the Earth Observing System (EOS).

2. To develop a foundation of experience for managing large amounts of satellite data for global change research prior to the launch of the Earth Observing System, thereby testing and proving the technologies and approaches for information management which will be needed by the community at large with the launch of the Earth Observing System.

The approach to Pathfinder is straightforward. The first step is the identification and acquisition of a pan-tropical, wall-to-wall Landsat digital data set of over 2500 Multi Spectral Scanner (MSS) and Thematic Mapper (TM) scenes from the EROS Data Center (EDC) archive and the archives of the foreign ground receiving stations with coverage of the study areas. A three-date data set has been selected based on data availability. The three dates, or epochs, being used are early-1970s (i. e., 1972-1974), mid-1980s (i. e., 1984 -1986), and early 1990s (i. e., 1989-1994). The exception to this plan is the use of 1978 data for the Amazon. This parsing of data analysis over three year epochs allows a much wider selection of low-cloud data from the

archive. Landsat MSS data is utilized for the two earliest epochs. The last epoch utilizes Landsat TM data. Once acquired, the digital data is then analyzed to create a science product data set: a digital map database, in a geographic information system, of the rate and extent of deforestation.

Digital Data Processing

Research and development activities for this project and a prototype project for the International Space Year suggest that the use of digital image processing in conjunction with editing, georeferencing and spatial analysis in a Geographic Information System are effective means for quantifying deforestation. Findings also indicate that the use of high resolution Landsat data may in fact yield much better precision than AVHRR-based analyses. The use of digital pre-processing with visual post-processing greatly reduces analysis time over that of hand digitization of a photographic product, and greatly reduces the confusion of classes associated with purely digital processing techniques.

Preliminary results from an accuracy assessment of the Amazon analysis revealed an overall accuracy of 89%.

After EDC pre-processes the imagery into a uniform, project-specific format, the digital data are first classified using traditional techniques based on unsupervised clustering and knowledge-based assignment of clusters to land cover classes. The output classes of interest are forest, deforested areas, secondary growth, non-forest vegetation, cloud, cloud shadow, and water. The secondary growth class represents areas that have been deforested and then abandoned and are regrowing (accumulating carbon). The digital classification is then converted to polygons and then plotted on clear vellum at 1:250,000 scale and compared with the 1:250,000 scale color composite prints provided by EDC. Digitizers check the label on each and every polygon for accuracy, make any necessary changes and add any missing polygons. This process is iterative, with quality assurance checking until the coverage is accepted for archiving. Quality control is carried out by trained supervisors with GIS training, forestry backgrounds and field experience. The accepted final coverages are stitched together scene by scene to build regional coverages in an edge-matching process. The edge-matching is performed to insure thematic and positional consistency within the overlap areas of the individual Landsat scenes. The final product is a seamless database.

Validation and Accuracy Assessment

To obtain an estimate of the accuracy of the final analysis, the project has developed a field-based accuracy assessment program. Objectives are to quantify the thematic and positional variance. This is done at three levels of analysis:

1. Experts in each region are consulted and insights are gained from their extensive knowledge of local conditions. To facilitate a close working relationship with experts in the countries and regions under study, a visiting scientists program provides support to colleagues from tropical countries to spend time in residence at the University of New Hampshire and University of Maryland. Visiting scientists spend anywhere from 2 to 12 months in residence.

2. Preliminary and cursory field excursions to various areas are conducted to get a good sense of on-the-ground conditions and to establish initial classification rules and procedures.

3. Systematic field validation exercises are conducted, where points on the field are selected and measurements are made using a Global Positioning System. The results of these field exercises are used to develop a statistical accuracy assessment using standard methods of presentation in contingency tables. In these field exercises, two aspects of accuracy are tested.

The first is thematic, assessing errors of omission and commission in classification of the images. The second, using the GPS and obvious features, assesses the geometric and positional accuracy of the image registration.

The project has established approximately 22 field test sites throughout the tropics. At each test site, as much ancillary data as possible is collected, as well as other sources of remote sensing data, including Spot 20 m multispectral data and JERS-1 ERS-1 SAR data. Field measurements are conducted at each test site. The test sites are also used for inter-laboratory comparisons, which helps with assessments of the variability between analyses conducted in the two different laboratories, and assessments of the variation in interpretation and classification within the laboratory. The latter is accomplished through repeated classification trials and comparisons with classifications performed using other data sources, such as Spot. Because the project also uses historical MSS data for the first two epochs, historical aerial photos are used to obtain reference data for the accuracy assessment. Some preliminary results from an accuracy assessment of the Amazon analysis revealed an overall accuracy of 89%.

Almost 30% of the disturbed forest area is in some form of secondary growth.

Some of these field test sites are also used for examining the land cover change dynamics between the nearly decadal assessments for each epoch. Annual Landsat and Spot observations are analyzed to look at annual rates of clearing and abandonment in an attempt to understand the land use practices driving the deforestation. These sites are spread out across the tropics in an attempt to characterize many of the more wide spread land use/land cover change dynamics associated with tropical deforestation.

Results from the Humid Tropical Forest (HTF) Project to date indicate that in the Amazon in 1986 there was 245,415 km2 of deforestation, and of the deforested area, 72,305 km2 were in secondary growth. This suggests an annual rate of deforestation from 1978 to 1986 of 18,000 km2 The secondary growth numbers highlight the fact that almost 30% of the disturbed forest area is in some form of secondary growth. Figures 18.1 and 18.2 present the extent of the 1986 deforestation and secondary growth, respectively. The full resolution data has been gridded to 16 km cells and shaded according to the percentage of each 16 km cell that has been deforested or is in secondary growth.

All of the Landsat data used by the HTF project is available from the Land Processes Distributed Active Archive Center (DAAC) at the EROS Data Center. Information on how to obtain data from the DAAC can be found at the EDC homepage (http://sun1.cr.usgs.gov /landdaac/landdaac.html). The derived products will initially be available from the Landsat Pathfinder HTF project (http://pathfinder-www.sr.unh.edu/pathfinder) and eventually from the DAAC at EDC. Preliminary data on the extent of forest in several countries in Southeast Asia is shown in Table 18.1.

Region	Forest Area 1973	Forest Area 1985	Rate (1973-1985)	% Loss
Thailand	224,976	169,413	4,630	24
Cambodia	51,620	41,197	868	20
Laos	176,370	163,818	1,046	7
Vietnam	193,711	158,759	2,912	18

Table 18.1

Preliminary estimates of the extent of forest in several countries in Southeast Asia. Areas are in square kilometers and rates are in square kilometers per year. The estimates are preliminary because the analysis is not complete.

Satellite remote sensing is the only means for resolving discrepancies or quantifying temporal and spatial variations in deforestation rates. Such data can thereby provide vastly improved forcing functions for global carbon models.

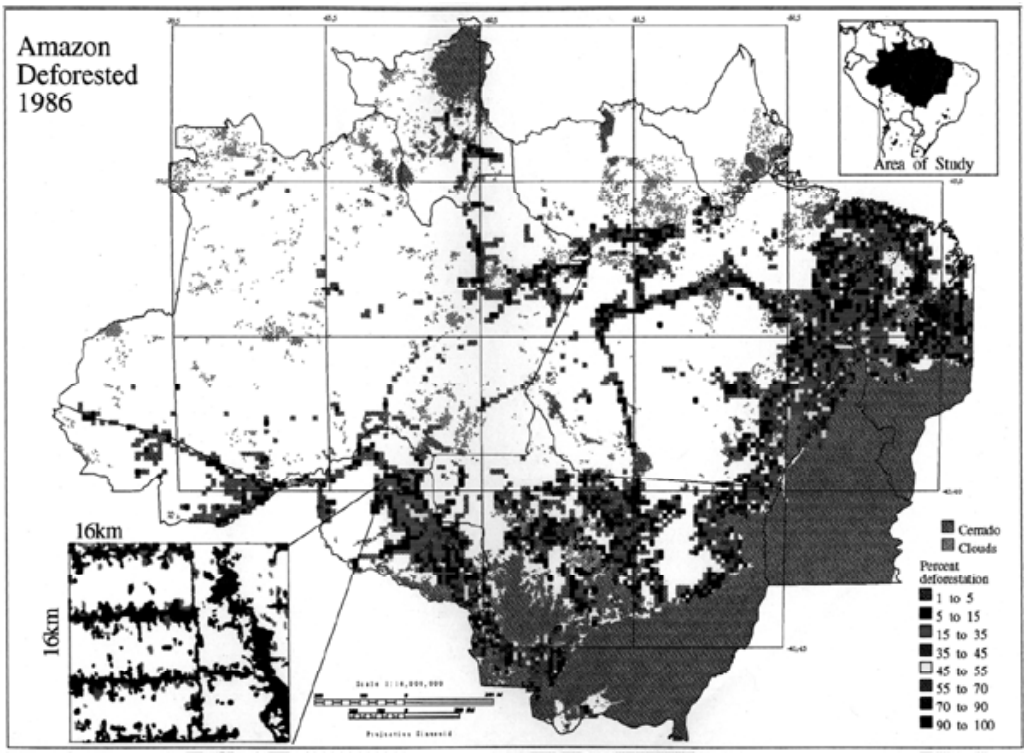

Figure 18.1
Extent of Amazon Deforested in 1986

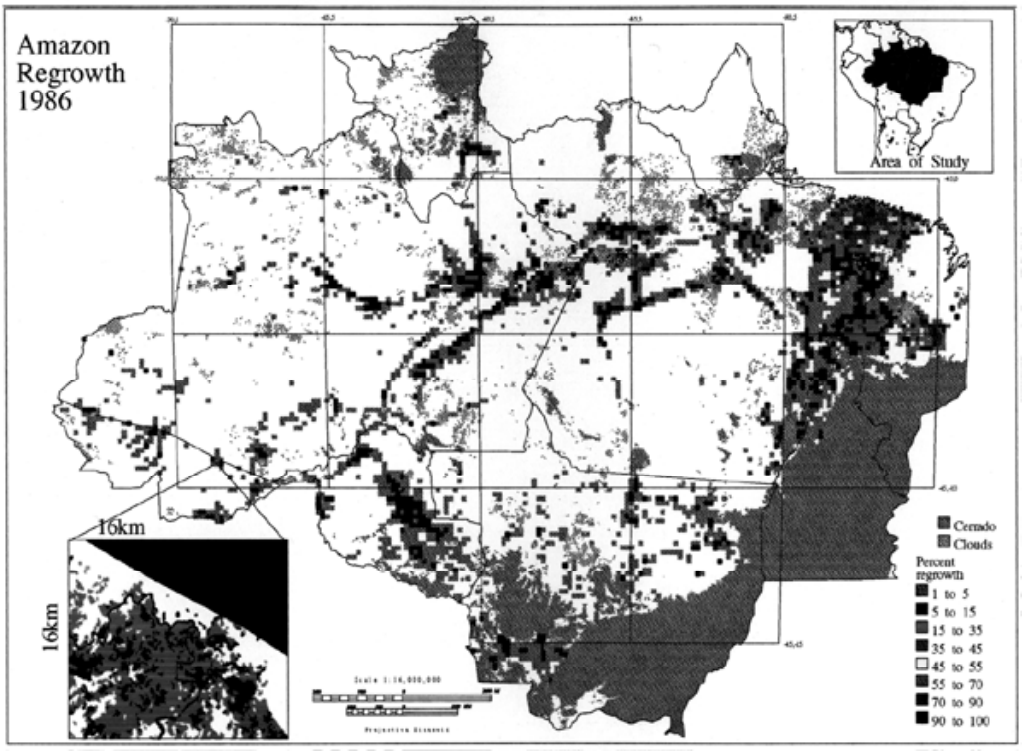

Figure 18.2
Extent of Amazon Regrowth in 1986

Human Impacts on Terrestrial Vegetation

Compton J. Tucker

Terrestrial Physics Lab
NASA/Goddard Space Flight Center
Greenbelt, Maryland

In forested parts of the world, it is relatively easy to see human impacts on terrestrial vegetation and to discern them from natural impacts. In non-forested areas, such as arid and semi-arid regions, it is much more difficult to distinguish human from natural impacts.

In attempting to evaluate human impacts on vegetation, the area of study is quite large - the entire terrestrial surface of the globe. Therefore, satellite data are needed to obtain the necessary coverage of space and time. In addition, smaller scale process studies that can be extrapolated to larger areas are needed, as well as output from models from which predictive capacity can be gained. In pursuing these various methodologies, there is the problem of differing scales. Coarser scales involve more abstraction as well as the possibility of more errors. Some studies need to go all the way down to the 1 meter by 1 meter scale, if not to the individual leaf, while others go all the way up to hundreds of square kilometers. In situ measurements, satellite data and models, are all needed to gain an understanding of change in global vegetative cover.

The issue of deforestation has received spurts of interest from the popular press. There is a great deal of confusion and widely varying claims regarding the actual rates of deforestation in Amazonia and elsewhere. Consequently, new research is needed to provide improvement over the present inadequacy of knowledge. This subject can be approached incrementally and much can be learned from the process.

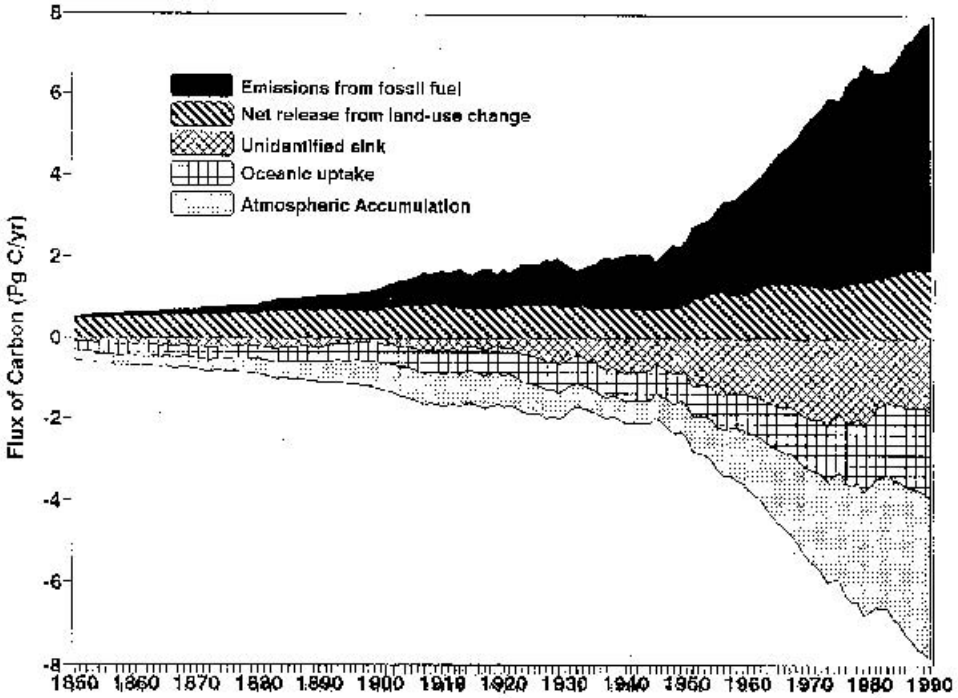

Figure 19.1
Flux of Carbon, 1850-1990

In forested parts of the world, it is relatively easy to see human impacts on terrestrial vegetation and to discern them from natural impacts. In non-forested areas, such as arid and semi-arid regions, it is much more difficult to distinguish human from natural impacts.

Figure 19.1 shows global sources and sinks of carbon and demonstrates the uncertainties that exist regarding the global carbon cycle. In some variables, there is a high degree of certainty, including the fossil fuel contribution and oceanic uptake. Other areas are not as well understood and need further refining, including the mid-latitude terrestrial carbon sink and the impacts of land use change.

There are naturally occurring variations in the climate system, such as the El Niño-Southern Oscillation (ENSO), which are closely correlated with regional climatic events. A good example is the direct correlation between an El Niño-induced rise of sea surface temperature (SST) in the Pacific and maize yield in Zimbabwe. Similarly, a satellite-derived vegetation index for Brazil is highly correlated with tropical Pacific SST. The alteration in the rainfall regime causes the vegetation index to rise with rising SST. These are examples of how natural phenomena, which may or may not be affected by humans, can affect rainfall and climate, and hence vegetation patterns on a regional scale. These stand in contrast to forest removal, where the role of humans is unequivocal.

It is important to avoid simplistic interpretations and recognize that there is large inter-annual variation.

The 1991 eruption of Mount Pinatubo injected a huge cloud of sulfate aerosols into the atmosphere, creating a significant climatic forcing, cooling the planet as a whole and possibly affecting vegetative response and patterns. This an example of a natural phenomenon which caused a global-scale perturbation of the system. There is so much interaction among the variables that much confusion exists with regard to causation.

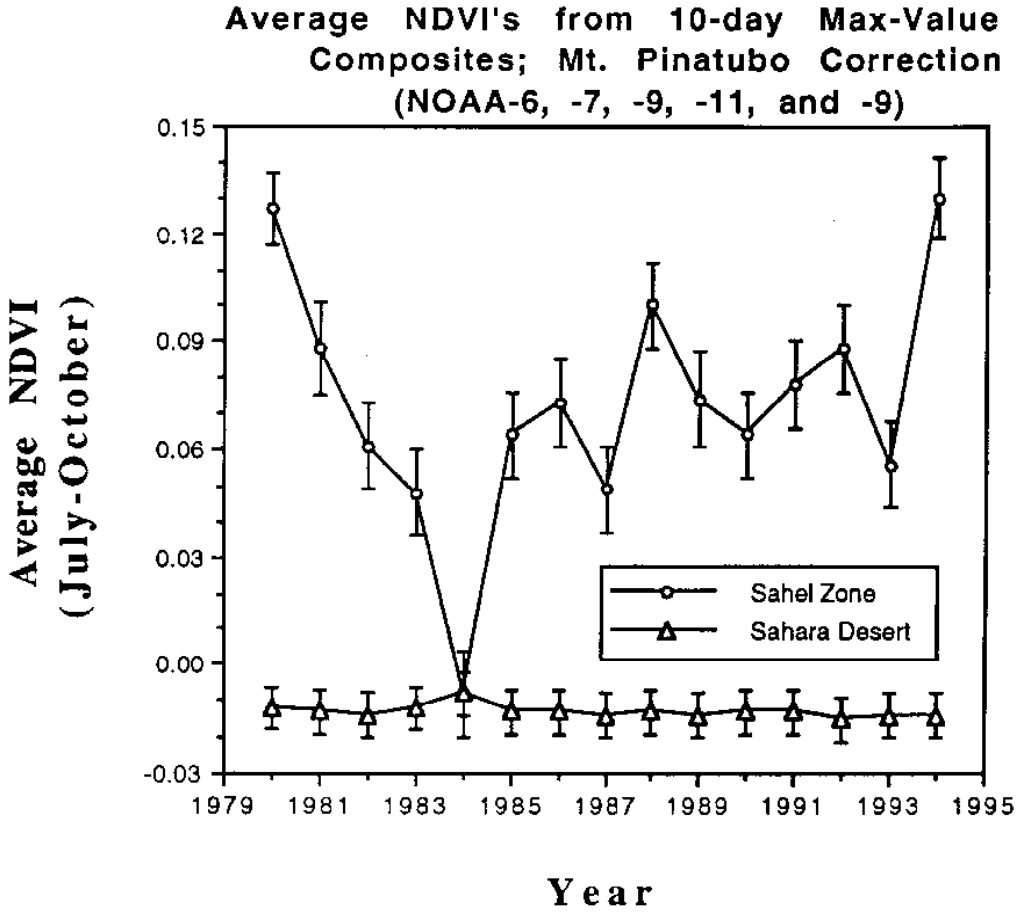

Figure 19.2
Average NDVI of the African Sahel zone

African Sahel

In the Sub-Saharan African Sahel, a region dominated by seasonal semi-arid grassland, rainfall records show that from 1949 to 1970, conditions were wetter than usual. This was followed by a period of approximately 15 dry years, a drought which led to allegations of anthropogenic regional climate forcing. It was suggested that the principal mechanism for initiating this feedback was overgrazing and removal of trees for firewood. Because these areas are arid and marginal to begin with, they are most at risk for these kinds of changes.

Charney et al. of MIT hypothesized that in creasing human land use in the arid zone would remove litter and vegetation, thereby drying the land and increasing its albedo. This would reflect more sunlight away, causing the region to become cooler, and lessening convective activity. This would decrease rainfall, further drying the land and continuing a climate feedback that would make the region drier. After examining this region with satellite data, Tucker believes it is difficult to sort out the human impact from the natural variability.

Figure 19.2 shows the importance of taking a longer timescale look at data before drawing conclusions. If the 1980 to 1984 numbers were all the data available, they would suggest that the system had crashed. But the longer time scale reveals that there has been a recovery of the vegetation. It is important to avoid simplistic interpretations and recognize that there is large interannual variation. A baseline is needed to discern human-caused versus natural variation. Is this global change or is it a basically stable system with a high degree of variation?

Pacific Northwest Forests

Because of gross changes in surface conditions between land which is forested and that which is not, it is relatively easy to discern human impact in these regions. A checker board pattern shows up in remotely sensed images of forests that have been cut corresponding to a pattern of private holdings within public lands. Landsat Thematic Mapper mosaics of late succession coniferous forests of the U. S. Pacific Northwest show that in that region, the remaining old growth forest is almost exclusively at higher elevations and on Federal land. The scarcity of old growth forest on private land is largely due to the high economic value of old growth trees - a 200 to 300-year-old Douglas Fir can be worth $5000 to $7000 just for the felled tree.

The darker areas in the image are old growth forests which have more variation in tree height and hence more shade. Cut forests have less shade because new-growth trees are mostly the same height. The forest of the U. S. Pacific Northwest is tremendously fragmented due to the high degree of timbering on private land and the Forest Service policy of distributing timber cuts. This high degree of habitat fragmentation causes great problems for the Northern Spotted Owl and other species that require large contiguous blocks of undisturbed old growth forest.

Brazilian Tropical Rainforest

Tucker and colleague David Skole undertook a study of satellite data, coupled with several site visits, in an attempt to get definitive answers and repeatable results regarding deforestation in Brazil over the last 20 years.

There are large areas with little human activity. The impact of native indigenous people is usually quite small, with a few exceptions. There are large tracts of undisturbed forest as well as areas that are severely fragmented. The transportation network is the principal conduit for

In the edges of forests, hunting, predation by feral animals, drying due to microclimate conditions, and other biological and physical effects, greatly impact the biodiversity in a one kilometer area around the edge.

colonization of the forest, which leads to deforestation. Where there are no roads, there is little deforestation. Prior to road building, lake areas were the main ones colonized, so new growth forests are often found there.

The region is not all Amazonian high forest. There is also some cerrado (savanna) which has been converted to agriculture, since it is easier to use cerrado for agriculture and the soils can be better than tropical forest. Thus, there tends to be less impact on tropical forest in these areas.

Skole and Tucker estimated deforestation over of 5 million km2 in the Brazilian Amazon. They found that in 1978, approximately 80,000 km2 were deforested, and that by 1988, this had increased to about 230,000 km 2 In addition to outright deforestation, they also examined areas of isolated forest (those cut off from areas of contiguous forest), and the totality of "edge effect." In the edges of forests, hunting, predation by feral animals, drying due to microclimate conditions, and other biological and physical effects, greatly impact the biodiversity in a one kilometer area around the edge.

The results of these investigations revealed a much higher figure for habitat fragmentation than for deforestation, which is important with regard to biodiversity.

The results of these investigations revealed a much higher figure for habitat fragmentation than for deforestation, which is important with regard to biodiversity. When isolated forest and edge effects were included, they found that 600,000 km2 of tropical forest were affected with regard to impacts on biodiversity. The use of satellite data and selected ground visits help to break out results like this in an effort to reduce uncertainty in this area.

In Brazil, from 1990 on, the government instituted close monitoring and policing of fires. They actively enforced existing laws and put an end to subsidies that encouraged rainforest destruction. Through these policies, Brazil's deforestation was reduced to about 10,000 to 12,000 km2 of new deforestation per year, a rate of clearing of about 1/4% per year, equal to a 400-year rotation. By comparison, on private land in the U.S., there is a 50- to 75-year rotation; and on Federal land about a 100-year rotation or a 1% clearing rate per year.

Smoke Emissions From Biomass Burning

Darold E. Ward

Intermountain Research Station, Forest Service
U. S. Department of Agriculture
Missoula, Montana

The International Global Atmospheric Chemistry Program (IGAC), a core project of the International Geosphere Biosphere Program (IGBP), has emphasized experiments in tropical regions of the world to reduce the uncertainties regarding the contribution of biomass burning to the buildup of greenhouse gases in the atmosphere. Most of the research discussed by Ward was done in response to the objectives for the IGAC Program and relates to the global carbon balance. Biomass burned globally is estimated at 6,366 teragrams per year at combustion efficiencies ranging from 0.80 to 0.97. Combustion efficiency is the ratio of carbon released as carbon dioxide (CO2) to the total carbon released by a fire. This is basically the efficiency with which a fire converts carbon to CO2.

In per capita terms, some developing countries may now be generating more CO2 through land use change than developed nations release from fossil fuel combustion.

According to the FAO, deforestation has increased from 11 million hectares in 1980 to nearly 17 million hectares in 1991. It is more difficult to quantify CO2 emissions from biomass burning than from fossil fuel use. In per capita terms, some developing countries may now be generating more CO2 through land use change than developed nations release from fossil fuel combustion.

The Vegetation Fire Information (VFI) System is a proposed method, accepted by IGAC, for assessing the temporal and spatial extent of fires in different ecosystems in different regions of the world and their contribution to smoke emissions [Malingreau et al., 1993]. The VFI System relies on satellite methods of detecting fires. AVHRR and other satellite systems do not typically detect all individual fires. Generally, very little information is provided regarding the size of fires, making additional data necessary. The temporal effect of change in area burned per lit-up pixel is adjusted based on the application of fire behavior models that respond to weather. The VFI System incorporates the effect of land-use change and succession models, to develop knowledge about fuel loading and the structure of fuel. It also makes use of fire behavior modeling coupled with land cover modeling, and emissions modeling to provide estimates of source strength for regional areas. The results from the VFI System are proposed to be checked by flying aircraft along transect lines to estimate the flux of emissions. Ultimately, through an iterative process, the predictability of source strength for a region can be improved to an acceptable level of accuracy.

Smoke Emissions

When biomass combines with oxygen in a heated environment, combustion occurs. The completeness of combustion in producing CO2 is dependent on the chemical mixture of fuel and air. Products of combustion, many of which technically are products of incomplete combustion, can be described by the combustion efficiency. The combustion efficiency ranges from 0.80 to

as high as 0.97. Variables affecting smoke emissions include fuel type, fuel load, fuel chemistry, fuel moisture content, packing ratio for the fuel particles, surface area to volume ratio, and method of ignition. Correlating fuel parameters and other factors of combustion can help predict combustion efficiency and emission factors for fires.

The average release of carbon from a fire is approximately as follows: 88% CO2, 9.5% Carbon Monoxide (CO), 0.5% Methane (CH4), 0.5% non-methane hydrocarbons (NMHC), and 1.5% in particles of less than 2.5 microns diameter (PM2.5).

Vegetation consumed by fire is about 50% carbon (ranging from 47.5% in savanna vegetation to 51-52% for coniferous ecosystems). The measured carbon in a unit volume of emissions above background levels is used in estimating the amount of fuel consumed in producing the emissions and expressed as an emission factor (g/kg).

The FASS is an instrument developed specifically to study smoke emissions from a range of fire conditions as a function of the rate of carbon release.

The Fire Atmosphere Sampling System

The Fire Atmosphere Sampling System (FASS) has been used extensively by Ward et al. [1992] for characterizing smoke emissions on areas with measured fuel characteristics (see Figure 20.1). The FASS is an instrument de veloped specifically to study smoke emissions from

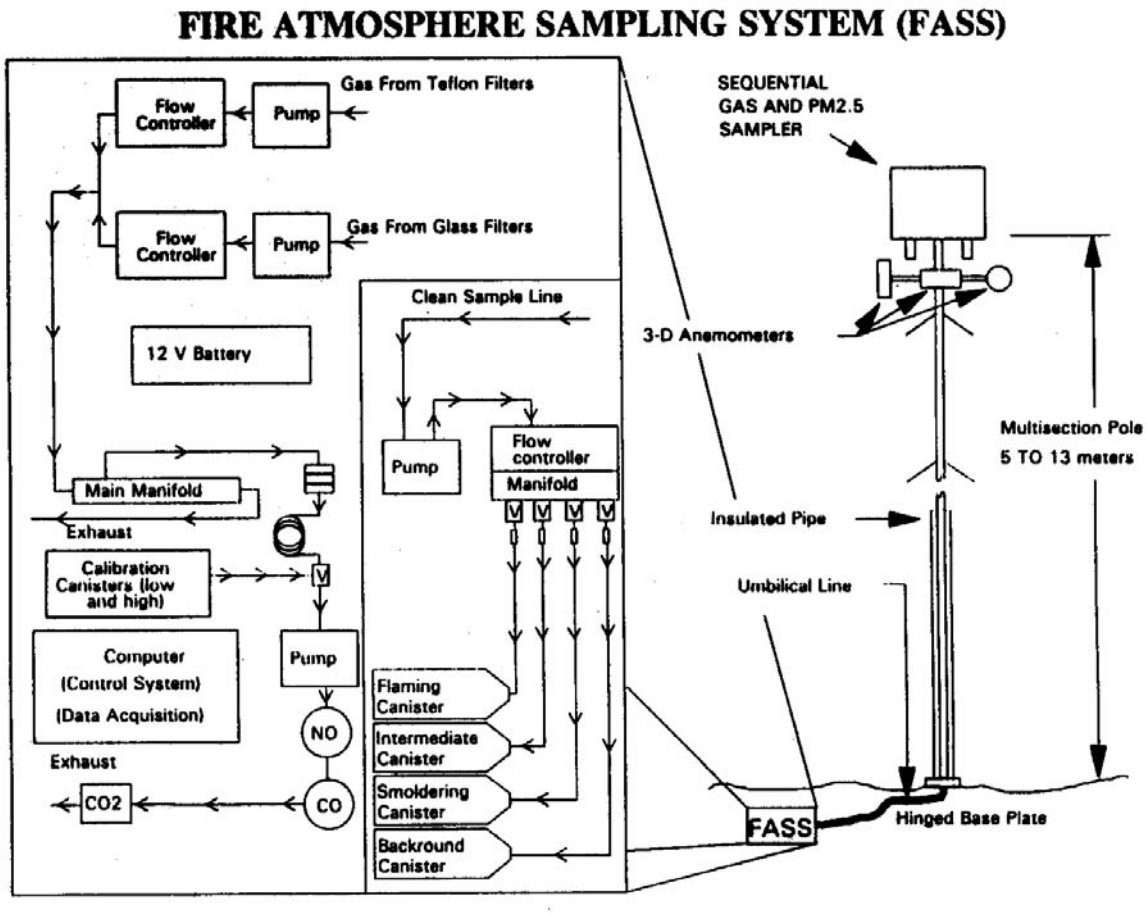

Figure 20.1

a range of fire conditions as a function of the rate of carbon release. It is computer controlled and measures CO2, CO, and NO concentrations, vector wind components, temperature, and other parameters that are logged once each second. Grab samples of particulate matter are collected concurrently with samples of the combustion gases by phase of combustion. A light absorption meter and integrating nephelometer measure the light absorption and scattering by particles by phase of combustion, respectively. Samples of the PM2.5 are collected on filters at the top of a tower and the gases are sampled through a line running from the top of the tower to the ground. The main part of the FASS is placed underground near the base of the tower. The FASS is completely automatic once it is armed and goes through background sampling, calibration, and phase of combustion sampling automatically.

Results And Discussion

Emission factors for the release of emissions of CH4 for savanna fires are about 12% of the emission factors for fires used to burn debris during conversion of primary forested areas. Emissions of CH4 from burning of cut second-growth forest sites is intermediate to savanna and primary forest sites. Emission factors for pasture burns in the Brazilian Amazon have been found to be about 20% larger than for cerrado area savanna burns.

For savanna ecosystems ranging from semi-arid to humid savanna ecosystems, models have been developed for predicting combustion efficiency using the ratio of the amount of grass to the sum of grass and litter. Models have also been developed for estimating emission factors for a range of compounds and particulate matter as a function of combustion efficiency for these same savanna ecosystems. There is a need to incorporate net primary productivity models into the system for smoke production for the African savanna ecosystems.

Carbon released from fires used for converting primary forested areas to agriculture in the Amazon can last for several days with over 50% of the biomass consumed through smoldering combustion. Areas of savanna burned by fires usually have smoldering combustion carbon released that is 10 to 15% of that during the flaming phase of combustion. Carbon models that are coupled with land use data by region are needed.

Emissions of hydrocarbons and other carbon-containing compounds were studied for charcoal making in Zambia and Brazil. A preponderance of the hydrocarbons are oxygenated for the two types of kilns studied: brick style for Brazil and earthen construction for Zambia. Both kiln types were operated using wood cut from open forested savanna ecosystems. The Zambian earthen kilns converted 23-25% of the wood to charcoal whereas the Brazilian brick kilns were of a higher efficiency, converting approximately 35% of the wood to charcoal. It is practical in Brazil to transport wood to the brick kilns, whereas in Zambia, this may be impossible. Fire management programs are needed to sustain the production of charcoal and recovery of the forested areas used in the production of wood for fire wood and the making of charcoal.

The Zambian earthen kilns converted 23-25% of the wood to charcoal whereas the Brazilian brick kilns were of a higher efficiency, converting approximately 35% of the wood to charcoal.

The FASS packages have been used to develop carbon release and emission factors for fires used with shifting cultivation in southern Africa. The chitemene style of agriculture is used to concentrate nutrients on large areas of 2 to 5 hectares on garden spots of 0.5 to 1 hect are. The tops and limbs from trees are harvested and used to create a uniformly deep pile for the garden spot. The pile is burned immediately prior to the onset of the rainy season, typically in October. Agriculture is practiced on each garden spot for 5-7 years before abandonment. The active pile burns and burns of the fallow chitemene sites have been studied for smoke emissions. The results for the fallow chitemene sites follow the same trends found by Ward et al. (1995) for

burns of miombo and dambo savanna ecosystems. Fire management practices are needed to decrease the time of recovery of forested areas to sustain the chitemene style of agriculture.

The VFI System will require good emission factors and biomass consumption models for the major ecosystems on a global scale. This research needs to be extended to other ecosystems, especially those in Asia, to complete the development of models for predicting emissions from fires.

References

Ward, D. E., R. A. Susott, J. B. Kauffman, R. E. Babbitt, D. L. Cummings, B. Dias, B. N. Holben, Y. J. Kaufman, R. A. Rasmussen, and A. W. Setzer. 1992. Smoke and fire characteristics for Cerrado and deforestation burns in Brazil BASE-B Experiment. J. Geophys. Res. 97:14,601-14,619.

Malingreau, J.-P., F. A. Albini, M. O. Andreae, S. Brown, J. S. Levine, J. M. Lobert, T. A. Kuhlbusch, L. Radke, A. Setzer, P. M. Vitousek, D. E. Ward, and J. Warnatz. 1993. Group Report: Quantification of fire characteristics from local to global scales, Fire in the Environment: The Ecological, Atmospheric, and Climatic Importance of Vegetation Fires . edited by P. J. Crutzen and J. G. Goldammer, John Wiley & Sons Ltd., pp. 329-343.

Ward, D. E., W. M. Hao, R. A. Susott, R. A. Babbitt, R. W. Shea, J. B. Kauffman, C. O. Justice. 1995. Effect of fuel composition on combustion efficiency and emission factors for African savanna ecosystems. Accepted for publication J. Geophys. Res.

Susott, R. A., S. P. Baker, G. Olbu, D. E. Ward, and J. B. Kauffman. 1995. “Carbon, hydrogen, and nitrogen content of tropical ecosystem fuels,” in Biomass Burning and Global Change, edited by J. S. Levine, in preparation.

Modeling Land Cover and Anthropogenic Changes in Biogeochemical Cycles

Michael White

University of Montana, School of Forestry
Missousla, Montana

Over the past two decades, scientists have developed an increasingly refined ability to quantify and monitor the surface of the Earth through the use of satellite remote sensing. In particular, as our understanding of humanity's role in altering global patterns of vegetation and weather has increased, so has our interest in the detection of anthropogenic changes in land cover.

The term land cover itself is open to multiple interpretations. Since the introduction of the first, and still widely used, comprehensive global land cover classification (Matthews, 1983), a proliferation of studies has led to considerable confusion as to the extent and definition of major biomes (see figure i.1,Townshend, 1991). Townshend concluded that the next step in land cover modeling should be a satellite-derived classification scheme.

Such a classification would help to fulfill a growing need for accurate, repeatable, and globally extensive land cover maps. While the number of desired land cover classes varies considerably by discipline, a biome level classification is often used for large-scale terrestrial ecosystem modeling. In fact, obtaining biome distribution is one of only four critical precursors to implementation of the current generation of large scale biogeochemical (BGC) computer simulation models. The second requirement is Leaf Area Index (LAI), a dimensionless variable representing the ratio of leaf to ground surface area. LAI can be approximated from remote sensing, most commonly as a function of the Normalized Difference Vegetation Index (NDVI) and biome type. Daily climate and topography are also required.

For individual biome types, such as grass, deciduous broadleaved, or evergreen needleleaved, White and colleagues have created detailed files which include factors such as respiration coefficients, carbon to nitrogen ratios, and other basic physiological parameters. This file, with the addition of LAI, topography and climate, is then used to execute one of the family of BGC models, ranging from stand to global levels. Outputs from BGC models include Net Primary Production (NPP), respiration, and evapotranspiration, among others.

As topography and climate are relatively easy to obtain, and LAI is calculated from NDVI and biome type, representing biome distribution becomes extremely important in regional to global ecological modeling.

The purpose of White's presentation was to provide a basic outline of current satellite-driven land cover modeling activities at the Numerical Terradynamic Simulation Group (NTSG) at the University of Montana. Throughout development, the group's goal has been to produce a land cover classification scheme which is 1) based on clearly defined vegetation structure; 2)

Obtaining biome distribution is one of only four critical precursors to implementation of the current generation of large scale biogeochemical computer simulation models. The other requirements are leaf area index, daily climate and topography.

driven by remotely sensed data; and 3) useful to large-scale carbon models. Within this overall framework, three primary stages have been completed.

Stage One, Original Logic

Running et al. (1994) presented the initial logical concept for a global vegetation land cover classification. A series of decisions is used to drive the implementation logic (Figure 21.1). First, permanence of above-ground woody biomass separates grasses and broad leaf crops from trees and shrubs. The length of the growing season, possibly defined as the length of time the NDVI curve stays above a threshold value (Figure 21.2), could be used to make this first decision; a longer duration above the threshold defines year-round biomass.

The addition of surface temperature and a seasonal trajectory component enhanced the operational capability of the original logic.

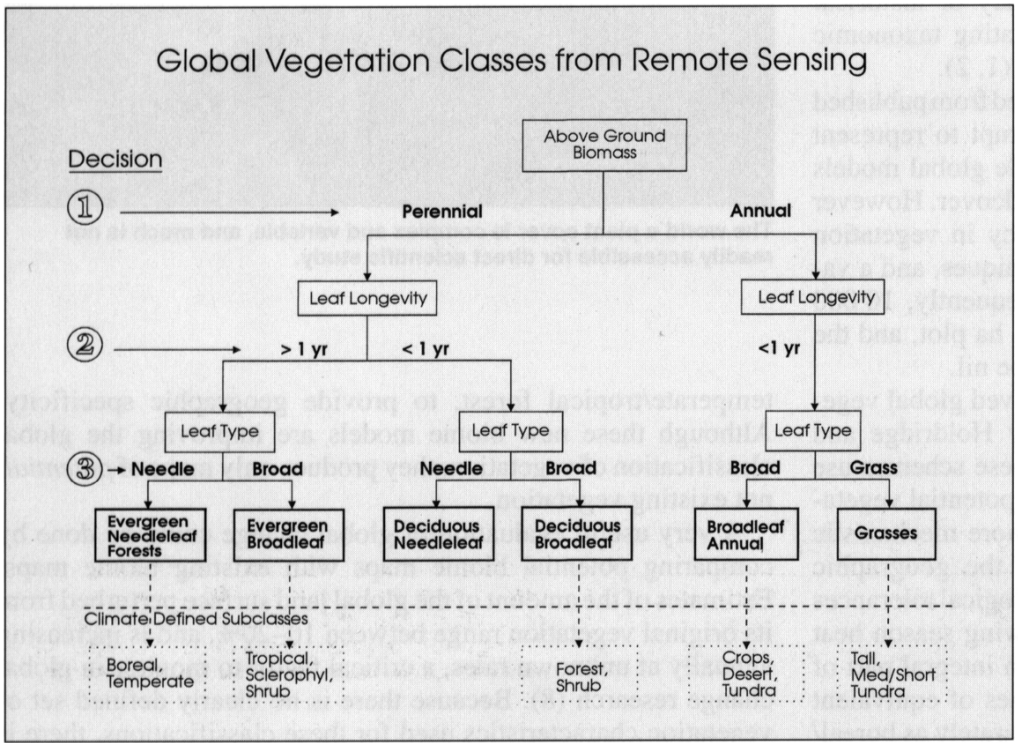

Figure 21.1
A flowchart of our global vegetation classification logic. Each simple box identifies the variable being defined, and each decision point is illustrated. The final six classes of vegetation are shown in bold. Below the dotted line, potential- climate defined subclasses corresponding to more common classification schemes are suggested.

Second, leaf longevity is used to distinguish between vegetation types which maintain leaf cover for more than one year and those that do not. The amplitude of the NDVI curve is theorized to differentiate between evergreen (low amplitude) and deciduous (high amplitude) vegetation types. For grasses and broadleaf annuals, this is not an issue, since all the cover types are deciduous. For trees and shrubs, though, this is an important distinction. Third, leaf type, needleleaf or broadleaf, is defined. This last division differentiates between, for example, oak (deciduous broadleaf) and pine (evergreen needleleaf). For theoretical discussion of possible implementation of this methodology and associated problems, see Running (1994).

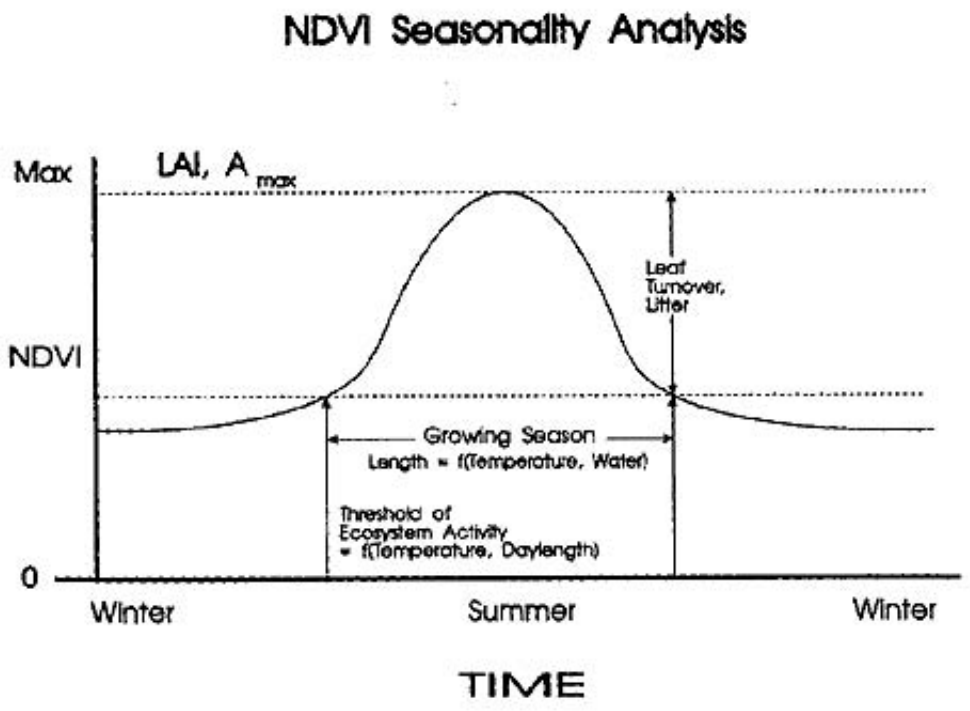

Figure 21.2
A conceptual diagram of how the seasonal trace of Normalized Difference Vegetation Index (NDVI) data may be used to distinguish perennial from annual above-ground biomass types, based on minimum thresholds, and leaf longevity, or evergreen from deciduous classes, based on NDVI amplitude.

Stage Two, Implementation

This logic defined the framework from which subsequent modifications were built. Using the 1991 bi-weekly composite NOAA/AVHRR dataset from the EROS Data Center, White and colleagues classified the biome cover of the conterminous U. S. (Nemani, in press). While similar to the logic outlined by Running, this classification included numerous modifications. Essentially, the addition of surface temperature and a seasonal trajectory component enhanced the operational capability of the original logic.

The first decision relies on surface temperature, calculated from thermal infrared (TIR) channels 4 and 5, to separate groups with typically high canopy temperatures (groups I and III, Figure 21.3) and groups with lower canopy temperatures (groups II and IV, Figure 21.3). A 35 degree threshold was used for this distinction, based on empirical evidence that well-watered closed canopies do not exceed 32 degrees C. It was assumed that even when water stressed, the aerodynamically rough canopies of forests will mix well with the atmosphere, and temperatures will usually not elevate by more than 2 to 3 degrees. Crop, grass, shrub, and barren areas, which are relatively smoother aerodynamically, will not mix well with the atmosphere and may reach canopy temperatures well above ambient levels.

Second, an NDVI threshold of 0.4 was used to separate group I (barren, shrub, and grass) from group III (crops) and group II (wetlands and non-vegetated) from group IV (forest).

Distinction of forest/non-forest was 90%. Forest type detection was also good, while shrubs and barren class detection was slightly lower. Grasses and crops were identified with the least success. In general, the classification captured the major distribution of significant biomes.

The underlying theory for this threshold is the assumption that at an NDVI of 0.4, 75% of photosynthetically active radiation (PAR) has been absorbed. Forests and crops, then, were assumed to absorb more than 75% of PAR.

The classification into four groups is iterated for each composite period. Typically, most classes begin in Group II, energy limited, and then move toward another group. Whichever group besides Group II the pixel occupies a majority of the time becomes the final group classification.

In areas where human land use has resulted in the removal of native forest vegetation for agriculture or grazing, there has been an evident reduction in LAI. Southeast Asia, western Europe, parts of Africa, and India, are areas where this pattern appears to dominate.

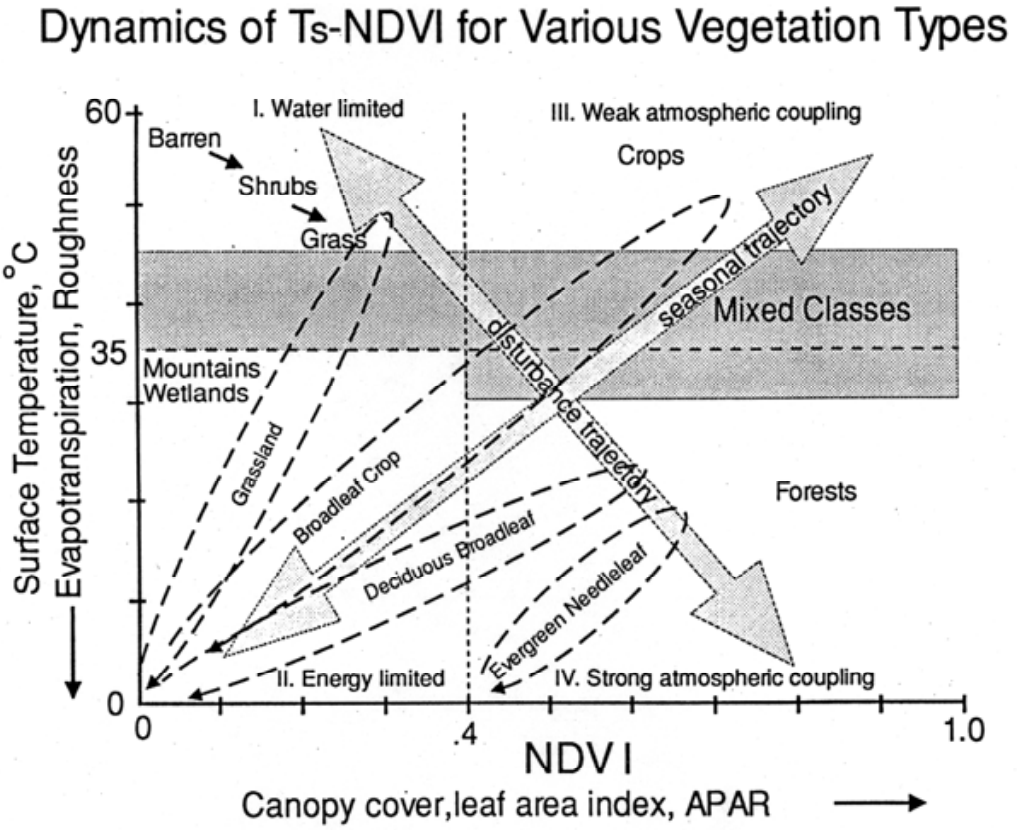

Figure 21.3
Dynamics of Ts- NDVI for Various Vegetation Types

Group I was further separated into barren, grass, and shrub by computing a growing season average NDVI, NDVIgs defined as the average of the NDVI composite periods with surface temperature above 5°C. Barren areas were assumed to have low NDVIgs, shrubs intermediate, and grass high. Group II, wetlands and non-vegetated, was also separated using NDVIgs. Group III was divided into deciduous and evergreen using NDVIgs. Further separation into broadleaf or needleleaf was achieved with a near infrared (NIR) threshold, based on empirical evidence that coniferous canopies, especially boreal forests, have low NIR reflectances. Crops required no further separation.

Results were validated by comparing the group's land cover image to a reclassification of Loveland's 1990 map. Distinction of forest/non-forest was 90%. Forest type detection was also good, while shrubs and barren class detection was slightly lower. Grasses and crops were identified with the least success, possibly because of common land cover mixing which is difficult to detect at 1 km resolution. In general, though, the classification captured the major distribution of significant biomes.

Stage Three, Anthropogenic Influences

An initial analysis of the impacts of human land use practices on global biogeochemical cycles has been completed (Nemani, in press). This area of work is controversial because of the difficulty in establishing pre-agricultural land cover distribution. Nonetheless, a dataset based on long-term climate and soil types was used to derive biome distribution, grided to 0.5 degrees. Standard physiognomic plant optimization theory was used to calculate a maximum historical LAI. Biome BGC, an NTSG ecosystem simulation model, was iterated until LAI reached a stable value. Modern biome distribution was taken from a current atlas-based land cover map. Biome distribution and the 1985-1990 NOAA Global Vegetation Index (GVI) were used to calculate current global LAI. Maximum values from each of the six years were selected and then averaged to arrive at a single NDVI value in the hope of minimizing cloud contamination.

While all usual Biome BGC outputs were generated, the focus here is on changes in LAI from historical to current conditions. LAI is assumed to be a crude surrogate for biomass. Two types of land use change seem to have resulted in distinct patterns of vegetation change. In areas where human land use has resulted in the removal of native forest vegetation for agriculture or grazing, there has been an evident reduction in LAI. Southeast Asia, western Europe, parts of Africa, and India, are areas where this pattern appears to dominate. Conversely, other areas of the world, such as the southeast United States and eastern Australia have experienced increases in LAI as a result of agricultural development.

White and colleagues recognize that the NOAA GVI has problems in terms of cloud contamination, multiple satellite calibration, and inadequate atmospheric corrections. Nonetheless, their simple analysis seems to have captured known patterns of global land use. Currently, the group is working to analyze global land use impacts using a remote sensing derived land cover map. Herein lies the potential for global change monitoring: to create decadal, remote sensing derived global land cover maps, and thus to monitor the ongoing impacts of human land use, and ultimately to suggest political and economic strategies to ameliorate negative impacts.

Herein lies the potential for global change monitoring: to create decadal, remote sensing derived global land cover maps, and thus to monitor the ongoing impacts of human land use, and ultimately to suggest political and economic strategies to ameliorate negative impacts.

Working Group Report on Land Cover Detection in Savanna and Steppe Regions of the World

Appendix 1: Session One Working Group 1

Changes in land use and environmental factors which alter the extent of woody vegetation in the savanna and steppe regions influence the energy, hydrological and biogeochemical fluxes within these ecosystems.

Background

In global change studies, the investigation of Earth surface properties needs to be dynamic in approach. However, past applications of remote sensing techniques have been more synoptic and provided current status of Earth surface and atmospheric conditions. Recently, a concerted effort has been undertaken to better document changes in Earth surface properties, especially in terrestrial ecosystems undergoing rapid changes.

Current issues related to land use change and changes in land cover are applying dynamic modeling and field studies to assess process level changes in association with changes in land cover related to environmental and land use changes. These studies are limited in space because site level studies are constrained by the number of sites that can be investigated. The linking of multi-temporal remote sensing studies and process level studies in order to develop a method of assessing regional and global dynamics to changes in climate or land use will be needed.

In the savanna and steppe regions of the world, land surface and ecosystem properties have not been well documented. These regions are important because of their areal extent and the human population which depends on them. These ecosystems are sensitive to changes in rainfall, temperature, and land management practices which determine the extent of woody and grass species cover. Changes in land use practices are continuing to modify these ecosystems due to population pressures and intensification of land use practices (e. g., grazing intensity, cropland expansion, agroforestry expansion, fuel wood extraction, etc.). These changes in land use and environmental factors which alter the extent of woody vegetation in the savanna and steppe regions influence the energy, hydrological and biogeochemical fluxes within these ecosystems. Changes in these fluxes influence local and global environmental changes, such as modifying carbon stocks, and changing evapotranspiration fluxes and forage availability and quality in the region. The two areas this group focused on are undergoing rapid land use change: the cerrado region of Brazil and the Eurasian steppe.

Objective

The objective of this experimental approach is:

* to determine the change in woody vegetation in the savanna and steppe regions of the world in order to predict changes in ecosystem properties that influence NPP, C storage, energy flux, and hydrological and biogeochemical dynamics; and
* to project different scenarios of change in woody extent of these ecosystems.

Detection of these changes during the past 30 years is possible with the remote sensing data and field observations available.

Many of these changes in woody land cover can take several decades to manifest themselves over large areas; however, fine scale changes can be detected with repeated observations. Short-term changes can be detected in situations where human activities related to grazing, fire, cropland conversion, or reforestation take place. The areal extent of these changes is usually large enough to detect using AVHRR-level remote sensing techniques. The initial test areas are the cerrado region of Brazil and the steppes of Asia.

In these areas, anthropogenic and natural processes modifying the woody extent will be identified and studied. Fire, grazing, and cropland conversion are key land use practices which contribute to changes in woody cover in these regions. Human activities can accelerate or reduce the rate of woody cover change through different applications of fire, grazing, and cultivation. Natural changes in climate patterns leading to drought or intensification of rainfall can modify the vegetation community. Climate variability in these systems is very large; a 30 -year analysis of the coefficient of variance of rainfall can exceed 50%. This characteristic variability results in a highly dynamic vegetation response and hampers our ability to detect changes solely due to human activities.

An integrated, multi-technique study approach is proposed, incorporating multi-temporal, multi-spatial monitoring with remote sensing, as well as modeling analysis and field studies.

Analytical Approach

An integrated, multi-technique approach is proposed for the study of changes in woody cover extent in the savanna and steppe regions of the world. This integrated approach will incorporate multi-temporal, multi-spatial monitoring of the land surface using remote sensing techniques (AVHRR, MSS, SPOT, TM, SAR, aerial photographs, etc.). Modeling analysis of ecological features of these systems will be used to assess current changes in ecosystem characteristics that can be used to evaluate current dynamics and future changes in woody dynamics of these systems. Field studies of processes influencing changes in land cover and measuring the rate of land cover change will be incorporated to supply more detailed information on factors affecting the rate of change in these systems. These field studies will incorporate information dealing with social-economic-political sectors as well as environmental features.

Remote sensing techniques

Remote sensing techniques can be applied to woody cover detection at several scales of analysis. At the fine spatial scale of resolution we are limited by the temporal resolution of analysis. However, synoptic, subdecadal to decadal analysis of land cover over the region can provide the needed information to determine the synoptic status of woody cover in the region. Ancillary data from field studies can then be applied to determine the ecological changes in the system that can be used for extrapolation studies.

Coarse spatial resolution analysis can be applied with higher temporal frequency and be used to document large scale changes in these systems. New techniques with unmixing of end-member analysis, spectral cluster analysis, and BRDF techniques can be used to determine different aspects of the land surface that would indicate changes in the woody extent and other changes in land cover features related to changes in grazing and fire intensity.

Spectral classifiers operate by grouping together those pixels with similar reflectance values over the various sensor bands. Since agricultural areas and savanna/steppe regions have

distinct spectral characteristics, especially if time of scene selection is chosen to optimize these differences, this technique is able to distinguish cover classes such as cropland and rangelands. Integration of the resulting clusters will be based both on the spectral statistics of the spectral bands as well as their spatial structure.

The high temporal frequency of AVHRR-like instruments can also be used to analyze for causal factors of change to the region. Fire is an example of an event that can quickly reduce woody cover. Malingreau et al. (1993) developed a conceptual framework describing the mechanics of a fire information system. The only method of monitoring fire activity is through the use of remote sensing. Nearly all fire detection is done using the NOAA-AVHRR (Advanced Very High Resolution Radiometer) 3 micron channel (1-km resolution). High resolution instruments are used to account for the average fire scar size and this is used in the algorithm for estimating area burned represented by a detected hot spot. GIS methods are extensively used in the application of models for estimating fire effects including the release of greenhouse gases and particulate matter from detected fires. Layers within the GIS framework must include total fuel loading, weather, appropriate fire model, and algorithms for estimating fuel consumption and emissions production (Scholes et al., 1995).

The angular distribution of radiation scattered by the Earth surface also contains information on the structural and optical properties of the surface. Potentially, this information may be retrieved through the inversion of surface bidirectional reflectance distribution function (BRDF) models.

There are several limitations of AVHRR for use as the driver of a fire information system:

1. Usually only a single afternoon pass for a given location is recorded. This is only a small window in the daily burning cycle. Adjustments must be made for the bias created through this undersampling.

2. The instrument saturates at a very low temperature (320°K).

3. The resolution of the instrument only detects the presence of a heated object or objects within a pixel. Thus, there may be multiple fires of varying size and intensity within a given pixel.

4. Clouds can interfere with fire detection.

These limitations must be accounted for through compensating for the instrument bias. Some of the limitations of AVHRR will be overcome with the launch of the Moderate Resolution Imaging Sensor (MODIS) as part of the Earth Observing System (EOS) platform (Kaufman et al. 1994). This system will considerably enhance the capability to measure smoke, clouds and fires by measuring their properties in additional channels that are more suitable (e. g., the blue channel for smoke measurements or the channel at 2.2 nm for cloud drop size measurements). The channel at 3.75 nm will be used for fire detection and will have a much higher temperature of saturation (500°K). This should allow separation of smoldering and flaming processes.

These limitations may also be addressed through the use of the international SAR sensors (e. g., ERS-1, ERS-2, RADARSAT, ENVISAT). Radar can directly observe land surfaces independent of cloud and smoke cover and time of day. Thus it may be possible to use AVHRR or MODIS data for fire detection and supplement these measurements with the detailed monitoring of the SAR for quantifying landscape change.

The angular distribution of radiation scattered by the Earth surface also contains information on the structural and optical properties of the surface. Potentially, this information may be retrieved through the inversion of surface bidirectional reflectance distribution function (BRDF)

models. In contrast to vegetation index methods, inversions produce quantitative estimates of biophysical parameters that do not depend on empirical relationships. While previous inversion work has largely been limited to use of data from ground-based radiometers, recent work (B. H. Braswell and J. L. Privette, personal communication) has shown that accurate inversions are possible with 1.1 km data from the AVHRR. Compared to other environmental satellite sensors, AVHRR employs a large field of view which results in relatively diverse angular measurements. This is advantageous to the inversion problem. Moreover, AVHRR samples each Earth target at least twice each 24 hours.

Since data from multiple AVHRR sensors are typically ingested each day, the potential for collecting a sufficient number of cloud-free samples during a relatively short period (~10 days) is significant. For example, LAI and leaf optical properties were accurately retrieved from data collected during the FIFE experiment. About 3 to 6 cloud-free samples, collected during an 11-day period, were used in each inver sion. By combining samples collected over adjacent land targets, Braswell successfully inverted the SAIL model with the PATHFINDER AVHRR data from Africa. Once model parameters are retrieved, the models may be used in forward mode to estimate albedo and fAPAR for any solar angle. Currently, techniques are being used to deconvolve AVHRR data collected over heterogeneous areas such that inversions may be possible at 180 m resolution (D. Baldwin, personal communication). Upon launch of MODIS (an AVHRR successor) and MISR (which collects samples at nine different view zenith angles per pass), global inversions may routinely be possible at relatively high resolution (100-300 m).

The availability of remote sensing data and the increasing availability of land surface statistical information has improved our ability to model terrestrial ecosystem dynamics over greater spatial extents.

Modeling Analysis

Ecosystem models can provide information on terrestrial ecosystems that cannot yet (or in the future) be measured remotely . However, knowledge of the spatial extent of various land surface properties that can be used to parameterize ecosystem models is currently limited. The availability of remote sensing data and the increasing availability of land surface statistical information has improved our ability to model terrestrial ecosystem dynamics over greater spatial extents and to verify the behavior of these models within a limited extent.

The current modeling capability of most ecosystem models does not need specific information on spatial patterning of woody and herbaceous vegetation in these regions. Aggregated spatial information is adequate for most modeling needs. In special applications more detailed pattern analysis is needed to simulate certain climate and mass fluxes from these systems. Land use information within these regions is important for simulations of current dynamics of these ecosystems, and the future changes in these systems.

Prediction of the ecosystem response to changes in land use and environmental conditions can be simulated assuming current trends of land use and climate.

Field Studies and Statistical Analysis

Current knowledge of ecosystem dynamics relative to climate variability and land use patterns is limited to relatively few sites. Extensive data on land cover and land use patterns are available, but work is needed to incorporate and collaborate these data within a process-level modeling system and a remote sensing framework.

Working Group on Land Cover Change in Humid Tropical Forests: Ideas Toward a Plan of Action

Appendix 2: Session One Working Group 2

It is impossible to discriminate many types of forest degradation. Only the most intensively logged areas are visible on TM images and the spectral distinction disappears within three years.

The area of interest is divided into three sub-areas:

1. Africa,

2. Southeast Asia (including insular tropical forest areas),

3. Amazonia (Brazilian and non-Brazilian).

The objectives, approaches and field studies mentioned here can also be adopted in studies of boreal and temperate forests.

Objectives

1. Determine changes in land cover types using remote sensing;

2. Determine land use intensities in anthropogenically affected cover types;

3. Obtain necessary parameters to feed climate models and models of the behaviors of biogeochemical cycles: carbon, trace gases, nutrients, hydrological cycles.

Note: The parameters which drive models which predict future rates of Humid Tropical Forest (HTF) loss or alteration (and the consequent fluxes of carbon, nutrients, water, trace gases, and climate change) include road building, population growth, economic alternatives outside the HTF, improvements in pasture management techniques, introduction of disease-resistant forage grasses, domestic and foreign market pressures for timber and meat, and very probably some other economic, political and social parameters. This working group does not include experts in these fields, so that predictive models of future land use will not be discussed here. Modelers with this expertise might be invited to a future meeting. The human dimension of Land Use Cover Changes in the HTF is also the subject of the Human Dimension Program of the IGBP.

Approach

1. Use whatever imagery is available, ideally MSS and TM, but it may be necessary to rely on AVHRR 1-km and orbital radar sensors (RADARSAT, JERS-1, ERS-1, dual polarizaton ENVISAT, dual polarized, one-time SIR-C covering ± 60° latitude) in some areas.

2. Identify the natural boundary between HTF and the neighboring savanna/woodland biome. Save this decision in a widely used GIS file format.

3. Classify HTF into at least four categories and include in a widely used GIS format:

a) Primary forest plus secondary forest over a threshold age [threshold spectral criterion];

b) Deforested: includes bare soil, short cycle crops, perennial crops;

c) Secondary forest up to the threshold age [threshold spectral criterion?]; and

d) Non-forest.

4. For deforested and secondary forest areas, determine the history of land use, pixel by pixel, in order to derive a classification based on the history of the pixel. Develop index of land use intensity based on this classification; for example, number of years pixel was classified as NPV/bare soil.

5. Modify the land use intensity index with such parameters as soil texture, soil fertility, land use type (pasture vs. swidden) to develop a site degradation index.

Field Studies

1. Ground truth spectral classes; i. e. supposed land-use/land-cover types, including the different stages input into the land use history classes, as seen in temporal series of images.

2. Determine behavior of carbon, trace gases, nutrients, and hydrology under different land use regimes and histories. For example after a single slash-and-burn of primary forest, after repeated crop/fallow cycles in swidden agriculture, and after long-term pasture.

3. Determine LAI, APAR, NPP, and GEP of different cover types.

4. Create a temporal transformation matrix where boxes represent different land cover or land use types, including different land use history/intensity classes. See recent work of P. Fearnside.

Problems

1. Availability of data: TM & MSS not available everywhere.

2. Archiving problems: encourage places like INPE to maintain readability and archival security of old MSS data. This is irreplaceable data spanning such important natural change periods as 1982/83 El Niño. Some data has already been lost. Express need of the scientific community in writing for this archival effort. Write to:

Dr. Luiz Alberto Vieira Dias
Chefe, Observacoes da Terra
INPE-Instituto Nacional de Pesquisas Espaciais
Caixa Postal 515
12.225 Sao Jose dos Campos, SP
BRAZIL

There is ambiguity in separation of anthropogenic secondary forest vs. some natural forests. This problem is greatest in SE Asia, a small problem in the non-Brazilian Amazon, but not a problem in the Brazilian Amazon. The error should be estimated for each region by field checking.

Note:Dr. Vieira Dias has stated that such letters from the scientific community, showing a demand for these products, is required in order to obtain the necessary funds for archiving and data recovery.

3. It is impossible to discriminate many types of forest degradation. Only the most intensively logged areas are visible on TM images and the spectral distinction disappears within three years.

4. There is ambiguity in separation of anthropogenic secondary forest vs. some natural forests. This problem is greatest in SE Asia, a small problem in the non-Brazilian Amazon, but not a problem in the Brazilian Amazon. The error should be estimated for each region by field checking.

Participant Roster

Rob Braswell
NCAR

Dennis Dye
Department of Geography
Boston University

William Emery
University of Colorado

Alfredo Huete
University of Arizona

Jean Iaquinta
Universite Blaise Pascal

Sietse Los
NASA/GSF
Biospheric Sciences Branch

Elaine Matthews
NASA/GISS

Kyle McDonald
Jet Propulsion Laboratory
NASA

Ranga B. Myneni
NASA/GSFC
NASA

Bruce Walker Nelson
INPA

Ivan Nijs
University of Antwerp

Greg Asner
University of Colorado

Dennis Ojima
Colorado State University

Bill Parton
Colorado State University

Jeff Privette
NASA/GSFC

Elijah Ramsey
Southern Science Center
NWRC

Brad Reed
EROS Data Center

Don Sabol
University of Washington
Remote Sensing Lab

Bill Salas
University of New Hampshire
CSRC/Morse Hall

Laura Stretch
Natural Resources Ecology Lab
Colorado State University

Compton J. Tucker
NASA/GSFC

Darold E. Ward
Intermountain Research Station
Intermountain Fire Sciences
Laboratory

Michael White
University of Montana

Aspen Global Change Institute
100 East Francis Street
Aspen CO 81611
http://www.agci.org
970 925 7376
agcimail@agci.org

Furthering the understanding of Earth Systems and Global Environmental Change